A GENERALIZED VALENCE BOND DESCRIPTION OF VACANCY AND IMPURITY STATES IN DIAMOND AND SILICON

Thesis by

Grover Timothy Surratt

In Partial Fulfillment of the Requirements

for the Degree of

Doctor of Philosophy

California Institute of Technology

Pasadena, California

1975

(Submitted December 17, 1975)

ACKNOWLEDGMENTS

I find that it is the interaction with different sorts of people with different viewpoints by which one learns, perhaps more so than from books and journals. I have had the opportunity to know some very good people over the past several years. I am particularly pleased to have had the chance to work with my advisor, Bill Goddard. His seemingly boundless enthusiasm and his scientific insight make him one-of-a-kind. I am very grateful to my friends and colleagues from Wright-Patterson AFB, particularly Bob Euwema, Tom Collins, Gordon Wepfer, Doug Wilhite and Dillon Scofield, from whom I learned a lot of semiconductor physics. I have enjoyed knowing and working with the members of our research group, particularly Larry Harding and Tom Upton.

Finally, I could not have done this without the support from my family. Mom, Dad and Walt have been a constant source of encouragement. Ultimately, it is to my wife, Catie, that I am most indebted for her patience, understanding and trust in me.

ABSTRACT

Generalized Valence Bond and Configuration Interaction calculations using a double zeta basis have been performed for the vacancy states of diamond and silicon and for the lithium and boron impurities in silicon. For the vacancy case it was found that the nature of the low-lying electronic states of the positive, negative and neutral charge species is easily understood in terms of simple valence bond concepts. Here the effect of symmetric distortion of the vacancy was included, but no other distortions were included. For those cases in which the ordering of the states is known, the experimental ordering is reproduced by the theoretical results. For the impurity case it is found that boron is strongly bound in a substitutional site whereas lithium is not. In both cases the states of the system can be predicted from a simple valence bond analysis. The calculated results are compared with experiment through the use of a dielectric continuum approximation to correct the energies of charged and ionic states.

TABLE OF CONTENTS

I. INTRODUCTION

The traditional approach to describing defect or impurity states in semiconductors begins with the energy band structure for the material.[1] The states are typically classified as shallow, meaning close to a band edge, or deep, meaning more than 0.1 eV from a band edge. The usual treatment of shallow levels involves describing the impurity wavefunction in terms of the energy-band states.[2] This leads to effective mass type theories. Deep levels have been described using modifications of effective mass theory,[3] but most calculations of defects (vacancies) have been some sort of cluster calculation. That is, the vacancy is treated as a missing atom in a finite cluster of atoms and the problem is solved as a molecular orbital problem.[4,5,6] In some cases an attempt is made to relate the calculated states to the band structure by using large clusters, but this is not always done.

The approach used here is based on the cluster approach, however no basic distinction is made between shallow and deep levels. The idea is to study the vacancy or impurity states in terms of relatively simple "chemical" ideas about bonds and electron states. A straightforward qualitative description of the states of interest can be given based on valence bond concepts. These qualitative ideas are then tested by performing ab initio Generalized Valence Bond (GVB)[7,8] and Configuration Interaction (CI) calculations. The emphasis here will be on obtaining a consistent localized picture of the various states. After this is done we will go back and relate the calculated quantities to the usual band structure picture. The systems that will be discussed

are the vacancy and (111) surface states in diamond and silicon and the lithium and boron impurity states in silicon.

II. QUALITATIVE DESCRIPTION OF THE STATES

Since the work of Coulson and Kearsley,[9] the conceptual basis for vacancies in covalent materials has been the "defect molecule". In this model one removes the atom or atoms to form the vacancy, breaking the bonds and leaving sufficient electrons to make the system neutral. For diamond and silicon this means that four tetrahedrally arranged dangling bond orbitals remain. The usual approach is then to treat the problem as a molecular orbital problem, combining the functions into symmetry orbitals and solving for the states of the system. This is the approach which has been followed by Coulson and Kearsley and others.[10] However, if one looked at the same defect molecule from the Generalized Valence Bond (GVB) viewpoint, a somewhat more intuitive structure emerges. If one were to solve for the GVB wavefunction for the defect molecule, one would expect to find a structure very much like the Coulson Kearsley defect molecule. That is, we would solve for four singly occupied non-orthogonal orbitals. These orbitals would be localized on each of the centers. The overall wavefunction would be an antisymmetric product of these orbitals and an appropriate spin function. We can start with these orbitals, call them ϕ_1, ϕ_2, ϕ_3, ϕ_4 on centers 1, 2, 3, 4 respectively, and construct a qualitative description of the first few states of the defect. The ground state would be a state in which the orbitals are coupled into two weak bonds. There are 3 combinations ($\phi_1 + \phi_2$, $\phi_1 + \phi_3$ or $\phi_1 + \phi_4$) but we know that there will be only 2 proper spin-eigenfunctions for the singlet case. In T_d symmetry this gives rise

to an E state. Suppose we consider one case in which ϕ_1 and ϕ_2 are bonded. If we look at the system as like two H_2 molecules, we can depict this state as

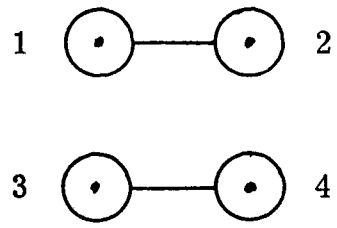

The first excited state is obtained by the excitation of one electron from the bond pair $(\phi_1 + \phi_2)^2$ into an antibonding orbital. The orbital form of this state is $(\phi_1 + \phi_2)(\phi_1 - \phi_2)$ which yields $\phi_1^2 - \phi_2^2$ as the singlet component. This is a wavefunction for an ionic state which is a combination of 2 electrons on center 1 and 2 electrons on center 2. One ionic structure can be depicted

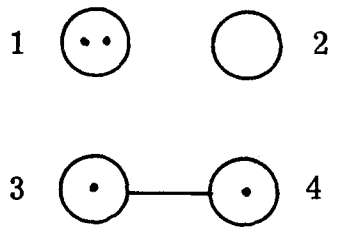

There are twelve such diagrams that can be constructed for a tetrahedral geometry. A group theoretical analysis of the states resulting from these diagrams gives A_1, E, T_1 and 2 T_2's. (The procedure used in this determination is outlined in Appendix A.) The next excited states would involve ionic states in both bonds and thus would be quite high in energy.

A triplet state of the vacancy can be obtained by singlet coupling one bond pair while triplet coupling the other pair of electrons. The diagram for this state is

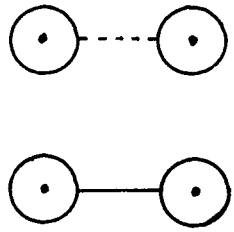

There are three ways to couple 4 electrons into a triplet and we find that this gives rise to a T_1 state. The first excited state of this structure is a single excitation in the 3-4 bond. The diagram for this state is

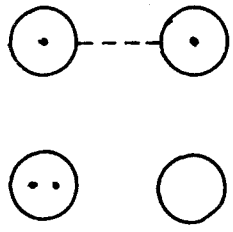

which gives rise to 12 states. Their symmetries are A_2, E, T_2 and 2 T_1's. There should be no other low-lying triplet states. There is one quintet state of A_2 symmetry in which the 4 orbitals are high-spin coupled.

The symmetry information may now be used with some other qualitative information to give a reasonable picture of the ordering of these states. The overlap between the dangling bond orbitals should be small since the center to center distance in the vacancy is about 1.6 times a normal bond length for the diamond lattice. This would

lead us to expect a small singlet-triplet splitting in any one bond.[11] Thus the predicted order of state is $^1E < {}^3T_1 < {}^5A_2$, with roughly the same splittings between the levels in zero order. The excitation energy to the first excited state for both the singlet and triplet should be about the same, since it involves the same sort of excitation in one bond. This picture is given in Figure II-1. Considering the interactions of the states, we obtain the splittings indicated in Figure II-1. In the singlet case the E ground state is lowered by interaction with the E excited state. The T_2 states interact strongly and are split more than the E states. The A_1 and T_1 states are left unchanged. Thus we expect the first excitation for the vacancy to be E to T_2. In the triplet case only the T_1 states can interact. Here we expect the ground state to be lowered slightly and the upper T_1 states to split apart. The A_2, E and T_2 remain at about the same energy. The $^5A_2$ state has no other states to interact with and thus stays fixed.

A similar analysis can be performed for the positive and negative ion states. The positive ion would be depicted

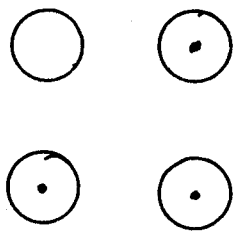

while the negative ion would be given by

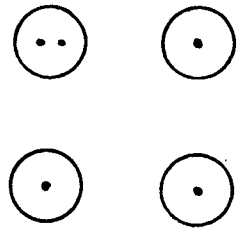

There are four structures in each case giving rise to 4 quartet and 8 doublet states. The symmetries of these are $^4A_2$, $^4T_1$, $^2E_1$, $^2T_1$, $^2T_2$.

Let us now turn to the case of the boron impurity. The GVB diagram for the boron atom is

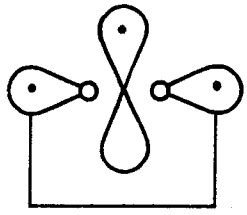

which represents a singly-occupied p_z orbital and a $s+p_x$ and $s-p_x$ pair of orbitals.[12] The bonding of B can be explained by considering how other species would bond to this structure. The case of B in Si is quite simple. Starting with Si vacancy as

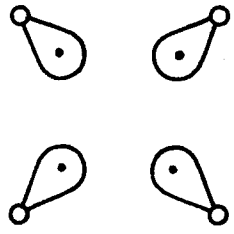

a bond could be formed to each of 3 Si lobes giving

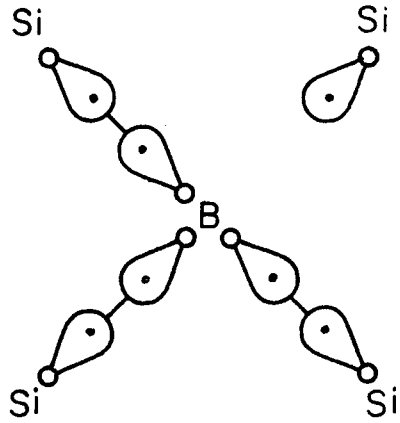

There are 4 equivalent structures for this complex leading to A_1 and T_2 states. The form of the acceptor which has trapped an electron is obtained by forming one more Si-B bond to obtain

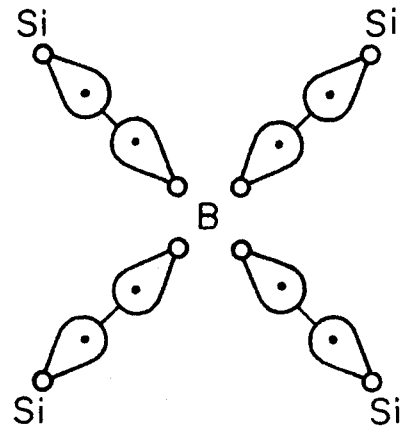

The case of lithium is a bit more difficult to visualize. The case of the ionized Li simply amounts to putting a positive charge in the middle of the vacancy. Thus we would expect pretty much the same picture as in the vacancy case but with the orbitals polarized toward the Li somewhat. To obtain the neutral state we must add a singly occupied orbital which overlaps strongly with each of the singly occupied

orbitals of the vacancy. Diagrammatically we write this

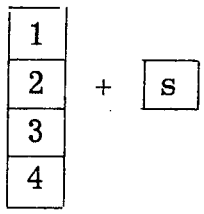

where this represents 4 singly occupied orbitals high spin (antisymmetrically) coupled (quintet state of the vacancy) plus a lithium s orbital. We could get structures such as

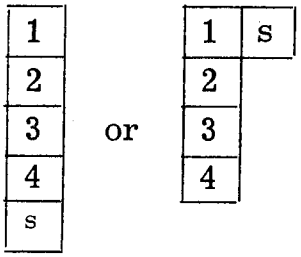

or recoupling the second structure into

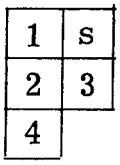

The totally antisymmetric structure is probably fairly high in energy since it requires 5 orthogonal orbitals in the vacancy. The next structure (quartet) amounts to forming one totally symmetric doubly occupied orbital or orbital pair and three orthogonal singly occupied orbitals.

The last structure is derived from the second by doublet coupling the high spin orbitals. The quartet should lead to symmetries A_2 and T_1 while the doublet states would be T_1, T_2, E. It is not clear whether the doublet or quartet would be lower.

The foregoing analysis, not only serves to quickly catalog what states to expect, but also indicates what sort of calculations would be appropriate for the various complexes studied.

The unreconstructed (111) surface for diamond lattice semiconductors is depicted as dangling bond orbitals on each surface atom pointed perpendicular to the surface. The quantities of interest in this case are the ionization potential and electron affinity of the surface orbitals and the geometry of the positive, negative and neutral species. For this study we assume that the dangling bond orbitals are very weakly coupled and thus roughly independent. This assumption is based on calculations by Redondo and Goddard[13] and on the geometrical argument that the orbitals are widely separated and essentially non-overlapping. If we choose a cluster consisting of one surface atom and its three bonded neighbors, we can study the motion of the surface atom with some confidence and still have a single surface orbital. The states of interest are then just a dangling bond orbital with zero, one or two electrons in it. For this picture there will be no orbital coupling and so there is no analysis to be made as was done for the vacancy.

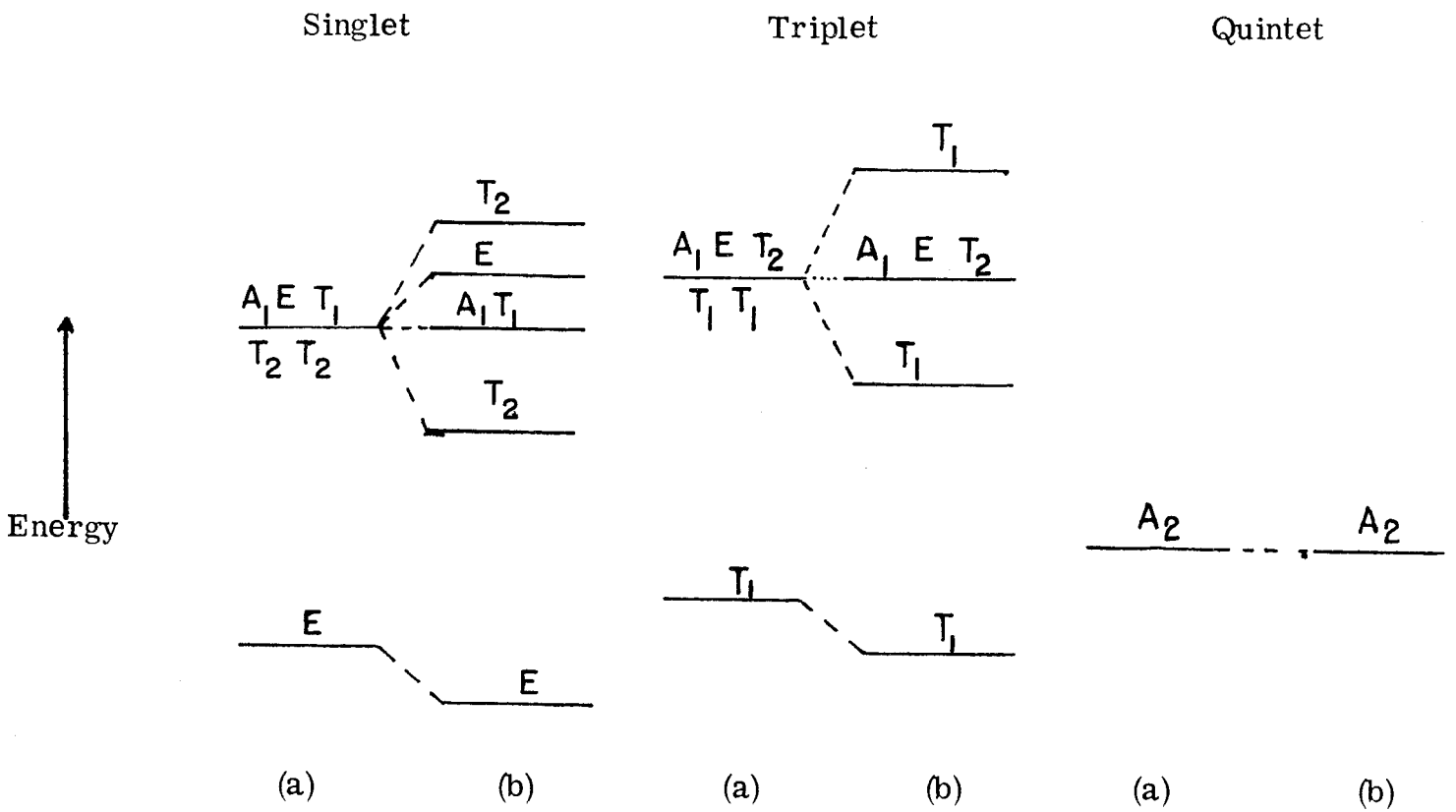

Figure II.1. States of the neutral vacancy as derived from a valence-bond analysis: (a) gives the ordering of the states if they are considered non-interacting; while (b) shows the effects of interactions. There is only a relative scale (i.e., ordering) implied.

III. CALCULATIONAL DETAILS

A. Geometries

Diamond and silicon both occur in the diamond structure,[14] which is a face-centered cubic lattice with two atoms per unit cell. The calculations in this work involve clusters of atoms that extend only to the second-nearest-neighbor position. Starting with the atom at the origin, the nearest-neighbor positions are $\frac{a}{4}(1,1,1)$, $\frac{a}{4}(1,-1,-1)$, $\frac{a}{4}(-1,1,-1)$ and $\frac{a}{4}(-1,-1,1)$ where a is the cubic lattice constant. The twelve second-nearest-neighbor positions are $\frac{a}{2}(\pm1,\pm1,0)$, $\frac{a}{2}(\pm1,0,\pm1)$, $\frac{a}{2}(0,\pm1,\pm1)$. The silicon and diamond lattice constants employed were 5.43 Å and 3.56 Å respectively.[14] In the calculations reported here, the second-nearest-neighbor atoms were replaced with hydrogen atoms. The hydrogens were placed along the appropriate bond directions, but using SiH and CH bond lengths of 1.479 Å and 1.09 Å respectively. These structures retained tetrahedral symmetry. The vacancy and impurity clusters were obtained by deleting the atom at the origin or replacing it with a B or Li. The (111) surface cluster was obtained by deleting the atom at $\frac{a}{4}(1,1,1)$ and its bonded hydrogens. The clusters are shown in Figures III.1 and III.2. The atoms are labelled for reference throughout later sections. The coordinates of the atoms are given in Tables III.1 and III.2 and are keyed to Figures. In some of the calculations to be discussed later, some changes in the coordinates will be made. However, the basis symmetry and labelling of each structure will be retained.

B. Basis Sets.

Two types of calculations were performed, one type was to obtain geometries and qualitative information about states, while the second type was to obtain quantitative descriptions of the states. For the former a minimum basis set (MBS) was used, while for the latter a "valence" double-zeta basis (DZ) was employed. In all cases the bases were of contracted Cartesian Gaussian functions. For the diamond calculations the MBS was an STO-4G set for carbon and hydrogen, while the DZ set was a [3s2p] contraction obtained by Dunning[15] from Huzinaga's[16] (9s5p) set. The hydrogen function in this case was Dunning's [2s] contracted function[17] scaled to a Slater function exponent of 1.2. In the silicon calculations an ab initio effective potential[18] was used to replace the $(1s)^2$ $(2s)^2$ $(2p)^6$ core of the Si. This potential as well as the MBS and DZ basis set optimized for use with the potential were calculated by A. Redondo.[19] The basis set used for boron is the Dunning[17] [4s2p] contraction of Huzinaga's (9s5p) basis, while the basis for lithium was obtained from the paper of Kahn, Hay and Shavitt.[20] The unpublished basis set information is given in Tables III.3-III.5.

C. Wavefunctions

The GVB[7, 8] wavefunction for a bonding pair of electrons is represented as

$$\frac{1}{\sqrt{2}} [(\phi_1 \phi_2 + \phi_2 \phi_1)(\alpha\beta - \beta\alpha)]$$

where ϕ_1 and ϕ_2 are allowed to be non-orthogonal. The form for more than two electrons is

$$\mathcal{A}\,[\,\phi_{a1}\,\phi_{b1}\,\phi_{a2}\,\phi_{b2}\cdots\chi\,]$$

where each electron is represented by a non-orthgonal orbital and the spin function χ is a general spin eigenfunction. ($\mathcal{A}$ is the antisymmetrizer.) Self-consistent wavefunctions of this general form are quite difficult to solve for and hence a more restricted form is generally used. The constraints made are that orbitals of different pairs are required to be orthgonal and that the spin function is taken as the product of singlet spin functions for the pairs of electrons. These constraints are the strong orthogonality and perfect pairing constraints respectively, and the wavefunction is referred to as the GVB Perfect Pairing (GVB-PP) wavefunction. Additionally, rather than solve for the orbitals of the form $(\phi_1\phi_2 + \phi_2\phi_1)$ it is advantageous to transform each pair to a natural orbital (NO) representation,

$$(\phi_1\phi_2 + \phi_2\phi_1) = C_g\phi_g\phi_g - C_u\phi_u\phi_u,\ \langle\phi_g|\phi_u\rangle = 0,$$

where ϕ_g and ϕ_u are the first and second natural orbitals. (The ϕ_1 and ϕ_2 are still referred to as GVB orbitals.) Normally the ϕ_g orbital is very much like a HF bonding molecular orbital, and the coefficient C_g is large, while ϕ_u resembles a HF antibonding orbital and C_u is small. Using only the first NO's in each term would give back the HF form of the wavefunction. Thus the HF and PP forms are quite compatible. In our calculations we have treated the bonds to the hydrogens and the core electrons as HF pairs, thus allowing only the valence orbitals associated with the defect to be correlated.

As described previously, one could eliminate the PP and SO restrictions by allowing more general spin functions and non-orthogonal pairs. While such calculations are tractable for a small number of electrons, it is computationally easier to remove these constraints by performing Configuration Interaction (CI) calculations based on the GVB-PP wavefunction. As in the GVB calculations, the interest is in the description of the vacancy or impurity, so all core, SiH or CH orbitals are removed by an appropriate transformation. The remaining NO's and singly occupied orbitals form the valence space for the CI calculations. The dominant configuration is usually taken as the one (ones) in which the first NO's are doubly occupied. The valence space is usually augmented by an extra set of orthogonal functions which constitute the virtual space. Within this basis, 4 types of CI calculations are employed here:

GVB-RCI: Double excitations within pairs from the dominant GVB configuration into the valence space are included in the CI.

GVB-CI: All excitations in the valence space are included in this case.

POL-CI: All single and double excitations in the full space are allowed with the restriction that there be at most one singly occupied orbital in the virtual space.

SD-CI: All single and double excitations from the dominant configurations into the full space are allowed.

In both the POL-CI and the SD-CI, the GVB-CI configurations are also included. The GVB-RCI serves to relax the PP restriction, while the

GVB-CI relaxes the SO constraint as well as including some other correlation terms.

D. Programs and Miscellanea

The programs used for these calculations are various parts of the Caltech MQM program library. The integrals were done using the Basch-Melius POLYATOM program with the exception of the STO-4G basis which were done using a modified version of GAUSSIAN 70. The SCF calculations were done using the Bobrowicz, Wadt, Goddard program GVB TWO. The CI calculations were done using the Bobrowicz, Winter, Ladner CI program. Properties were calculated using a version of the NYU properties program of Moskowitz as modified by Ermler. Other assorted programs of mixed local heritage were also used. In the case that POLYATOM was used for integral calculation, a post-test value of 10^{-8} was used. For GAUSS70 this value was set to 10^{-7}. All SCF calculations were converged to a SQCDIF of 10^{-6}.

TABLE III.1 Coordinates (in a.u.) for the basic tetrahedral cluster for diamond and silicon. The centers are numbered with reference to Figure III.1.

C0	(0.0, 0.0, 0.0)	SI0	(0.0, 0.0, 0.0)
C1	(-1.6852, -1.6852, 1.6852)	SI1	(-2.5658, -2.5658, 2.5658)
C2	(1.6852, 1.6852, 1.6852)	SI2	(2.5658, 2.5658, 2.5658)
C3	(1.6852, -1.6852, -1.6852)	SI3	(2.5658, -2.5658, -2.5658)
C4	(-1.6852, 1.6852, -1.6852)	SI4	(-2.5658, 2.5658, -2.5658)
H1	(2.8744, 2.8744, 0.4959)	H1	(4.1803, 4.1803, 0.9513)
H2	(2.8744, -2.8744, -0.4959)	H2	(4.1803, -4.1803, -0.9513)
H3	(-2.8744, 2.8744, -0.4959)	H3	(-4.1803, 4.1803, -0.9513)
H4	(-2.8744, -2.8744, 0.4959)	H4	(-4.1803, -4.1803, 0.9513)
H5	(2.8744, 0.4959, 2.8744)	H5	(4.1803, 0.9513, 4.1803)
H6	(-2.8744, 0.4959, -2.8744)	H6	(-4.1803, 0.9513, -4.1803)
H7	(-2.8744, -0.4959, 2.8744)	H7	(-4.1803, -0.9513, 4.1803)
H8	(2.8744, -0.4959, -2.8744)	H8	(4.1803, -0.9513, -4.1803)
H9	(0.4959, 2.8744, 28744)	H9	(0.9513, 4.1803, 4.1803)
H10	(-0.4959, -2.8744, 2.8744)	H10	(-0.9513, -4.1803, 4.1803)
H11	(0.4959, -2.8744, -2.8744)	H11	(0.9513, -4.1803, -4.1803)
H12	(-0.4959, 2.8744, -2.8744)	H12	(-0.9513, 4.1803, -4.1803)

TABLE III.2 Coordinates (in a.u.) for the (111) surface cluster for diamond and silicon. The centers are numbered with reference to Figure III.2.

C1	(0.0, 0.0, 0.0)	SI1	(0.0, 0.0, 0.0)
C2	(1.6852, -1.6852, -1.6852)	SI2	(2.5658, -2.5658, -2.5658)
C3	(-1.6852, 1.6852, -1.6852)	SI3	(-2.5658, 2.5658, -2.5658)
C4	(-1.6852, -1.6852, 1.6852)	SI4	(-2.5658, -2.5658, 2.5658)
H1	(-2.8744, -2.8744, 0.4959)	H1	(-4.1803, -4.1803, 0.9513)
H2	(-2.8744, 0.4959, -2.8744)	H2	(-4.1803, 0.9513, -4.1803)
H3	(0.4959, -2.8744, -2.8744)	H3	(0.9513, -4.1803, -4.1803)
H4	(2.8744, -2.8744, -0.4959)	H4	(4.1803, -4.1803, -0.9513
H5	(-2.8744, 2.8744, -0.4959)	H5	(-4.1803, 4.1803, -0.9513)
H6	(-2.8744, -0.4959, 2.8744)	H6	(-4.1803, -0.9513, 4.1803)
H7	(2.8744, -0.4959, -2.8744)	H7	(4.1803, -0.9513, -4.1803)
H8	(-0.4959, -2.8744, 2.8744)	H8	(-0.9513, -4.1803, 4.1803)
H9	(-0.4959, 2.8744, -2.8744)	H9	(-0.9513, 4.1803, -4.1803)

TABLE III.3 Contracted Cartesian Gaussian Valence Double Zeta Basis for Carbon[15]

Function	Exponent	Coefficient
1s	4233.0	.001220
	634.9	.009342
	146.1	.045452
	42.5	.154657
	14.19	.358866
	5.148	.438632
	1.967	.145918
2s	5.148	-.168367
	.4962	1.060091
3s	.1533	1.0
1p	18.16	.018539
	3.986	.115436
	1.143	.386188
	.3594	.640114
2p	.1146	1.0

TABLE III.4 Ab initio Effective Potential[a] for Si.[19] The form of the potential is $V_\ell(r) = \Sigma_i C_{\ell i} r^{n_i-2} e^{-\alpha_i r^2}$

Term	n_i	α_i	C_i
V_s-V_d	0	.1570859	.24891789
	2	3.5641009	30.31756200
	0	1.8478285	4.0800434
V_p-V_e	0	.9686443	.86954814
	2	4.0620237	36.58557100
	0	.2389864	.45326622
V_b	2	.0991736	-.0118962
	1	.290009	-.07889166
	1	3.2105169	-3.5910011

a) See Reference 18(a) for computational details with regard to this form of effective potential.

TABLE III.5 Cartesian Gaussian Basis Set for Si and H.[19] The minimum basis set is obtained by using the first function of each type, the double zeta basis by using both. Only a minimum basis for hydrogen was used in either case.

	Function	Exponent	Coefficient
Silicon	1s	4.051	.0436619
		1.484	-.2748724
		.2704	.4527114
		.09932	.4247582
	2s	.2704	-.2004077
		.09932	.4247582
	1p	4.185	-.0047173
		1.483	-.0365421
		.335	.3147023
		.09699	.1447246
	2p	.335	-.0307358
		.09699	.1447246
Hydrogen	1s	5.663728	.0871988
		.857387	.5046466
		.190504	.8087388

FIGURE CAPTIONS

Figure III.1. Vacancy and Impurity Cluster for diamond and silicon as viewed from the [001] direction.

Figure III.2. Surface complex for the (111) surface as viewed from the [111] direction. The dashed circles indicate a hydrogen directly behind a silicon or carbon.

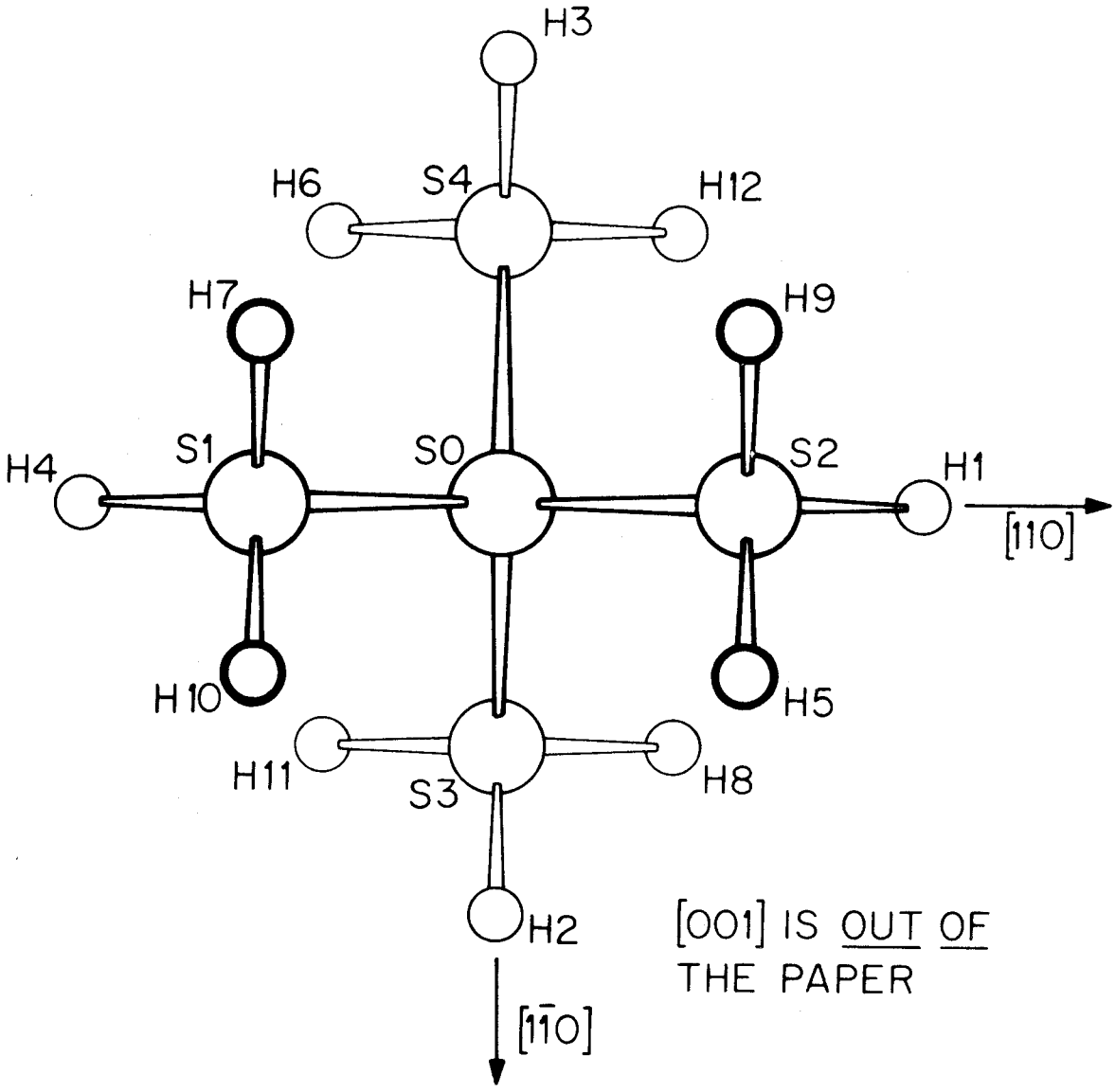
H3
H6
S4
H12
H7
H9
S1
S0
S2
H4
H1
[110]
H10
H5
H11
S3
H8
H2
[001] IS OUT OF
THE PAPER
[1$\bar{1}$0]

Figure III.1.

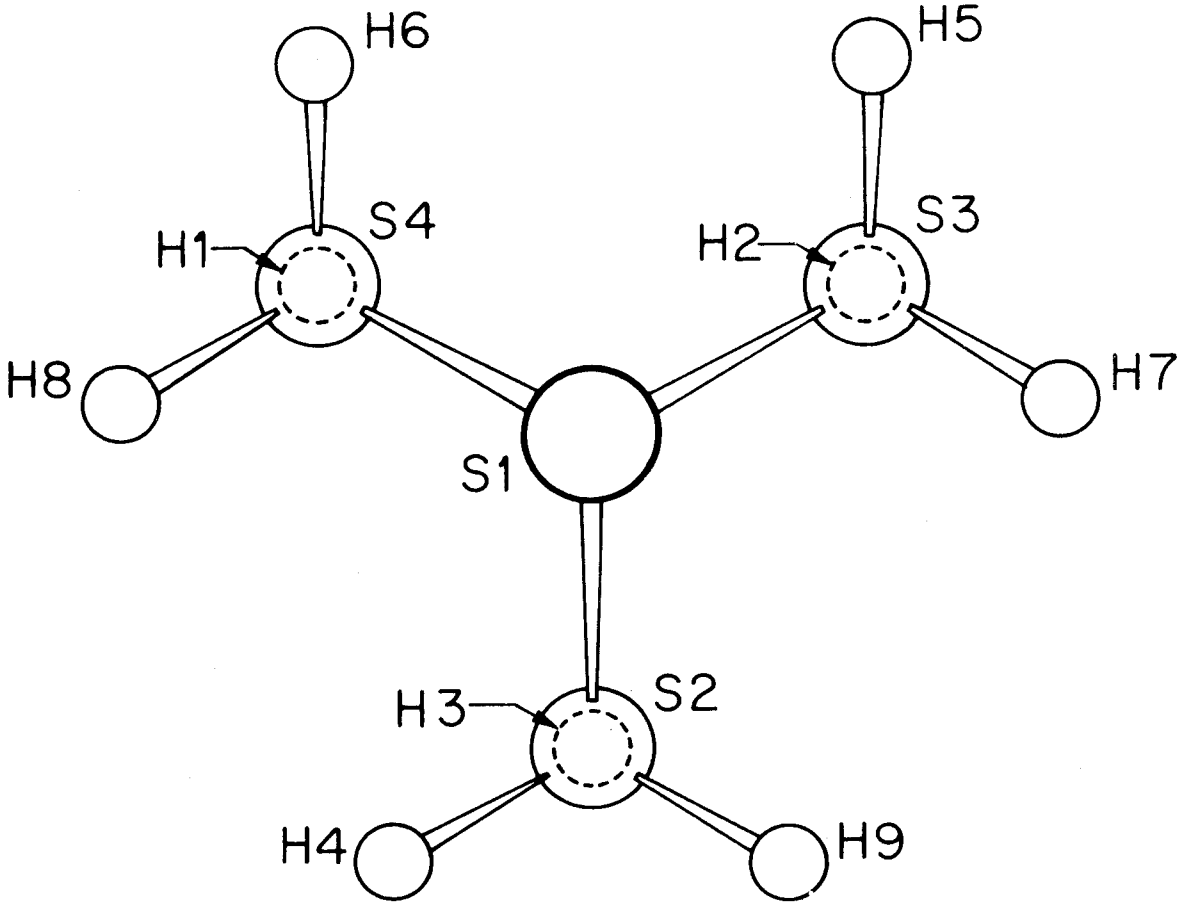

Figure III.2.

IV. DIAMOND VACANCY AND SURFACE STATES

The qualitative description of the vacancy states was given in section II. In order to provide a test of those ideas, a calculation of the quartet state of the vacancy was carried out using the STO-4G basis. This resulted in four singly occupied orbitals, all symmetry functions for the T_d point group. These four orbitals were recombined to form four equivalent (orthogonal) orbitals centered on the four carbon sites (see Figure III.1). Using these four orbitals we carried out full CI calculations for the singlet, triplet and quintet states. This yielded a ^1E ground state for the vacancy, a low-lying (0.44 eV) $^3T_1$ state and an excited singlet of $^1T_2$ symmetry. The $^5A_2$ state was found to be 1.77 eV above the ground state. Thus even at a very simple level, computationally, the qualitative predictions of section II prove to be correct.

Given that an adequate description of the system could be obtained, the next task was to obtain a reasonable geometry for the vacancy. Removing the center atom to leave 4 dangling bond orbitals can give rise to two major types of distortions.

(i) Each first neighbor of the vacancy is bonded to three second neighbors. In this circumstance the C–C bonds are expected to shorten slightly, leading to a movement of the first neighbor about 0.08 from the center of the vacancy.

(ii) To whatever extent the dangling bond orbitals of the different first neighbors overlap ($\sim .04$), weak bonding

between them could lead to additional distortions. Thus one component of the ^1E state has bonding of the form

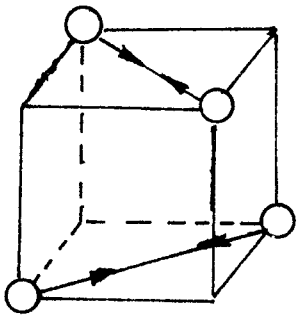

and hence should lead to D_{2d} distortions as indicated by the arrows.

Experimentally the ground state of the neutral vacancy in diamond is believed to be tetrahedral[21] which may be taken as support for (i) as being dominant.

To calculate the distortions in (i) we considered each first neighbor C to be bonded to three tetrahedral CH_3 groups. The carbons were all positioned at the appropriate locations of the diamond lattice. The position of the first carbon along its [111] axis was then optimized. Thus this calculation corresponds directly to the (111) surface model as discussed in sections II and III.

The calculations were performed on the C_4H_9 cluster using an STO-4G basis for various distances of the center atom along the [111] direction. C_{3V} symmetry was used leading to a $^2A_1$ state. The resulting values of the total energy are tabulated in Table IV.1. The minimum was found by a parabolic fit to the three points closest to the

minimum. The minimum point was also calculated. A cubic spline fit to the data is given in Figure IV.1. The minimum point is at -0.1812 a.u. = -.096 Å along the [111] axis. This corresponds to a bond length of 1.515 Å as opposed to a diamond bond length of 1.5445 Å. This bond length is in good agreement with C-C bond lengths calculated for organic radicals using a similar basis.[22] The distance between the surface (111) plane and the second (111) plane is one third of the bond length for the unrelaxed geometry. Thus the relaxation "into" the crystal is 18.6 % of this distance.

This information was next used to construct a model for the relaxed vacancy. The appropriate point to note in the C_4H_9 calculation is that only C1 (Figure III.2) moved. The analogous thing in the vacancy case is to move the nearest-neighbor shell outward but to fix the second nearest neighbor shell. However the second shell is the one we wish to replace with hydrogens. The consistent choice in this case is to preserve the bond angles to the center carbon as obtained from the C_4H_9 calculation but to replace the C-C bonds with C-H bonds. The carbon positions for the vacancy become (1.7898, 1.7898, 1.7898) (in a.u.) plus equivalent locations while the hydrogen positions are (2.9268, 2.9268, 0.5023) plus equivalent locations.

Using this geometry and the valence double zeta basis, GVB-PP calculations were performed on the ^1E ground state and the $^1T_1$ excited state. In actuality the states solved for were the structures indicated in section II. The ground state was treated as GVB(2-PP) wavefunction for the vacancy orbitals and a HF treatment of the

remainder of the cluster. The bonds were chosen to be between centers 1 and 2 and between 3 and 4 by employing C_{2V} symmetry with the C_2 axis along the z axis of the cluster. For the first excited state we expect a form of the wavefunction which is $(\phi_1 + \phi_2)(\phi_1 - \phi_2) = \phi_1\phi_1 - \phi_2\phi_2$ in one bond region and a GVB pair in the other. The form used was to singly occupy and singlet couple the first and second natural orbitals of one bond pair while leaving the second bond unchanged from the ground state calculation. The results of these calculations are given in Table IV.2. The orbitals for the vacancy states are given in Figures IV.2 and IV.3.

The ground state is much as had been predicted. The GVB orbitals overlap about .25 while for a strong bond an overlap of .7 would be typical. In Figure IV.2 we can see that the orbitals have delocalized slightly toward each other but are basically tetrahedral dangling bond orbitals in nature. Comparing the GVB calculation with the HF quintet calculation, the total splitting between singlet and quintet is .938 eV.

The nature of the $^1T_2$ state can be seen in Figure IV.3 with some help from Table IV.2. The GVB orbitals in Figure IV.3 are no longer dangling bond orbitals. Instead they are quite similar in the bond region (between 3 and 4) but are delocalized back onto centers 1 and 2, with one orbital delocalized toward each center. The antisymmetric $(\phi_3 - \phi_4)$ singlet orbital is in the 3-4 bond region as well,

while the symmetric singlet orbital is between centers 1 and 2. The net effect is that the $(\phi_3-\phi_4)$ orbital represents the transfer of an electron from one bond to the other while the delocalization of the GVB orbitals represents some "back transfer." From Table IV.2 we can learn a little more about the GVB orbitals. The energy lowering is small and the contribution of the first NO is almost all of the orbital. This indicates that the GVB pair is nearly a doubly occupied orbital. The large overlap of the GVB orbitals also indicates that the GVB orbitals are occupying the same region of space. The effect of polarization in the CH bonds is significant as well. If we divide the cluster in half with a plane perpendicular to the z axis (between bonds 1-2 and 3-4) we see from the Mulliken populations that there is $\sim$1.8 electron transferred from the 1-2 side to the 3-4 side. The carbon contribution to this is only $\sim$0.8 electron so that $\sim$1.0 electron shift comes from the CH bonds. The excitation energy to this state from the ^{1}E is 5.66 eV.

Next we wish to investigate the spectrum of states predicted by the VB analysis of section II. This is done via a CI calculation based on the GVB orbitals. The valence space was chosen as the four vacancy NO's from the GVB(2-PP) calculation. A set of virtual functions was obtained in the following manner. Using outermost (smallest exponent) s function and p functions on each center, 4 s-like and 4 p-like symmetry functions were constructed. In the

case of the p functions, a lobe directed at the origin from each center was used in constructing the symmetry functions. The resulting 8 functions were orthogonalized to all of the occupied functions in the ground state GVB calculation. A SD-CI was done over the 12 basis function space using all members of the GVB-CI as dominant configurations. The configurations were classified by C_{2V} symmetry and the CI calculations were done for each of the four irreducible representations. In this manner the singlet and triplet states of the neutral vacancy were calculated along with the doublet and quartet states of the positive and negative vacancy. These results are presented in Tables IV.3 and IV.4. The degeneracies of the C_{2V} states are not exactly correct due to the fact that the NO's are not exactly combinations of tetrahedral orbitals.

Overall one can see that the ordering of the singlet and triplet states is that predicted by the simple VB analysis. In Table IV.3 we report all of the states predicted by the VB analysis plus the next highest singlet and triplet states. The last states are the ones corresponding to the excitations in each structure and are at relatively high energy as predicted. One disconcerting fact is that the ^1E to $^1T_2$ excitation energy is larger for the CI calculation than for the SCF calculations. Comparing the SCF and CI calculations we see that the energy of the ^1E state is 17 millihartree (1 mh = .027 eV = .628 kcal) lower for the CI calculation, while the $^1T_2$ CI energy is only 2 mh below the SCF value. The key to this difference is that in the SCF calculation the C–H bonds were allowed to readjust while in the CI calculations the bonds were fixed as those from the ^1E SCF calculation. For comparison, an SCF calculation was performed on the $^1T_2$ state using the 12 basis function space used for the CI calculations. In this way the CH bonds were fixed as those for the ^1E state and only the 4 vacancy orbitals were solved for. This result is given in Table IV.2 [$^1T_2$ (12BF)]. We see that the energy for this constrained calculation is 30 mh higher. Some of this differences is undoubtedly due to there being less variational freedom in the 12 basis function space for describing the vacancy orbitals. Thus while this value should be taken as the maximum effect due to charge rearrangement in the CH bonds, it does indicate that such effects may be significant in the excited states.

In Tables IV.5 to IV.8 we present the dominant terms in the CI wavefunctions for the low-lying states of the various calculations. While the CI calculations were not done using the GVB orbitals as a basis, the NO basis that was used is a basis of localized functions. This allows us to interpret the CI wavefunctions in terms of valence bond structures as well as determining the origin of various correlation effects.

The singlet states are very much like their GVB description. In Table IV.5 we see that for the A_1 component of the ^1E state, the first four configurations are just the GVB configurations. The next two configurations are terms which serve to change the shapes of the bonding orbitals.

To interpret the $^1T_2$ states it is helpful to expand the wavefunctions to obtain the appropriate components. The first two configurations of the A_1 component of the $^1T_2$ state give

$$(u_1^2 - u_2^2)\, g_1\, g_2^{23}$$

which corresponds roughly to structures like

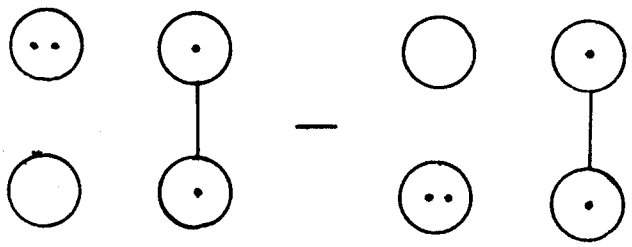

The second two configurations can be expanded to give a form

$$(\ell_1 r_1 + r_1 \ell_1)(\ell_2^2 + r_2^2) - (\ell_2 r_2 + r_2 \ell_2)(\ell_1^2 + r_1^2)$$

which corresponds to structures such as

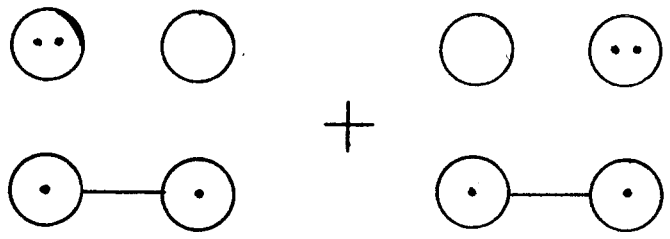

The first configuration of the B_1 component of the $^1T_2$ state corresponds to a structure like

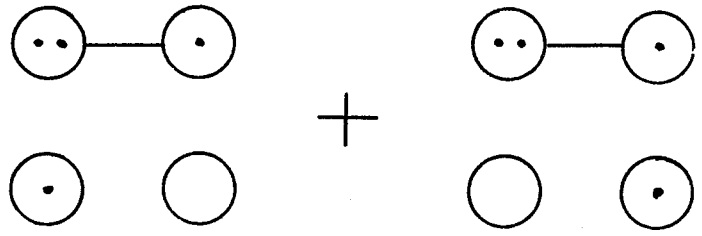

which can be interpreted as being like a He_2^+ in one bond coupled to an H^+ in the other.[24] The second two configurations are just a bond pair coupled with an ionic bond such as

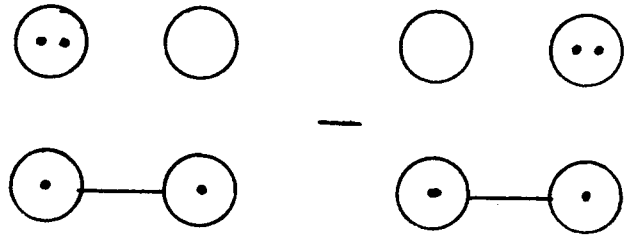

What this points out, in effect, is what we missed in the original analysis. That is, by forming a state such as $g^2 u = (\ell\ell r - rr\ell)$ in one bond we get what amounts to the bonding state for He_2^+ on one side. While this state is definitely above the H_2 state $\ell r + r\ell$, it is below the $\ell^2 - r^2$ ionic state of H_2. The point that should be made is that the form of the wavefunction employed makes it possible to use such interpretations and that the structure of the states can still be understood in terms of simple bonding concepts.

In the initial VB analysis of section II, the considerations used were relatively simple. The states were taken as well defined combinations of singlet and triplet states in two well defined bonds. In the GVB calculations the orientations of the bonds was fixed so that in doing the CI calculations, the resulting states are not as easily interpreted as if we were using truly localized functions. There are also some states which arise from considering more complicated sorts of spin couplings. For instance, given the low-lying triplet state of one bond, we could consider taking two triplets, one in each bond, and recoupling them. This line of reasoning was used to get the quintet state, but it also gives rise to a singlet and triplet state. The singlet state is the A_2 component of the ^1E state. The triplet state is the A_2 component of the 1^3T_1 state. The CI wavefunction for the 1^3T_1 as given in Table IV.6 gives the coefficients for the spin eigenfunctions for the orbital ordering $\sigma_1 \sigma_2 \sigma_1^* \sigma_2^*$ (refer to Table IV.4 for notation). If one changes the ordering to $\sigma_1 \sigma_1^* \sigma_2 \sigma_2^*$, then the spin eigenfunction is given by $.079\ \chi_1 - .802\ \chi_2 + .484\ \chi_3$. If the state were purely the triplet

state obtained from coupling two triplets, the spin eigenfunction would be $-.816\ \chi_2 + .577\ \chi_3$, however, this is the major component of the state. This state gives the same energy as the B_1 components of the 1^3T_1 which is simply a GVB pair in one bond and a triplet in the other.

For the 2^3T_1 state, we again have to reorder the orbitals in the A_2 component. Doing so we obtain a spin eigenfunction for the first configuration which is $.512\ \chi_1 - .043\ \chi_2 - .597\ \chi_3$. The χ_1 term leads to an ionic singlet state coupled to a covalent triplet while in χ_3 the singlet and triplet are interchanged. This could be depicted

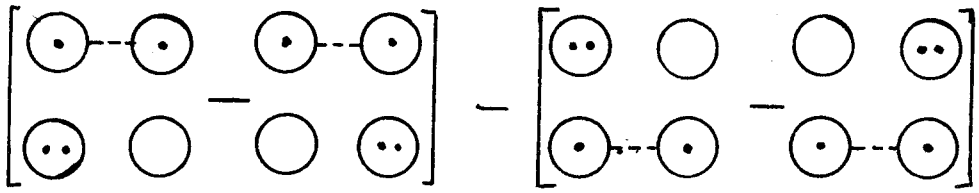

The B_1 component of the 2^3T_1 corresponds to an He_2^+ state triplet coupled to a single electron in the other bond. If we write He_2^+ as $\ell_1\ \ell_1\ r_1$ and $\sigma_2 = \ell_2 + r_2$, then the wavefunction is $[\ell_1\ \ell_1\ (r_1\ \ell_2 + r_1\ r_2)\ \alpha\beta(\alpha\beta + \beta\alpha)]$ which is a state triplet coupled "across" the vacancy relative to our usual sense. Such states would be depicted

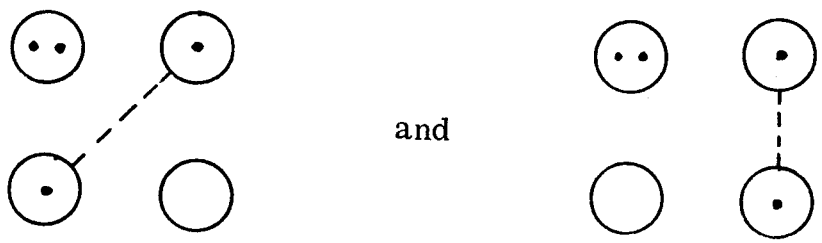

which is just another orientation for the A_2 state.

As an alternative way of viewing the positive and negative ion states, it is helpful to look at the states of He_2^+, H_2 and H_2^+. In He_2^+ the VB ground state is $\mathcal{A}[(\ell\ell r - rr\ell)\alpha\beta\alpha]$ which is equivalent to the MO wavefunction $\mathcal{A}[ggu\alpha\beta\alpha]$, where $g = \ell + r$, $u = \ell - r$, and ℓ and r may be thought of as atomic orbitals on the left and right centers. In the case of He_2^+ the first excited state is $\mathcal{A}[uug\alpha\beta\alpha]$. The energy splitting between these two states has a dependence on overlap which is $\frac{S}{1-S^2} \approx s$, for small s, $S = \langle \ell | r \rangle$. H_2^+ hs the same dependence for the splitting between the g and u states. For H_2, however, the first two states are $\ell r + r\ell$ and $\ell r - r\ell$, which represent a singlet and a triplet respectively. The singlet-triplet splitting has an overlap dependence which is $\frac{S^2}{1-S^2} \approx S^2$, for small s. In the region of low overlap, the splitting between the H_2 states will be less than the splitting between the states of either He_2^+ or H_2^+. Thus we should build up the positive and negative ion states by starting with the lowest state of H_2^+ and He_2^+ respectively, and then coupling these states with the singlet and triplet states of H_2 to form our picture. Both He_2^+ and H_2^+ are doublet states, so combining the doublet with the H_2 singlet gives only a doublet, but combining the doublet and triplet we can expect to get both doublet and quartet wavefunctions.

In Tables IV.7 and IV.8 we give the dominant terms in the CI wavefunctions for the positive and negative ion states. Consider first the negative ion states. The dominant configurations of the first two states ($^1A_1$ and A_2 component of $^2T_1$) are the same. They both correspond to structures

where 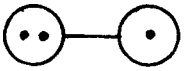 is the He_2^+ ground state while 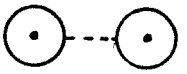 is the H_2 triplet state. For the ground state of the negative ion the coupling between the two structures is "triplet" so that the quartet state emerges as the ground state. The excited state corresponds to the same two structures "singlet" coupled to give a doublet state. The first configuration of the $^2T_1(A_2)$ is $\mathcal{A}[\sigma_1^2\sigma_2\sigma_1^*\sigma_2^*(.516\ \chi_1 - .429\ \chi_2)]$. If we permute the order of the electrons, then we obtain an expansion $\mathcal{A}[\sigma_1^2\sigma_2\sigma_2^*\sigma_1^*(.113\ \chi_1 - .662\ \chi_2)]$. χ_2 corresponds to the third and fourth electrons triplet coupled with the last electron coupled to form a doublet. Thus the dominant terms in the two states correspond directly with the structures given. The B_1 component of the $^2T_1$ state corresponds to the structure

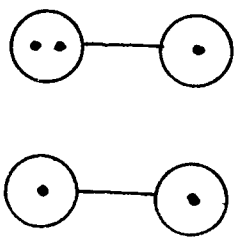

where 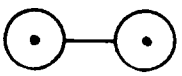 is just the singlet H_2 state. The B_2 component (not given in the Table) is the same but with the bonds interchanged

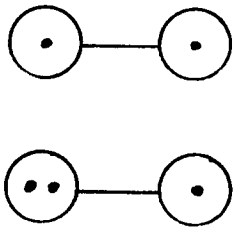

In the case of the positive ion, the relevant states are those of H_2 and H_2^+. The A_1 component of the $^2T_2$ state is a combination of structures such as

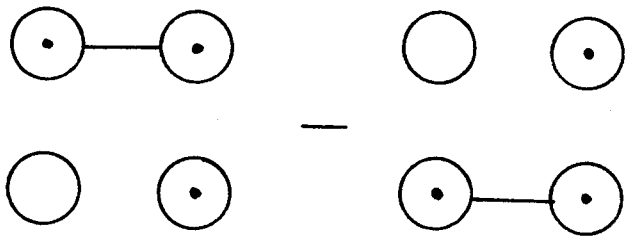

The B_1 component of the $^2T_2$ state is a combination of ionic H_2 states with the H_2^+ g or u function to give structures such as

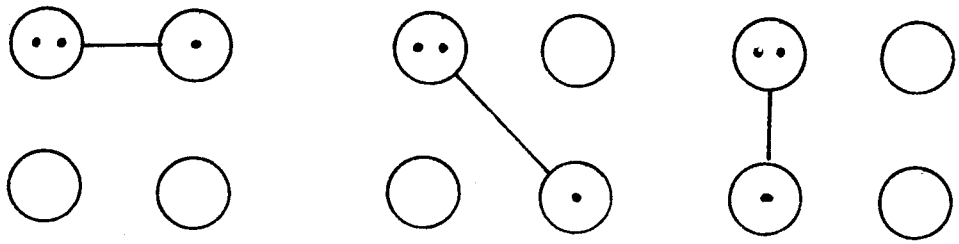

which is just He_2^+ back again. The quartet states of the positive vacancy arise from the various combinations of 3 electrons on the 4 centers high spin coupled.

One point which remains is the overall ordering of the positive and negative ion states of the vacancy. In the two cases the states are ordered almost exactly oppositely. A relatively straightforward analysis of these states is given in Appendix B. Here we will just give the results. First consider the quartet states of the positive ion. Suppose we construct the states from 4 equivalent localized orbitals, one on each center. We will label the orbitals a, b, c, d. If we start with one wavefunction, say $\mathcal{A}(bcd\,\alpha\alpha\alpha)$, then on appropriate rotation we produce the wavefunctions $\mathcal{A}(adc\,\alpha\alpha\alpha)$, $\mathcal{A}(dab\,\alpha\alpha\alpha)$, $\mathcal{A}(cba\,\alpha\alpha\alpha)$. These four wavefunctions can be used as the basis for a CI calculation which gives the result

$$E_{^4A_2} = A - \frac{3\tau}{1-3\sigma}$$

$$E_{^4T_1} = A + \frac{\tau}{1+\sigma}$$

where $\sigma = \langle a|b\rangle$ and $\tau = \langle a|h|b\rangle - \sigma\langle a|h|a\rangle$, in which h is the one electron part of the Hamiltonian. As explained in the Appendix, τ is expected to be negative while σ is of course positive. Thus the ordering of the states is $^4A_2$ <u>above</u> $^4T_1$. For the negative ion quartets, the wavefunctions are of the form $\mathcal{A}(a^2bcd\,\alpha\beta\alpha\alpha\alpha)$. The effect of the additional two functions is to cause a sign change in the matrix elements which lead to the τ and σ terms, thus the energy expressions become

$$E_{^4A_2} = A' + \frac{3\tau}{1+3\sigma}$$

$$E_{^4T_1} = A' + \frac{\tau}{1-\sigma}$$

where σ and τ have the same definition as above. Therefore the negative ion quartet states order $^4A_2$ below $^4T_1$. For the positive ion doublet states each spatial configuration (e.g., cdb) leads to two spin eigenfunctions resulting in eight wavefunctions. For the case of the spatial configuration cdb the two wavefunctions are of the form $\mathcal{A}[\text{cdb}\,(\alpha\beta\alpha - \beta\alpha\alpha)]$ and $\mathcal{A}[\text{cdb}\,(2\alpha\alpha\beta - \alpha\beta\alpha - \beta\alpha\alpha)]$, that is, singlet paired cd and triplet paired cd respectively. These two functions can be appropriately rotated as in the quartet case to give the eight wavefunctions. Going through the same process of evaluating matrix elements, constructing symmetry functions and evaluating the energy expression, one obtains

$$E_{^2T_2} = A + \frac{2\tau}{1+2\sigma}$$

$$E_{^2E} = A$$

$$E_{^2T_1} = A - \frac{2\tau}{1-2\sigma}$$

Thus given that τ is negative the states are ordered $^2T_2 < {}^2E < {}^2T_1$. What is even more interesting is that the overall order for the positive ion states

$$^2T_2 < {}^4T_1 < {}^2E < {}^2T_1 < {}^4A_2$$

is produced, and that is in the same order as found in the SD-CI

calculation. For the negative ion doublets we expect a sign change in the τ terms just as we found in going from positive ion quartets to negative ion quartets. The energy expressions one would expect are

$$E_{^2T_2} = A' - \frac{2\tau}{1 - 2\sigma}$$

$$E_{^2E} = A'$$

$$E_{^2T_1} = A' + \frac{2\tau}{1 - 2\sigma}$$

and thus the ordering of the states would invert relative to the positive ion. Therefore the expected overall ordering of the negative ion states is

$$^4A_2 < {}^2T_1 < {}^2E < {}^4T_1 < {}^2T_2 .$$

This is the calculated (SD-CI) order for the first three states, but the $^2T_2$ state is 0.5 eV below the $^4T_1$.

In the negative ion case we simply argued about the form of the energy expressions. We might expect to find extra exchange terms in the doublet states which would raise them relative to the quartet states. If we assume $\sigma \approx 0.2$ then we find that $\tau = -.56$ eV for the doublets and $\tau = -.86$ for the quartets using the SD-CI energy differences, which supports the assumption that there are additional positive terms entering into τ for the doublets.

The crucial step in the analysis is the fact that τ is negative, which we get from a simple VB analysis of the states of H_2^+. Thus we again find that relatively simple ideas about bonding can lead directly

to information such as the ordering of states in more complicated systems.

Calculations on the (111) surface complex using the DZ were performed using the minimum point geometry obtained from the STO-4G calculations. The energies obtained are reported in Table IV.9. These calculations give a vertical ionization potential of 7.32 eV and an electron affinity of -2.56 eV. The effect of correlating the lone pair in the negative ion would be expected to be 0.66 eV by comparison with CH_3 and CH_3^-. Also by comparison with CH_3, the outer C on the positive ion would tend to move even further into the plane while the negative ion would tend to move back out toward tetrahedral. We will use these calculations later to relate to the infinite crystal.

TABLE IV.1. Total energy of the diamond (111) surface complex as a function of the distance of the surface atom from the origin. The distance is in a.u. measured in the [111] direction. The energy is in a.u.

Distance	Energy
+0.1	-155.920295
0.0	-155.928168
-0.1	-155.932563
-0.1812	-155.933658
-0.2	-155.933607
-0.4	-155.926549

TABLE IV.2. GVB Calculations for the ^1E abd $^1T_2$ states of the neutral vacancy in diamond. The calculations are described in the text. The HF calculations of the $^5A_2$ state is included for comparison.

Calculation	Total Energy	C_1 [a]	C_2 [a]	ΔE [b]	S_{ab} [c]
$^5A_2$ HF (44 BF)	-158.091502	--	--	--	--
^1E GVB(2-PP) (44BF)	-158.125985	.8574	-.5147	-0.1109	.2498
$^1T_2$ GVB(2-PP) (44BF)	-157.917901	.9985	-.0550	-0.0016	.8955
$^1T_2$ GVB(1-PP) (12BF)	-157.887244	.9949	-.1004	-0.0037	.8167

a) Coefficients of the natural orbitals: $\phi_a \phi_b + \phi_b \phi_a = C_1 \phi_1 \phi_1 + C_2 \phi_2 \phi_2$.

b) Energy lowering due to the presence of the second NO.

c) Overlap of the GVB orbitals $S_{ab} = \langle \phi_a | \phi_b \rangle$.

Mulliken Populations for the two lowest singlet vacancy states.

Centers[d]	^1E	$^1T_2$ (44BF)
$C_{1,2}$	6.4876	6.2323
$C_{3,4}$	6.4876	6.8384
$H_{1,4}$	.8389	.7536
$H_{5,7,9,10}$	.8367	.7973
$H_{2,3}$	.8389	.8939
$H_{6,8,11,12}$	.8367	.8436

TABLE IV.3 SD-CI Calculations for the Singlet and Triplet States of the Neutral Vacancy. Total energies are in a.u., excitation energies are in eV.

T_d Designation	C.I. Total Energy for C_{2v} States (a.u.)				Excitation Energy (eV)	
	A_1	A_2	B_1	B_2	$E_i - E^1E$	$E_i - E^3T_1$
^1E	-158.143155	-158.141375			0.0	
$^1T_2$	-157.918377		-157.920279	-157.920277	6.06	
$^1A_1$	-157.857793				7.74	
$^1T_1$		-157.788279	-157.789065	-157.789065	9.62	
^1E	-157.752034	-157.752521			10.61	
$^1T_1$	-157.698606		-157.697631	-157.697626	12.09	
$^1T_1$		-157.581319	-157.582389	-157.582402	15.24	
$^3T_1$		-158.129483	-158.130655	-158.130654	0.33	0.0
$^3T_1$		-157.878047	-157.878570	-158.878570	7.18	6.85
$^3A_2$		-157.790852			9.56	9.24
^3E	-157.787813	-157.789379			9.60	9.27
$^3T_2$	-157.786745		-157.786382	-157.786382	9.68	9.35
$^3T_1$		-157.655491	-157.6 3507	-157.653507	13.28	12.95
$^3T_2$	-157.579551		-157.579648	-157.579663	15.31	14.98
$^5A_2$		-158.097289			1.20	0.88

TABLE IV.4 SD-CI Calculation for the Negative and Positive Charge States of the Vacancy.

T_d State	C.I. Total Energies for C_{2v} States (a.u.)				Excitation Energy (eV)	
Negative Ion	A_1	A_2	B_1	B_2	$E_i - E^4A_2$	$E_i - E^2T$
$^4A_2$		-158.079891			0.0	
$^4T_1$		-157.934094	-157.933344	-157.933341	3.98	
$^2T_1$		-158.052419	-158.052258	-158.052259	0.75	0.0
^2E	-157.986006	-157.986431			2.55	1.80
$^2T_2$	-157.954296		-157.954051	-157.954048	3.42	2.67
Positive Ion					$E_i - E^2T_1$	$E_i - E^4T_2$
$^2T_2$	-157.830864		-157.828494	-157.828494	0.0	
^2E	-157.708781	-157.704636			3.33	
$^2T_1$		-157.628305	-157.630060	-157.630059	5.44	
$^4T_1$		-157.735597	-157.737344	-157.739345	2.48	0.0
$^4A_2$		-157.563437			7.23	4.75

TABLE IV.5 Dominant Terms in the Configuration Interaction Wavefunctions for the First Singlet States of the Neutral Vacancy in Diamond. The term in parentheses by the state designation is the C_{2V} symmetry. The configurations are given in occupation number notation. The energy lowering ΔE is in millihartree (1 mh = .0272 eV).

State	Configuration[a]								Coefficient		Energy Lowering
	σ_1	σ_2	σ_1^*	σ_2^*	v_1	v_2	v_3	v_4	$C\chi_1$[b]	$C\chi_2$	ΔE[c]
$^1E(A_1)$	2	2	0	0	0	0	0	0	.695	-	222.9
	0	2	2	0	0	0	0	0	-.448	-	109.0
	2	0	0	2	0	0	0	0	-.448	-	109.0
	0	0	2	2	0	0	0	0	.259	-	45.2
	1	1	2	0	0	0	0	0	-.148	-	10.1
	1	1	0	2	0	0	0	0	-.148	-	10.1
$^1T_2(A_1)$	1	1	2	0	0	0	0	0	-.492	-	71.9
	1	1	0	2	0	0	0	0	.492	-	71.9
	2	0	0	2	0	0	0	0	.432	-	48.2
	0	2	2	0	0	0	0	0	-.432	-	48.2
	1	1	1	0	0	0	1	0	-.150	-.049	20.1
	1	1	0	1	0	0	0	1	.150	-.049	20.1
	2	0	2	0	0	0	0	0	-.129	-	10.0
	0	2	0	2	0	0	0	0	.129	-	10.0
	+ 16 configurations involving excitations to the virtuals										39.2

TABLE IV.5 Continued

	σ_1	σ_2	σ_1^*	σ_2^*	v_1	v_2	v_3	v_4	CX_1	CX_2	ΔE
$^1T_2(B_1)$	2	1	1	0	0	0	0	0	.790	--	187.7
	1	2	1	0	0	0	0	0	-.485	--	90.7
	1	0	1	2	0	0	0	0	.217	--	24.2
	1	1	1	0	1	0	0	0	-.137	.057	19.9
	2	1	0	0	0	0	1	0	.136	--	13.5
	1	2	0	0	0	0	1	0	-.115	--	0.3
	+ 8 configurations involving excitations to virtuals										23.0

a) The following notation is used for the functions
σ_1, σ_2 GVB 1st NO's corresponding to 1+2 and 3+4 respectively.
σ_1^*, σ_2^* GVB 2nd NO's corresponding to 1-2 and 3-4 respectively.
v_1, v_2 p-like virtual functions of types 1+2 and 3+4 respectively.
v_3, v_4 p-like virtual functions of types 1-2 and 3-4 respectively.
The C_{2v} symmetries of the functions are, in order, $a_1\, a_1\, b_1 b_2\, a_1\, a_1\, b_1\, b_2$.

b) Coefficients of the configuration by spin-eigenfunction. Doubly occupied orbitals are singlet coupled. The two electron singlet spin eigenfunction is $\frac{1}{\sqrt{2}}(\alpha\beta - \beta\alpha)$. The two 4 electron spin eigenfunctions are

$$X_1 = \tfrac{1}{2}(\alpha\beta\,\alpha\beta - \alpha\beta\,\beta\alpha + \beta\alpha\,\beta\alpha)$$

$$X_2 = \frac{1}{\sqrt{12}}(2\alpha\alpha\beta\beta - \beta\alpha\beta\alpha - \alpha\beta\,\alpha\beta + 2\,\beta\beta\,\alpha\alpha - \beta\alpha\,\alpha\beta)$$

c) The energy lowering is defined as the amount the energy would increase by deleting the configuration without adjusting the coefficients of the other configurations.

TABLE IV.6 Dominant terms in the configuration interaction wavefunctions for the first triplet states of the neutral vacancy in diamond. The table headings are explained in Table IV.5.

State	Configuration								Coefficient			
	σ_1	σ_2	σ_1^*	σ_2^*	v_1	v_2	v_3	v_4	$C\chi_1$[a]	$C\chi_2$	$C\chi_3$	ΔE
$1^3T_1(A_2)$	1	1	1	1	0	0	0	0	-.736	-.332	-.470	400.1
	2	0	1	1	0	0	0	0	-.242	--	--	25.2
	0	2	1	1	0	0	0	0	-.242	--	--	25.2
	1	1	0	1	0	0	1	0	-.037	-.005	-.018	1.5
	1	1	1	0	0	0	0	1	-.037	-.015	-.011	1.5
$1^3T_1(B_1)$	1	2	1	0	0	0	0	0	.833	--	--	306.1
	1	0	1	2	0	0	0	0	-.481	--	--	99.5
	2	1	1	0	0	0	0	0	-.251	--	--	21.4
	0	1	1	2	0	0	0	0	-.083	--	--	3.6
	1	1	1	0	0	1	0	0	.005	-.027	-.016	1.1
$2^3T_1(A_2)$	1	1	1	1	0	0	0	0	.293	-.422	-.597	44.8
	2	0	1	1	0	0	0	0	.388	--	--	27.0
	0	2	1	1	0	0	0	0	.388	--	--	27.0
	1	1	0	1	0	0	1	0	.079	-.083	-.016	7.9
	1	1	1	0	0	0	0	1	.079	.012	-.083	7.6
	0	1	1	1	1	0	0	0	.061	-.069	-.019	6.6
	1	0	1	1	0	1	0	0	.059	.044	-.009	5.3
	+ 10 configurations											26.2

TABLE IV.6 Continued

	σ_1	σ_2	σ_1^*	σ_2^*	v_1	v_2	v_3	v_4	$C\chi_1$	$C\chi_2$	$C\chi_3$	ΔE
$2^3T_1(B_1)$	2	1	1	0	0	0	0	0	.845			137.2
	1	1	0	1	1	0	0	0	-.042	.139	.086	21.9
	1	0	1	2	0	0	0	0	-.449	.116	-.158	16.6
	2	1	0	0	0	0	1	0	--	--	--	8.7
	+ 4 configurations											18.9

a) The 4 electron triplet spin eigenfunctions are

$$\chi_1 = \frac{1}{\sqrt{2}} (\alpha\beta\alpha\alpha - \beta\alpha\alpha\alpha)$$

$$\chi_2 = -\frac{1}{\sqrt{6}} (2\alpha\alpha\beta\alpha - \alpha\beta\alpha\alpha - \beta\alpha\alpha\alpha)$$

$$\chi_3 = \frac{1}{\sqrt{12}} (3\alpha\alpha\alpha\beta - \alpha\alpha\beta\alpha - \alpha\beta\alpha\alpha - \beta\alpha\alpha\alpha)$$

TABLE IV.7 Dominant terms in the CI wavefunctions for selected states of the Negative charge states of the vacancy in diamond. The table headings are explained in Table IV.5.

State	Configuration								Coefficient[a]					
	σ_1	σ_2	σ_1^*	σ_2^*	v_1	v_2	v_3	v_4	$C\chi_1$	$C\chi_2$	$C\chi_3$	$C\chi_4$	$C\chi_5$	ΔE
$^4A_2(A_2)$	2	1	1	1	0	0	0	0	.676	--	--	--	--	125.6
	1	2	1	1	0	0	0	0	-.676	--	--	--	--	125.6
	1	1	1	1	1	0	0	0	-.033	.106	+.063	-.002	--	14.1
	2	1	0	1	0	0	1	0	.121	--	--	--	--	10.6
	1	2	1	0	0	0	0	1	-.121	--	--	--	--	10.6
	+ 11 configurations													31.8
$^2T_1(A_2)$	2	1	1	1	0	0	0	0	.516	.429	--	--	--	168.6
	1	2	1	1	0	0	0	0	-.113	-.662	--	--	--	103.2
	1	1	1	1	1	0	0	0	.098	-.049	-.016	+.065	.037	17.6
	1	1	1	1	0	1	0	0	.005	.013	.108	.054	-.036	17.2
	2	1	0	1	0	0	1	0	.097	.073	--	--	--	12.8
	2	1	1	0	0	0	0	1	-.015	-.121	--	--	--	10.6
	+ 10 configurations													24.6

TABLE IV.7 Continued

	σ_1	σ_2	σ_1^*	σ_2^*	v_1	v_2	v_3	v_4	$C\chi_1$	$C\chi_2$	$C\chi_3$	$C\chi_4$	$C\chi_5$	ΔE
$^2T_1(B_1)$	2	2	1	0	0	0	0	0	.637	--	--	--	--	147.6
	2	0	1	2	0	0	0	0	-.513	--	--	--	--	144.6
	1	1	1	2	0	0	0	0	-.433	-.159	--	--	--	88.4
	1	1	1	1	0	0	0	1	.080	.041	.108	.039	.113	20.8
	1	2	0	1	1	0	0	0	.112	.071	--	--	--	17.1
	2	2	0	0	0	0	1	0	.122	--	--	--	--	11.8
	1	0	1	2	1	0	0	0	-.081	-.052	--	--	--	10.7
	+ 13 configurations													41.4

a) The five electron quartet spin eigenfunctions are

$$\chi_1 = \frac{1}{\sqrt{2}} (\alpha\beta\alpha\alpha\alpha - \beta\alpha\alpha\alpha\alpha)$$

$$\chi_2 = \frac{1}{\sqrt{6}} (2\alpha\alpha\beta\alpha\alpha - \alpha\beta\alpha\alpha\alpha - \beta\alpha\alpha\alpha\alpha)$$

$$\chi_3 = \frac{1}{\sqrt{12}} (3\alpha\alpha\alpha\beta\alpha - \alpha\alpha\beta\alpha\alpha - \alpha\beta\alpha\alpha\alpha - \beta\alpha\alpha\alpha\alpha)$$

$$\chi_4 = \frac{1}{\sqrt{20}} (4\alpha\alpha\alpha\alpha\beta - \alpha\alpha\alpha\beta\alpha - \alpha\alpha\beta\alpha\alpha - \alpha\beta\alpha\alpha\alpha - \beta\alpha\alpha\alpha\alpha)$$

The five electron doublet spin eigenfunctions may be found on pages 94-95 of ref. 25.

TABLE IV. 8 Dominant terms in the CI wavefunctions for selected states of the positive charge states of the vacancy in diamond. The table headings are explained in Table IV. 5.

State	Configuration								Coefficients		
	σ_1	σ_2	σ_1^*	σ_2^*	v_1	v_2	v_3	v_4	$C\chi_1$ [a]	$C\chi_2$	ΔE
$^2T_2(A_1)$	2	1	0	0	0	0	0	0	.635	-	124.2
	1	2	0	0	0	0	0	0	-.635	-	124.2
	1	0	0	2	0	0	0	0	.302	-	38.9
	0	1	2	0	0	0	0	0	-.302	-	38.9
	0	1	0	2	0	0	0	0	-.052	-	15.9
	1	0	2	0	0	0	0	0	-.052	-	15.9
$^2T_2(B)$	1	1	1	0	0	0	0	0	-.759	-.311	300.0
	0	2	1	0	0	0	0	0	-.485	-	82.9
	2	0	1	0	0	0	0	0	-.231	-	25.8
	0	0	1	2	0	0	0	0	+.175	-	14.9
$^4T_1(A_2)$	1	0	1	1	0	0	0	0	.706	-	89.1
	0	1	1	1	0	0	0	0	.706	-	89.1
$^4T_1(B_1)$	1	1	1	0	0	0	0	0	.997	-	827.4

a) The three electron doublet spin eigenfunctions are

$$\chi_1 = \frac{1}{\sqrt{2}} (\alpha\beta\alpha - \beta\alpha\alpha)$$

$$\chi_2 = -\frac{1}{\sqrt{6}} (2\alpha\alpha\beta - \alpha\beta\alpha - \beta\alpha\alpha)$$

TABLE IV.9. Hartree-Fock calculations for the positive, negative and neutral charge states of the diamond surface cluster.

	Total Energy	ϵ_π	ΔE
C_4H_9	-156.619345	-.358464	0.0
$C_4H_9^+$	-156.350446	--	0.268899
$C_4H_9^-(1)$[a]	-156.494034	+.096708	0.125311
$C_4H_9^-(2)$[a]	-156.525278	+.030258	0.094067

a) The negative ion calculation (1) used fixed CH bonds and carbon (1s) core while calculation (2) allowed full variational freedom.

FIGURE CAPTIONS

Figure IV.1. Total Energy of the (111) surface complex for diamond as a function of displacement of the apical carbon along the [111] direction. Positive distances are away from the surface.

Figure IV.2.1. The GVB orbitals for the ^1E state of the neutral vacancy in diamond. The spacing of the contour levels is .05 a.u. with dashed lines being negative. This spacing is used for all of the diamond orbitals. The centers are labelled according to Table III.1.

Figure IV.2.2. The natural orbitals of one bond pair of the ^1E state of the neutral vacancy in diamond.

Figure IV.3.1. The GVB orbitals for the $^1T_2$ state of the neutral vacancy in diamond.

Figure IV.3.2. A GVB orbital for the $^1T_2$ state of the neutral vacancy in diamond displayed in three planes. This shows the delocalization of this orbital onto a third center.

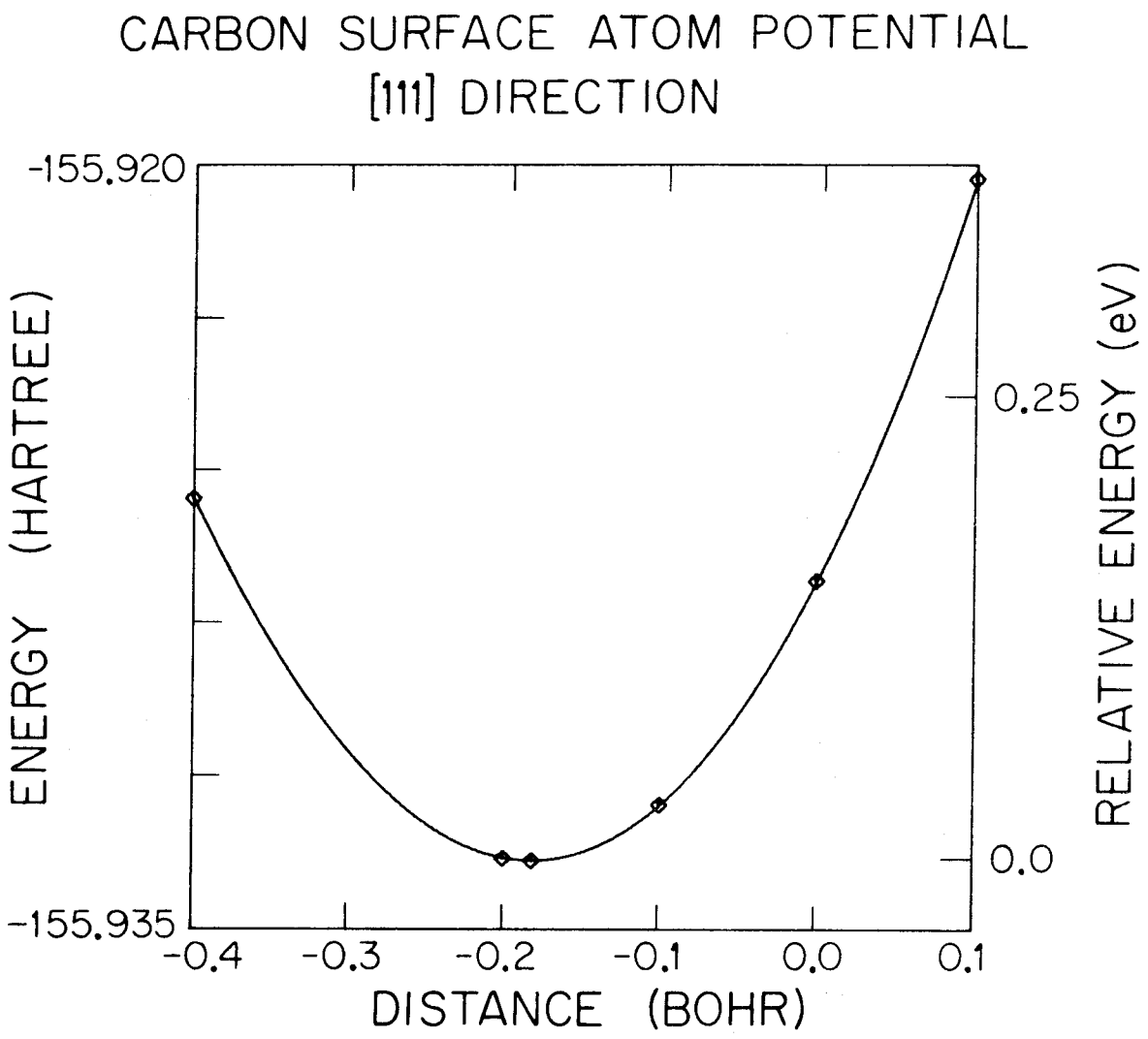
CARBON SURFACE ATOM POTENTIAL
[111] DIRECTION
-155.920
-155.935
ENERGY (HARTREE)
0.25
0.0
RELATIVE ENERGY (eV)
-0.4
-0.3
-0.2
-0.1
0.0
0.1
DISTANCE (BOHR)

Figure IV.1.

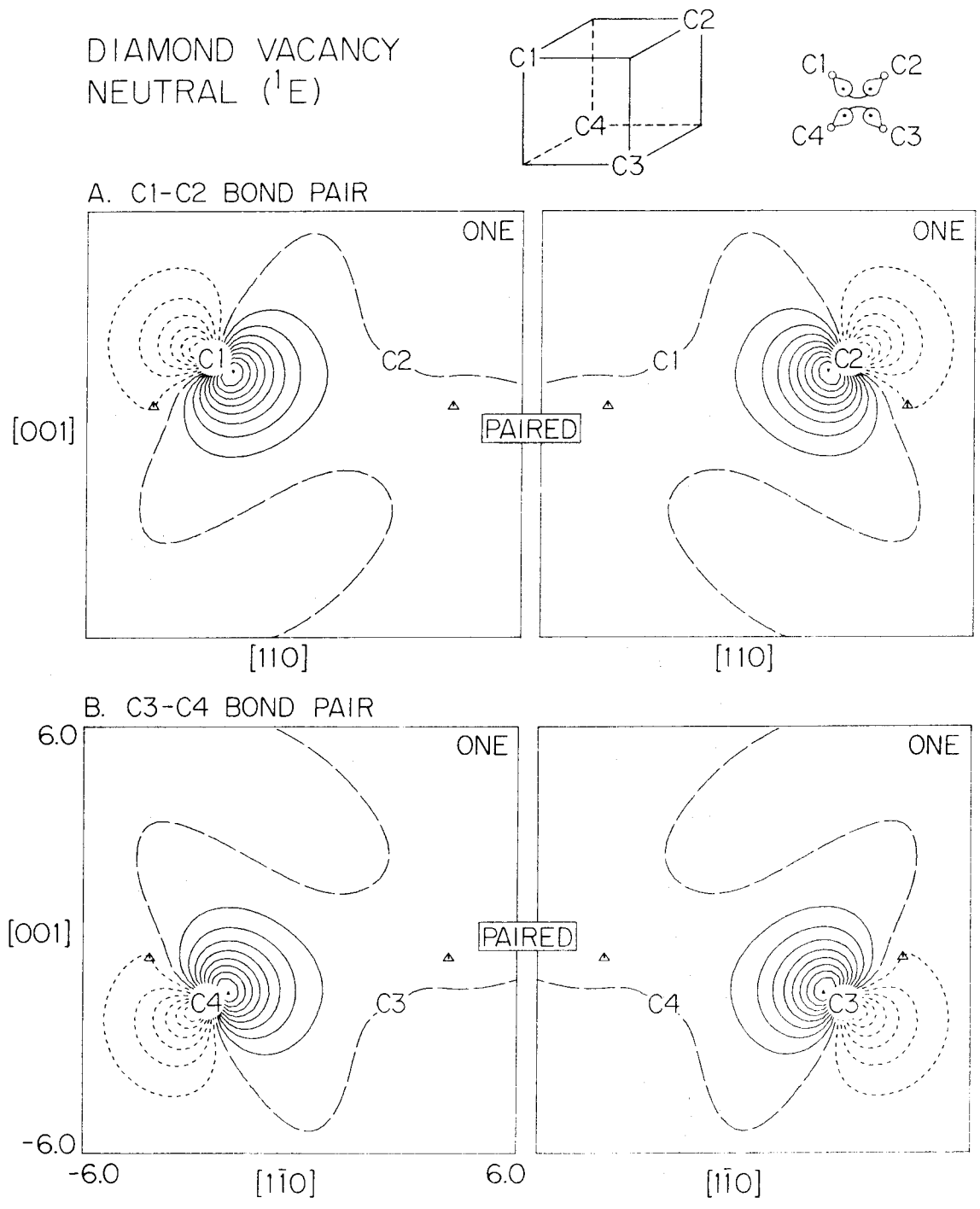
DIAMOND VACANCY
NEUTRAL (^{1}E)
C1
C2
C3
C4
A. C1-C2 BOND PAIR
ONE
ONE
PAIRED
[001]
[110]
[110]
B. C3-C4 BOND PAIR
6.0
-6.0
-6.0
6.0
[1$\bar{1}$0]
[1$\bar{1}$0]

Figure IV.2.1.

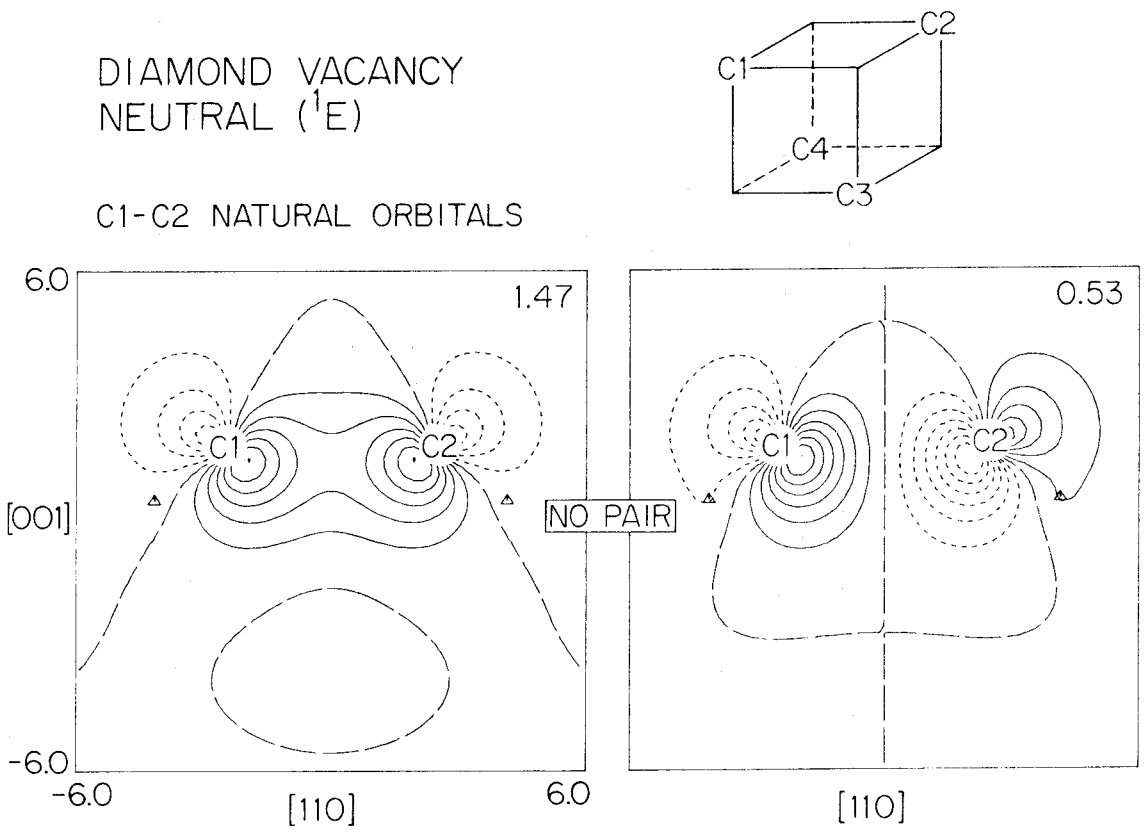
DIAMOND VACANCY
NEUTRAL (^{1}E)
C1-C2 NATURAL ORBITALS
C1
C2
C4
C3
6.0
1.47
C1
C2
[001]
NO PAIR
-6.0
-6.0
[110]
6.0
0.53
C1
C2
[110]

Figure IV.2.2.

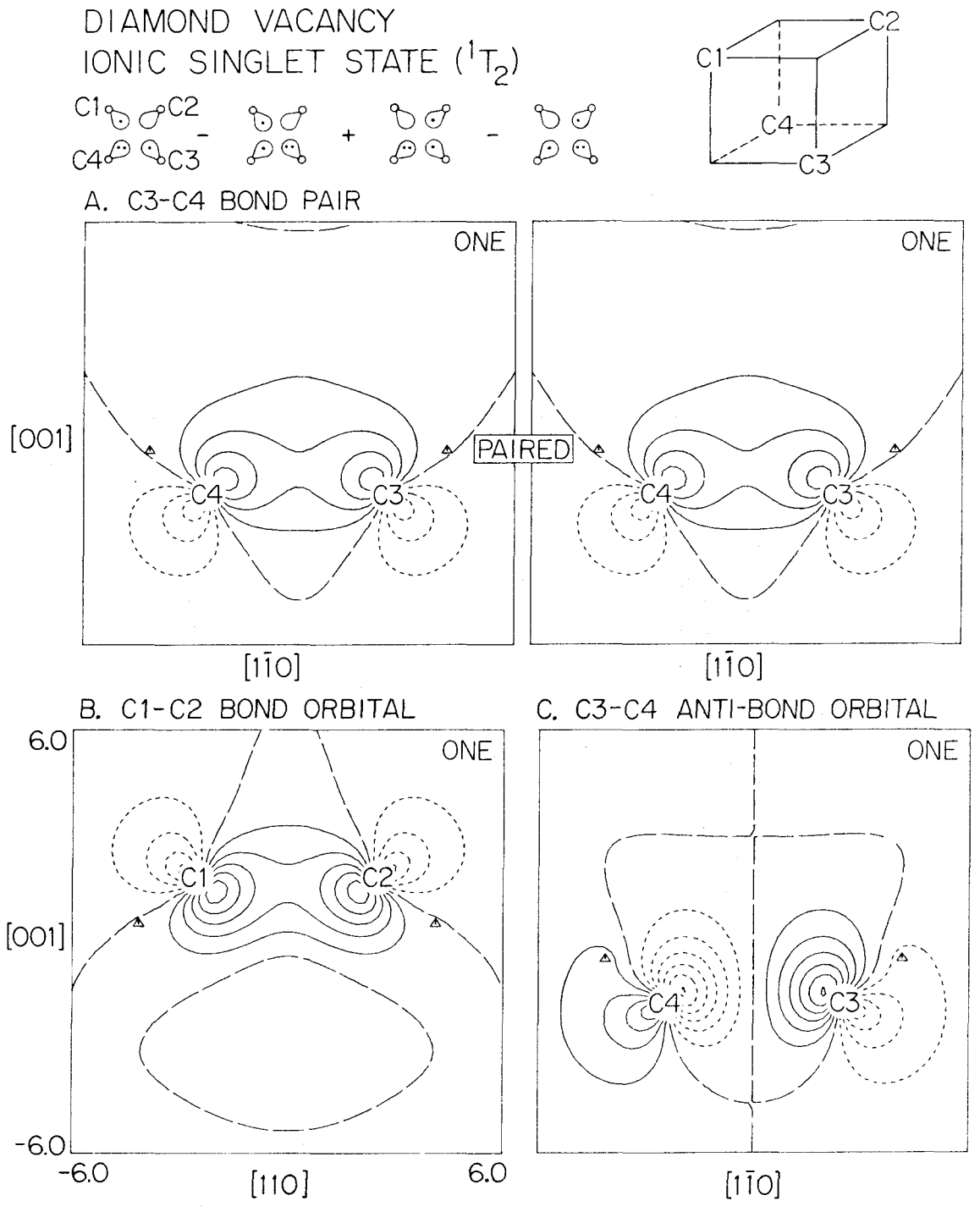
DIAMOND VACANCY
IONIC SINGLET STATE ($^1T_2$)
C1
C2
C4
C3
A. C3-C4 BOND PAIR
ONE
ONE
[001]
PAIRED
C4
C3
C4
C3
[1$\bar{1}$0]
[1$\bar{1}$0]
B. C1-C2 BOND ORBITAL
C. C3-C4 ANTI-BOND ORBITAL
6.0
ONE
ONE
C1
C2
[001]
C4
C3
-6.0
-6.0
[110]
6.0
[1$\bar{1}$0]

Figure IV.3.1.

DIAMOND VACANCY - IONIC SINGLET STATE ($^1T_2$)

A GVB BONDING ORBITAL

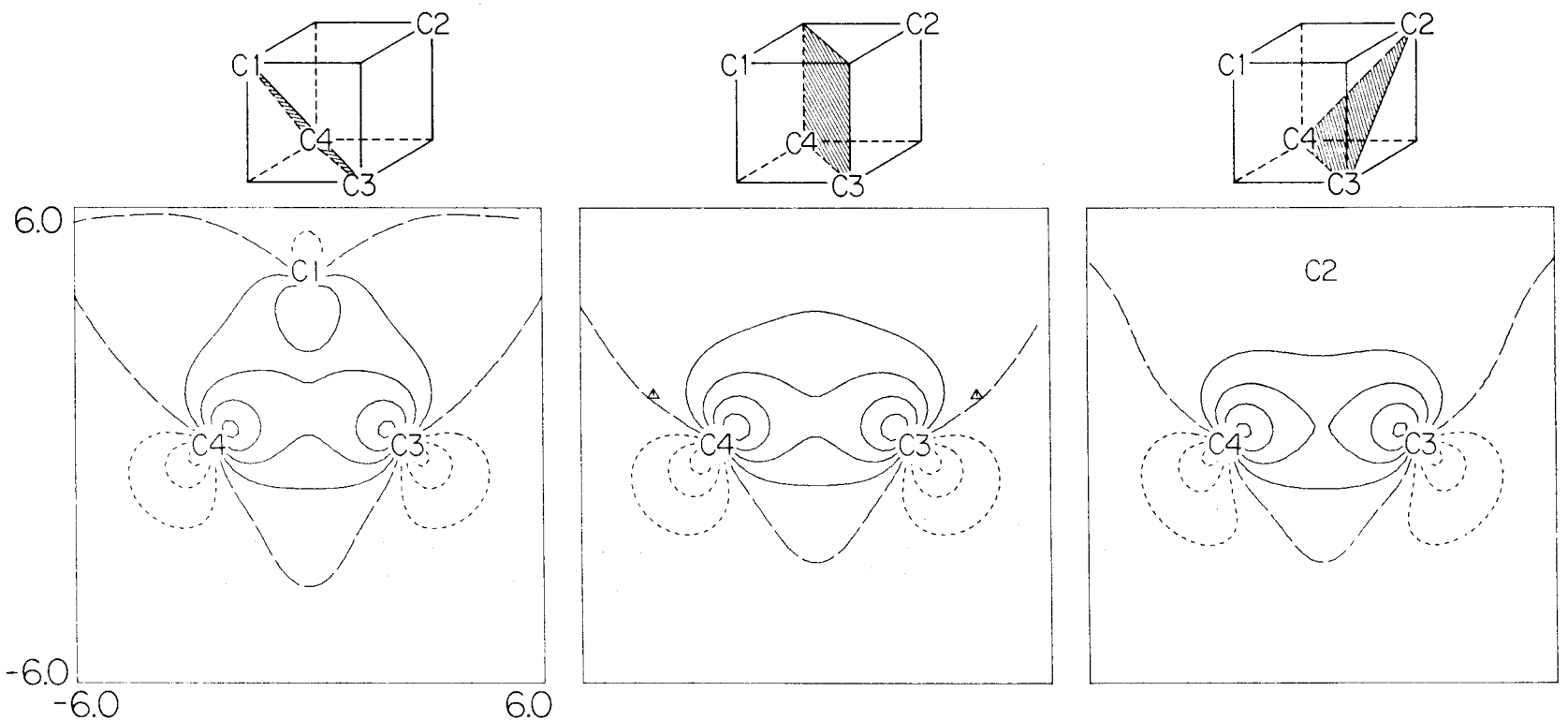

Figure IV.3.2.

V. SILICON VACANCY STATES

The states of the silicon vacancy were calculated in much the same way as the diamond vacancy states. In general we find that the description of these systems is the same. In fact, the only real difference is that in silicon the $^2T_2$ state of the positive ion is slightly above the $^4T_1$ while in diamond it was slightly below. Due to this similarity, the description here will parallel that of section IV and unless otherwise states, the basic considerations in doing the calculations are the same.

In the study of silicon it was decided to first obtain the optimum geometry by doing the Si_4H_9 calculations and then to look at the vacancy. Although the neutral vacancy in silicon is not observed experimentally, it is known that the positive and negative charge states of the vacancy exhibit Jahn-Teller distortion.[26] On the basis of a simple molecular orbital model Watkins argues that the neutral should exhibit a distortion to D_{2d} symmetry as well.[26] With our model complex we cannot accurately include such distortions without going to a valence force field model such as used by Larkins and Stoneham.[27] Instead we decided to solve for the symmetric outward distortion as before and to ignore other distortions as somewhat smaller. This set of calculations was done using the minimum basis set for silicon moving the surface atom along the [111] axis of the (111) surface complex as before. The results of this calculation are given in Table V.1 and in Figure V.1. The minimum was found to be at -0.159 a.u. along the [111] direction. Since the distance between (111) planes in the case of

silicon is 1.481 a.u., this represents a 10.8% relaxation into the crystal. Proceeding as before to calculate the "relaxed" positions we find that the silicon positions are given by (2.65775, 2.65775, 2.65775) in a.u. plus equivalent positions while the hydrogen positions are (4.23229, 4.23229, 0.96614) plus equivalent positions.

For the vacancy, an initial calculation was performed using the minimum basis set. The state solved for was the $^5A_2$. In this calculation the four dangling bond orbitals are quite distinct from the SiH bonds. The vectors for the SiH bonds were subsequently used in the calculations using the DZ basis. Since the inner function on the Si in the DZ basis is the same function as used in the MBS, and since a MBS hydrogen function was used in each case, the SiH vectors can simply be used without modification in the DZ calculation. Computationally this means that in the DZ calculation the SiH vectors were constrained to rotate among themselves (i.e., put into their own pseudo-symmetry class). At first the DZ calculations were performed with the SiH bonds "fixed." Later they were allowed full variational freedom in certain calculations.

In Tables V.2 and V.3 we present the results for a number of calculations on the vacancy. In addition to the ^1E and $^1T_2$ states, we calculated self-consistent wavefunctions for the 1^3T_1, the $^2T_2$ of the positive ion and the $^2T_1$ state of the negative vacancy. For the ^1E ground state three calculations were performed. The calculation was performed for both fixed and free SiH bonds as discussed above. In addition we calculated the ^1E state using the original (Table III.1)

geometry. This last calculation indicates that the energy change is quite small (.13 eV) in going from this geometry to the outwardly relaxed geometry. The effect of allowing the orbitals of the SiH bonds to readjust is a relatively large (~ .5 eV) effect. In Table V.3 we see that in the fixed SiH bond case the hydrogens each have 0.12 extra electron while for the free SiH case there is 0.09 extra electron on each hydrogen. Thus we see that the bonds are slightly ionic, which might affect the calculations of the other states. The GVB orbitals and the natural orbitals for the ^1E state are given in Figure V.2. The GVB orbitals are dangling bond orbitals polarized along the bond direction as in diamond.

In the case of the $^1T_2$ state, four different calculations were performed. Using the fixed SiH bonds we solved for this state as a GVB pair plus two singly occupied (orthogonal) singlet coupled orbitals. Comparing Tables IV.2 and V.2 we see that the description of the $^1T_2$ state is quite similar in diamond and silicon. Since the first NO of the GVB pair is essentially doubly occupied, the GVB pair was replaced by a doubly occupied HF orbital. The effect was to raise the energy only 2.5 mh = .07 eV. Thus viewing the state as a HF doubly occupied orbital (plus the two singlet orbitals) is quite reasonable. If the state is forced to be a covalent bond on one side and an ionic bond on the other, i.e., our first VB description, we find that the energy is raised by 54 mh = 1.47 eV. While this structure did contribute to the CI description of the $^1T_2$ state, it clearly is not a major component. In diamond we saw that the CH bond polarization of the

$^1T_2$ state amounted to ~ 1.0 eV due to electron transfer in the system. In the silicon case allowing the SiH bonds to rearrange gave a 25 mh = .68 eV energy lowering. From Table V.3 we see that there is ~ 1.5 electron transfer from the 1-2 bond to the 3-4 bond if we make the same division we did in diamond. In this case however we find that almost all of this effect (~ 1.4 electron) is due to the silicon. This is to be expected since the hydrogen basis is only a minimum basis description and thus will not allow for much polarization.

The orbitals for the $^1T_2$ state are given in Figure V.3. The orbitals are quite similar to the diamond case. Comparing the symmetric and anti-symmetric (g and u) singlet orbitals with the first and second NO's of the ^1E state, we see that the g orbital is slightly more diffuse than the second NO. This is to be expected since in the first case there is approximately one electron between the two centers (1 and 2) while in the second there are three electrons. The GVB orbitals are bonding orbitals between centers 3 and 4 but somewhat delocalized onto centers 1 or 2 as in the diamond case.

The excitation energy from ^1E to $^1T_2$ is 4.09 eV for the calculations using the fixed SiH bonds and 3.82 eV for the free SiH bonds. The difference is primarily due to the extra energy lowering in the $^1T_2$ state upon freeing the SiH bonds.

The $^3T_1$ state is an interesting contrast to the $^1T_2$ state. In this case, as can be seen in Figure V.4, the GVB pair is relatively unaffected by the presence of the triplet orbitals. The triplet orbitals themselves are simply the first and second natural orbitals of a GVB pair in bond 3-4. The difference is that they are triplet coupled and

each singly occupied. Thus we see that in this case the original VB analysis was quite reasonable. In Table V.3 we see that the differences in the pair CI coefficients and overlap between the ^1E pairs and the $^3T_1$ pair are small. The excitation energy of the $^3T_1$ state relative to the ^1E is 0.18 eV. We also find that the $^5A_2$ state is 0.44 eV above the ground state.

For the positive ion we simply removed an electron from one of the bond pairs. This gives one of the two VB structures which constitute the A_1 component of the $^2T_2$ state. The orbitals from this calculation are given in Figure V.5. The singly occupied orbital is like the first NO of a vacancy bond pair but is slightly more contracted. The orbitals of the bond pair are slightly delocalized toward the singly occupied orbital as well as along the bond direction. From Table V.2 we can see that the GVB orbitals are pointed more into the vacancy by the increase in the overlap, which is 0.42 for the positive ion bond pair as opposed to 0.23 for the vacancy bond pair. We find that the vertical ionization potential for the vacancy is 8.49 eV.

For the negative ion case we want to add an electron to the vacancy. Given that each bond is basically a g^2 configuration, we want a state which is g^2 in one and g^2u in the other. What was done computationally was to add an antisymmetric (b_1) orbital along the 1-2 bond. The orbitals for this state (B_1 component of the $^2T_1$) are given in Figure V.6. We see that in the bond where the b_1 orbital was added the GVB orbitals move toward each other. At the same time the b_1 orbital delocalizes back onto the hydrogens (only one of which is shown) out of the bond region. This effect can be seen in the

increased overlap (S_{ab} = 0.31) for the 1-2 bond. The second bond pair is relatively unaffected by the presence of the b_1 orbital. From Table V.2 we see that its overlap, CI coefficients and energy lowering are about the same as for a normal vacancy pair. We find that the electron affinity of the vacancy is negative with the value -7.56 eV. (We will find later that this is an excited state of the negative ion.)

The overall picture of the low-lying vacancy states in silicon, then, is (i) very much like the picture for diamond and (ii) well described qualitatively by the arguments given in sections II and IV. Our next task, then, is to explore the spectrum of states for the silicon vacancy. As in diamond, we performed SD-CI calculations over a 12 basis function space constructed exactly as in the diamond case. The GVB calculation from which the CI basis was derived used the fixed SiH bonds. In the SCF calculations we saw that using the fixed SiH bonds caused a 0.2 eV larger excitation energy for ^1E to $^1T_2$ than if the bonds were allowed to adjust. Thus for charge transfer types of excited states, we might expect these sorts of errors in the calculations. Since the GVB NO's used to construct the CI basis are C_{2v} symmetry functions and not T_d symmetry functions, the degeneracies for the T_d states will not be exact, as also happened in diamond. The SD-CI was done over the 12 basis function space using all members of the GVB-RCI as basic configurations.

The total energies for the singlet, triplet and quintet states from the SD-CI calculations are given in Table V.4. The overall structure predicted in Figure II.1 is maintained, but the ordering of

the $^3T_2$, ^3E and $^3A_2$ states is different between diamond and silicon. In diamond these three states are within a 0.12 eV energy range while for silicon they are ordered oppositely from diamond and occur in a 0.3 eV energy range. The splitting between the ^1E and $^3T_1$ states is 0.18 eV, which is the same as the SCF results. The energy difference between the ^1E and $^5A_2$ state is 0.60 eV, which is 0.16 eV more than in the SCF calculation. Comparing Tables V.4 and V.2 we see that the total CI energy lowering is the same for the ^1E, $^1T_2$ and $^3T_1$ states, 0.27 eV, while for the $^5A_2$ it is 0.11 eV. Thus the excitation energy from ^1E to $^1T_2$ is the same as the SCF value (for fixed SiH bonds).

The dominant terms in the CI wavefunctions for the first two singlet states are given in Table V.5. If we compare this with Table IV.5 we find that the CI description for diamond and silicon are very similar. The A_1 component of the ^1E state is just the GVB description with small terms that serve to change the shape of the orbitals. For the A_2 component we find that reordering the orbitals of the first configuration to give $\sigma_1 \sigma_1^* \sigma_2 \sigma_2^*$, one obtains the spin-eigenfunction $-0.04\ \chi_1 + .94\ \chi_2$. Thus this state is a triplet in each bond coupled into a singlet state.

The A_1 and B_1 components of the $^1T_2$ state are the same as we found in diamond. If we consider the A_1, B_1 and B_2 components at once, then what we have are three of the ways we can combine and He_2^+ state with an H_2^+ state. The B_1 and B_2 components are

B_1: 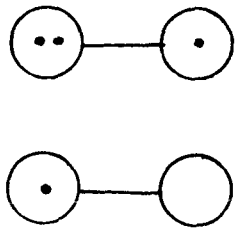

B_2: 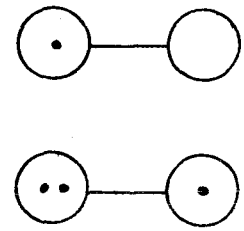

primarily while the A_1 state is a combination of structures such as

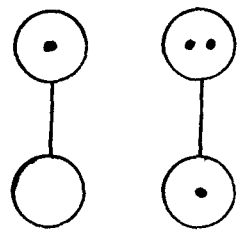

Each of these structures is corrected with the appropriate ionic structure such as

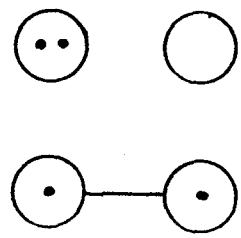

in the case of the B_1 component.

As described in section IV, the low-lying states of the vacancy derive in part from considering the states that can be constructed from two triplet coupled bonds. We saw previously that the A_2 component of the ^1E state is the singlet state arising from this combination.

If we reorder the orbitals for the A_2 component of the first triplet state (as given in Table V. 6) to the order $\sigma_1 \sigma_1^* \sigma_2 \sigma_2^*$, then the spin eigenfunction becomes $-.07\ \chi_1 + .809\ \chi_2 - .486\ \chi_3$, where χ_1, χ_2 and χ_3 are given in the table. If the state were a pure mixture of two triplets constituting a triplet, the spin eigenfunction would be $\sqrt{\frac{2}{3}}\ \chi_2 - \sqrt{\frac{1}{3}}\ \chi_3 = .816\ \chi_2 - .577\ \chi_3$. We can see, however, that this last spin coupling is the major component of the spin eigenfunction. The B_1 state is just the VB structure

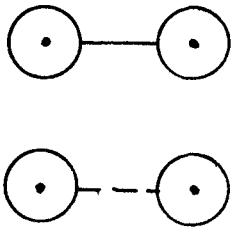

containing a bond pair and a triplet coupled pair. In the B_2 state we would find the same thing with the sides reversed.

In the case of the A_2 component of the 2^3T_1 state it is also helpful to reorder the orbitals as done above. The resulting spin eigenfunction is $-.520\ \chi_1 - .071\ \chi_2 + .587\ \chi_3$. The χ_1 terms leads, as in the diamond case, to a state which is a combination of an ionic singlet in one bond and a covalent triplet in the other, while the χ_3 term has the sides interchanged. That is, the state is a combination of structures of the form

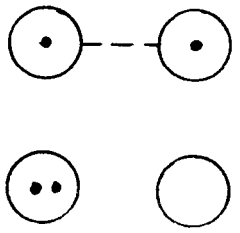

The B_1 component of the 2^3T_1 state can be viewed as a He_2^+ triplet coupled to a H_2^+. This sort of state can be depicted

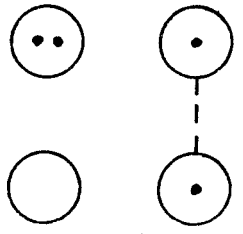

The calculated energies for the positive and negative ion states of the vacancy are given in Table V.7. Comparing the SCF calculation for the $^2T_2$ state of the positive ion with the CI result, we see that the energy is lowered by 33 mh = .91 eV. In the negative ion case the effect is 286 mh = 7.78 eV. This last result is quite surprising at first and will be discussed later.

In Table V.7 we see that ordering of the positive and negative ion states is just as predicted by the analysis given in Appendix B. The difference between silicon and diamond is that in silicon the $^4T_1$ of the negative ion is below the $^2T_2$ while in diamond it is not. In deriving the formulas obtained in Appendix B we made several qualitative arguments about the dependence of the integrals involved. The

difference in ordering is probably more an indication of the limits of the qualitative argument than anything else. One might attempt to argue on the basis of a difference in size of appropriate exchange integrals, however for the $^2T_2$ state there are 0.5 eV of energy lowerings due to excitation to the virtual orbitals, which is of the order of the differences involved.

Now we will consider the large energy difference between the SCF and CI wavefunctions. From the dominant terms in the B_1 component of the $^2T_2$ state (Table V.8) we see that the major contribution comes from a wavefunction of the form

$$\sigma_1^2 \sigma_1^* (C_1 \sigma_2^2 - C_2 \sigma_2^{*2}) = g_1^2 u_1 (C_1 g_2^2 - C_2 u_2^2)$$

which is the He_2^+ ground state in one bond and a GVB pair in the other bond. The selfconsistent calculation was for a state of the form

$$(C_1^1 \sigma_1^2 - C_2^1 \sigma_1^{*2}) (C_1^2 \sigma_2^2 - C_2^2 \sigma_2^{*2}) v_3$$

which is an excited state (v_3 being a b_1 symmetry virtual). The large energy difference, then, is due to the fact that we were not really comparing the same states.

Examining the other states given in Table V.8 we see that the A_2 components of the $^4A_2$ and $^2T_1$ states both arise from the structures

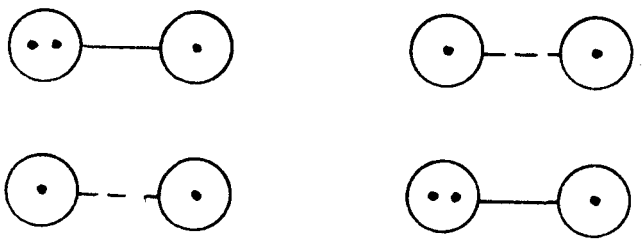

where in the quartet case the doublet (He_2^+ structure) and triplet are high spin coupled while in the doublet case they are "singlet" coupled to give a doublet. If we reorder the orbitals for the first configuration of the $^2T_1$ state we obtain the transformed spin eigenfunction $-.111\ \chi_1 - .692\ \chi_1$ which is just like the description found in the diamond case for the corresponding state.

The CI wavefunctions for the positive ion states are given in Table V.9. Once again we see that the A_2 component of the $^2T_2$ state is the resonant combination

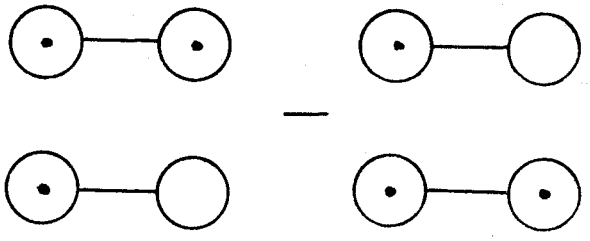

which is a GVB pair in one bond and a singly occupied orbital in the other. The GVB calculation for this state was a calculation for just one of two structures in the wavefunction. Since the dominant terms (> 1 mh) are simply the two GVB structures, we could say that the .91 eV energy difference between the SCF and CI calculations is stabilization due to allowing both structures, i.e., the resonance energy. The B_1 component of the $^2T_2$ state can be viewed as a triplet in one bond coupled to a single electron in the other. The positive ion quartets are simply the possible combinations of three electrons in four orbitals high spin coupled.

Thus we find that the vacancy states in diamond and silicon

are very similar. The differences that do occur are small and probably arise from minor differences in overlaps and interaction integrals. Overall we find that the use of relatively simple VB arguments leads to explanations of the form of the wavefunctions for the various states and provides a reasonable idea of the ordering of the energy levels.

TABLE V.1. Total energy of the Si (111) surface complex as a function of the position of the surface atom taken in the [111] direction. The origin is for tetrahedral bond angles, positive is away from the surface. All quantities are in Hartree atomic units.

Distance in [111]	Energy
0.2	-19.909681
0.0	-19.915003
-0.2	-19.916103
-0.4	-19.913491
-0.159[a]	-19.916200

a) The calculated minimum.

TABLE V.2. GVB calculations for various states of the vacancy in silicon. The calculations are described in the text. All quantities are in Hartree atomic units.

	State	SiH[d]	Energy	C_1[a]	C_2[a]	ΔE[b]	S_{ab}	Comments
1.	^1E	Fixed[d]	-21.476647	.846215	-.532842	.071860	.226495	Relaxed Si Positions
2.	^1E	Fixed	-21.471674	.862486	-.506080	.065916	.260423	Tetrahedral Si Positions
3.	^1E	Free	-21.491605	.848504	-.529188	.073275	.231775	Relaxed Si Positions
4.	$^1T_2$	Fixed	-21.3264	.992907	-.118885	.003186	-	
5.	$^1T_2$	Fixed	-21.272471	.846567	-.532282	.071770	.227932	Fixed Bond Pair
6.	$^1T_2$	Fixed	-21.323928	-	-	-	-	HF Bond Pair
7.	$^1T_2$	Free	-21.351058	.996387	-.084930	.001966	.842913	
8.	$^3T_1$	Fixed	-21.470127	.871873	-.489733	.062499	.280053	
9.	$^2T_2$	Fixed	-21.164489	.925994	-.377537	.039469	.420742	Positive Ion
10.	$^2T_1$	Fixed	-21.198923	.834376	-.551196	.073831	.204378	Negative Ion Pair 1
				.884880	-.465819	.052653	.310255	Negative Ion Pair 2
11.	$^5A_2$	Fixed	-21.460531	-	-	-	-	

a) Coefficients of the natural orbitals: $\phi_a \phi_b + \phi_b \phi_a = C_1 \phi_1 \phi_2 + C_2 \phi_2 \phi_2$.

b) Energy lowering due to the presence of the second NO. This is the amount the energy would increase if the second term in the NO expansion were deleted with the other orbitals held constant.

c) Overlap of the GVB orbitals, $S_{ab} = \langle \phi_a | \phi_b \rangle$.

d) Fixed implies that the SiH bonds come from a MBS calculation of the ^1E state.

TABLE V.3. Mulliken Populations for some of the GVB calculations in Table V.2. The numbers on the left refer to the appropriate row of Table V.2. The center numbers are with reference to Table III.1.

	State	$Si_{1,2}$	$Si_{3,4}$	$H_{1,4}$	$H_{5,7,9,10}$	$H_{2,3}$	$H_{6,8,11,12}$
1.	^1E	3.632	3.632	1.120	1.124	1.120	1.124
2.	^1E	3.623	3.623	1.122	1.127	1.122	1.127
3.	^1E	3.710	3.710	1.096	1.097	1.096	1.097
6.	$^1T_2$	3.245	4.009	1.118	1.125	1.129	1.125
7.	$^1T_2$	3.351	4.071	1.077	1.092	1.115	1.101

TABLE V.4. SD-CI Calculations for the singlet and triplet states of the neutral vacancy in Silicon. Total Energies are in a.u., excitation energies are in eV.

T_d Designation	CI Total Energies for C_{2V} States (a.u.)				Excitation Energies (eV)	
	A_1	A_2	B_1	B_2	$E_i - E_{^1E}$	$E_i - E_{^3T_1}$
^1E	-21.486363	-21.485933			0.00	
$^1T_2$	-21.335833		-21.336575	-21.336575	4.08	
$^1A_1$	-21.290872				5.31	
$^1T_1$		-21.258426	-21.258401	-21.258402	6.20	
^1E	-21.236703	-21.237016			6.78	
$^1T_2$	-21.195963		-21.195857	-21.195858	7.90	
1^3T_1		-21.478894	-21.480096	-21.480096	0.18	0.00
2^3T_1		-21.304564	-21.315541	-21.315539	4.74	4.56
$^3T_2$	-21.255113		-21.254923	-21.254923	6.29	6.11
^3E	-21.249408	-21.248464			6.45	6.28
$^3A_2$		-21.244475			6.58	6.40
3^3T_1		-21.162360	-21.174500	-21.174502	8.59	8.41
$^5A_2$		-21.464144			0.60	0.42

TABLE V.5. Dominant terms in the Configuration Interaction wavefunctions for the lower singlet states of the neutral vacancy in Silicon. The term in parentheses by the state designation is the C_{2V} symmetry used. The configurations are given in occupation number formalism. The energy lowering, ΔE, is in millihartree (1 mh = .0272 eV).

State	Configuration[a]								Coefficient[b]		Energy[c] Lowering
$^1E\ (A_1)$	σ_1	σ_2	σ_1^*	σ_2^*	v_1	v_2	v_3	v_4	C_{χ_1}	C_{χ_2}	ΔE
	2	2	0	0	0	0	0	0	.682	-	134.0
	0	2	2	0	0	0	0	0	-.456	-	68.9
	2	0	0	2	0	0	0	0	-.456	-	68.9
	0	0	2	2	0	0	0	0	.277	-	31.0
	1	1	0	2	0	0	0	0	-.140	-	5.4
	1	1	2	0	0	0	0	0	-.140	-	5.4
$^1E\ (A_2)$	1	1	1	1	0	0	0	0	-.830	.433	411.1
	0	2	1	1	0	0	0	0	-.245	-	16.5
	2	0	1	1	0	0	0	0	-.244	-	16.5
$^1T_2\ (A_1)$	1	1	0	2	0	0	0	0	.505	-	39.9
	1	1	2	0	0	0	0	0	-.505	-	39.9
	0	2	2	0	0	0	0	0	-.449	-	28.4
	2	0	0	2	0	0	0	0	.449	-	28.4
	0	2	0	2	0	0	0	0	.124	-	5.4
	2	0	2	0	0	0	0	0	-.124	-	5.3
	1	1	0	1	0	0	0	1	-.083	-.022	5.3
	1	1	1	0	0	0	1	0	-.083	-.022	5.3
	+ 12 configurations[d]										18.0

TABLE V.5. Continued

	σ_1	σ_2	σ_1^*	σ_2^*	v_1	v_2	v_3	v_4	C_{χ_1}	C_{χ_2}	ΔE
$^1T_2(B_1)$	2	1	1	0	0	0	0	0	-.806	-	108.2
	1	2	1	0	0	0	0	0	.487	-	52.8
	1	0	1	2	0	0	0	0	-.333	-	16.0
	1	1	1	0	1	0	0	0	.098	-.040	8.4
	2	1	0	0	0	0	1	0	-.077	-	4.0
	+ 6 configurations[d]										15.5

a) The followin notation is used for the functions
σ_1, σ_2 GVB 1st NO's corresponding to 1+2 and 3+4 respectively
σ_1^*, σ_2^* GVB 2nd NO's corresponding to 1-2 and 3-4 respectively
v_1, v_2 p-like virtual functions of types 1+2 and 3+4
v_3, v_4 p-like virtual functions of types 1-2 and 3-4
The C_{2V} symmetries of the functions are, in order, $a_1a_1b_1b_2a_1a_1b_1b_2$. The actual orbital ordering used in the CI is $\sigma_2\sigma_1\sigma_1^*\sigma_2^*v_1v_2v_3v_4$ so the coefficients of spin eigenfunctions refer to this ordering.

b) Coefficients of the configuration by spin eigenfunction. Doubly-occupied orbitals are singlet coupled. The two four electron singlet spin eigenfunctions are

$$\chi_1 = \tfrac{1}{2}(\alpha\beta\alpha\beta - \alpha\beta\beta\alpha - \beta\alpha\alpha\beta + \beta\alpha\beta\alpha)$$

$$\chi_2 = \frac{-1}{\sqrt{12}}(2\alpha\alpha\beta\beta - \beta\alpha\beta\alpha - \alpha\beta\beta\alpha + 2\beta\beta\alpha\alpha - \beta\alpha\alpha\beta - \alpha\beta\alpha\beta)$$

c) The energy lowering is defined as the amount the energy would increase by deleting the configuration without adjusting the coefficients of the other configurations.

d) These configurations involve excitations from the dominant configurations, usually a single excitation to the virtual of the same symmetry, which serve to modify the shapes of the orbitals slightly.

TABLE V.6. Dominant terms in the Configuration Interaction wavefunctions for the triplet states of the neutral vacancy in silicon. The table headings are explained in Table V.5.

State	Configuration								Coefficient[a]			Energy Lowering
	σ_1	σ_2	σ_1^*	σ_2^*	v_1	v_2	v_3	v_4	C_{χ_1}	C_{χ_2}	C_{χ_3}	ΔE
$1^3T_1(A_2)$	1	1	1	1	0	0	0	0	.736	-.344	-.486	246.5
	0	2	1	1	0	0	0	0	.225	-	-	13.3
	2	0	1	1	0	0	0	0	.225	-	-	13.3
$1^3T_1(B_1)$	1	2	1	0	0	0	0	0	.826	-	-	183.6
	1	0	1	2	0	0	0	0	-.504	-	-	66.3
	2	1	1	0	0	0	0	0	-.229	-	-	11.1
	0	1	1	2	0	0	0	0	-.088	-	-	2.4
$2^3T_1(A_2)$	1	1	1	1	0	0	0	0	.322	.415	.587	18.8
	2	0	1	1	0	0	0	0	.407	-	-	17.0
	0	2	1	1	0	0	0	0	.407	-	-	17.0
	0	1	1	1	1	0	0	0	-.029	-.011	.076	3.9
	1	0	1	1	0	1	0	0	-.016	-.009	.084	3.9
$2^3T_1(B_1)$	2	1	1	0	0	0	0	0	-.811	-	-	67.1
	1	0	1	2	0	0	0	0	.485	-	-	9.2
	0	1	1	2	0	0	0	0	.228	-	-	7.9
	1	1	1	0	0	0	0	0	-.019	.026	.101	7.5

a) The 4 electron triplet spin eigenfunctions are

$$\chi_1 = \frac{1}{\sqrt{2}} (\alpha\beta\alpha\alpha - \beta\alpha\alpha\alpha)$$

$$\chi_2 = -\frac{1}{\sqrt{6}} (2\alpha\alpha\beta\alpha - \alpha\beta\alpha\alpha - \beta\alpha\alpha\alpha)$$

$$\chi_3 = \frac{1}{\sqrt{12}} (3\alpha\alpha\alpha\beta - \alpha\alpha\beta\alpha - \alpha\beta\alpha\alpha - \beta\alpha\alpha\alpha)$$

TABLE V.7. SD-CI Calculations for the negative and positive charge states of the vacancy in Silicon. Total energies are in a.u., excitation energies are in eV.

T_d Designation	C.I. Total Energies for C_{2v} States (a.u.)				Excitation Energies (eV)	
Negative Ion	A_1	A_2	B_1	B_2	$E_i - E_{^4A_2}$	$E_i - E_{^2T_2}$
$^4A_2$		-21.508084			0.0	
$^4T_1$		-21.414425	-21.413793	-21.413793	2.56	
$^2T_1$		-21.474534	-21.484965	-21.484982	0.72	0.00
^2E	-21.444596	-21.429629			1.93	1.21
$^2T_2$	-21.417331		-21.400728	-21.400984	2.77	2.04
Positive Ion					$E_i - E_{^2T_2}$	$E_i - E_{^4T_1}$
$^2T_2$	-21.198590		-21.198052	-21.198051	0.00	
^2E	-21.124796	-21.124198			2.01	
$^2T_1$		-21.075720	-21.075992	-21.075992	3.33	
$^4T_1$		-21.148843	-21.145964	-21.151362	1.35	0.00
$^4A_2$		-21.039080			4.33	2.98

TABLE V.8. Dominant terms in the Configuration Interaction wavefunctions for selected states of the negatively charged vacancy. The table headings are explained in Table V.5.

State	Configuration								Coefficients[a]				Energy Lowering
	σ_1	σ_2	σ_1^*	σ_2^*	v_1	v_2	v_3	v_4	C_{χ_1}	C_{χ_2}	C_{χ_3}	C_{χ_4}	ΔE
$^4A_2(A_2)$	1	2	1	1	0	0	0	0	.695	-	-	-	68.1
	2	1	1	1	0	0	0	0	-.695	-	-	-	68.0
	1	1	1	1	1	0	0	0	.015	-.021	-.014	.081	5.1
	1	1	1	1	0	1	0	0	-.019	.012	.028	.063	3.7
	1	2	1	0	0	0	0	1	-.059	-	-	-	2.4
	2	1	0	1	0	0	1	0	.059	-	-	-	2.4
$^2T_1(A_2)$	2	1	1	1	0	0	0	0	-.543	-.441	-	-	92.7
	1	2	1	1	0	0	0	0	.111	.692	-	-	41.8
	1	2	1	0	0	0	0	1	-.006	-.071	-	-	3.2
	2	1	0	1	0	0	1	0	-.006	-.071	-	-	3.2
$^2T_1(B_1)$	2	2	1	0	0	0	0	0	.696	-	-	-	108.5
	2	0	1	2	0	0	0	0	-.552	-	-	-	96.2
	1	1	1	2	0	0	0	0	-.385	.140	-	-	34.5
	1	2	1	0	1	0	0	0	+.010	.092	-	-	6.3
	1	0	1	2	1	0	0	0	-.008	-.065	-	-	3.7

a) The three electron doublet spin eigenfunctions are

$$\chi_1 = \frac{1}{\sqrt{2}} (\alpha\beta\alpha - \beta\alpha\alpha)$$

$$\chi_2 = -\frac{1}{\sqrt{6}} (2\alpha\alpha\beta - \alpha\beta\alpha - \beta\alpha\alpha)$$

The five electron quartet spin eigenfunctions are

TABLE V.8. Continued

$$\chi_1 = \frac{1}{\sqrt{2}} (\alpha\beta\alpha\alpha\alpha - \beta\alpha\alpha\alpha\alpha)$$

$$\chi_2 = \frac{1}{\sqrt{6}} (2\alpha\alpha\beta\alpha\alpha - \alpha\beta\alpha\alpha\alpha - \beta\alpha\alpha\alpha\alpha)$$

$$\chi_3 = \frac{1}{\sqrt{12}} (3\alpha\alpha\alpha\beta\alpha - \alpha\alpha\beta\alpha\alpha - \alpha\beta\alpha\alpha\alpha - \beta\alpha\alpha\alpha\alpha)$$

$$\chi_4 = \frac{1}{\sqrt{20}} (4\alpha\alpha\alpha\alpha\beta - \alpha\alpha\alpha\beta\alpha - \alpha\alpha\beta\alpha\alpha - \alpha\beta\alpha\alpha\alpha - \beta\alpha\alpha\alpha\alpha)$$

TABLE V.9. Dominant terms in the Configuration Interaction wavefunctions for selected states of the positively charged vacancy in silicon. The table headings are explained in Table V.5.

State	Configuration								Coefficient[a]		Energy Lowering
	σ_1	σ_2	σ_1^*	σ_2^*	v_1	v_2	v_3	v_4	C_{χ_1}	C_{χ_2}	ΔE
$^2T_2(A_1)$	1	2	0	0	0	0	0	0	.629	-	76.1
	2	1	0	0	0	0	0	0	-.629	-	76.0
	1	0	0	2	0	0	0	0	-.313	-	25.1
	0	1	2	0	0	0	0	0	.313	-	25.1
$^2T_2(B_1)$	1	1	1	0	0	0	0	0	.759	-.318	182.7
	0	2	1	0	0	0	0	0	.482	-	51.1
	2	0	1	0	0	0	0	0	.220	-	14.5
	0	0	1	2	0	0	0	0	-.185	-	10.0
$^4T_2(A_2)$	0	1	1	1	0	0	0	0	.719	-	63.7
	1	0	1	1	0	0	0	0	.686	-	52.8
	0	0	1	1	1	0	0	0	.539	-	2.0
	0	0	1	1	0	1	0	0	.499	-	1.9
$^4T_2(B_1)$	1	1	1	0	0	0	0	0	.997	-	574.8

a) The three electron doublet spin eigenfunctions are

$$\chi_1 = \frac{1}{\sqrt{2}} (\alpha\beta\alpha - \beta\alpha\alpha)$$

$$\chi_2 = -\frac{1}{\sqrt{6}} (\alpha\alpha\beta - \alpha\beta\alpha - \beta\alpha\alpha)$$

FIGURE CAPTIONS

Figure V.1. Total Energy of the (111) surface complex for silicon as a function of displacement of the apical silicon along the [111] direction. Positive distances are away from the surface.

Figure V.2.1. The GVB orbitals for the ^1E state of the neutral vacancy in silicon. The spacing of the contour lines is .03 a.u. with dashed lines being negative. This spacing is used for all of the silicon orbitals. The centers are labelled according to Table III.1.

Figure V.2.2. The natural orbitals of one bond pair of the ^1E state of neutral vacancy in silicon.

Figure V.3.1. The GVB orbitals of the $^1T_2$ state of the neutral vacancy in silicon.

Figure V.3.2. A GVB orbital for the $^1T_2$ state of the neutral vacancy in silicon displayed in three planes. This shows the delocalization of this orbital onto a third center.

Figure V.4. The GVB orbitals of the $^3T_1$ state of the neutral vacancy in silicon.

Figure V.5. The GVB orbitals of the $^2T_2$ state of the silicon vacancy positive ion.

FIGURE CAPTIONS (continued)

Figure V.6. The GVB orbitals of the $^2T_1$ state of the silicon vacancy negative ion.

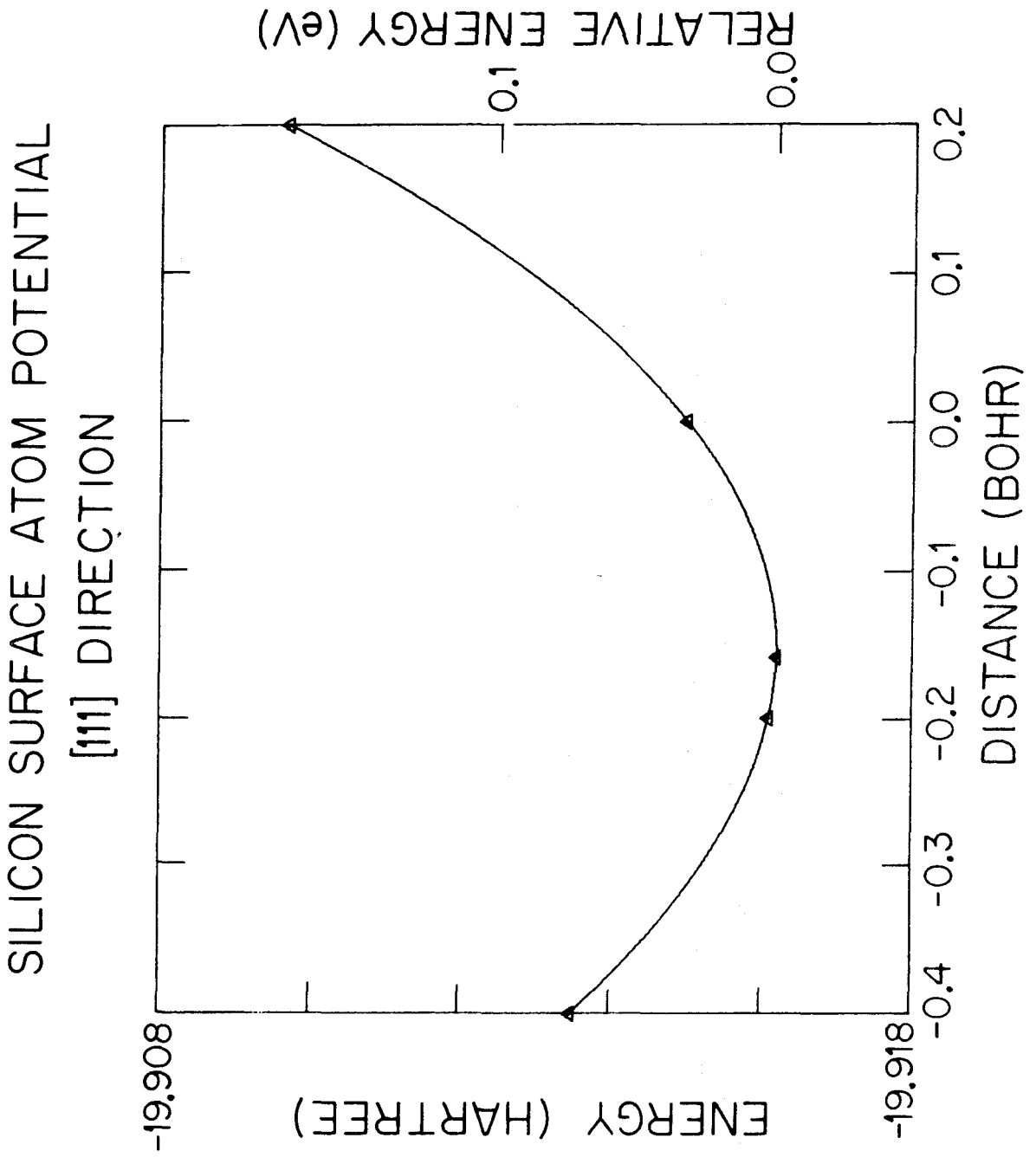
SILICON SURFACE ATOM POTENTIAL
[111] DIRECTION
ENERGY (HARTREE)
RELATIVE ENERGY (eV)
DISTANCE (BOHR)
-19.908
-19.918
0.1
0.0
0.2
0.1
0.0
-0.1
-0.2
-0.3
-0.4

Figure V.1.

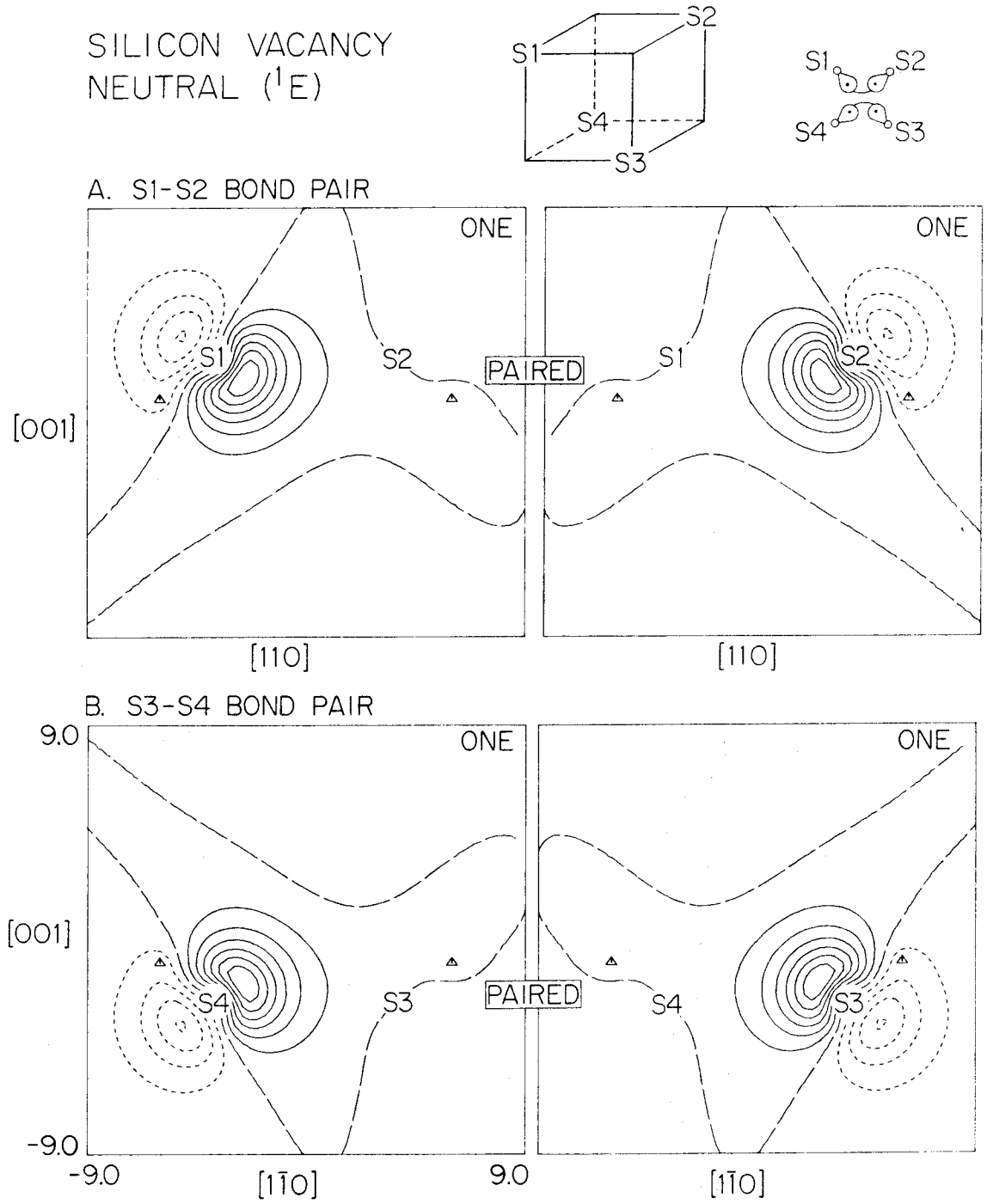
SILICON VACANCY
NEUTRAL (^{1}E)
S1
S2
S3
S4
A. S1-S2 BOND PAIR
ONE
PAIRED
[001]
[110]
B. S3-S4 BOND PAIR
9.0
-9.0
[1$\bar{1}$0]

Figure V.2.1.

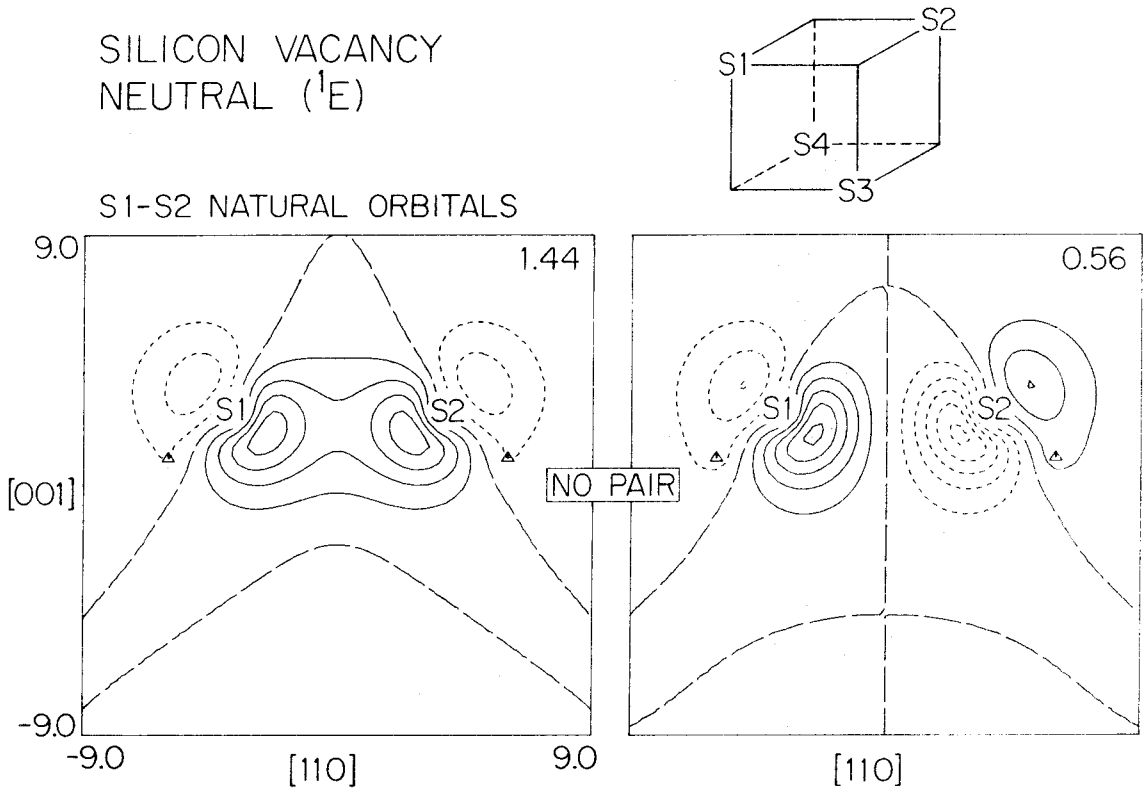
SILICON VACANCY
NEUTRAL (^{1}E)
S1
S2
S3
S4
S1-S2 NATURAL ORBITALS
9.0
1.44
0.56
S1
S2
S1
S2
NO PAIR
[001]
-9.0
-9.0
[110]
9.0
[110]

Figure V.2.2.

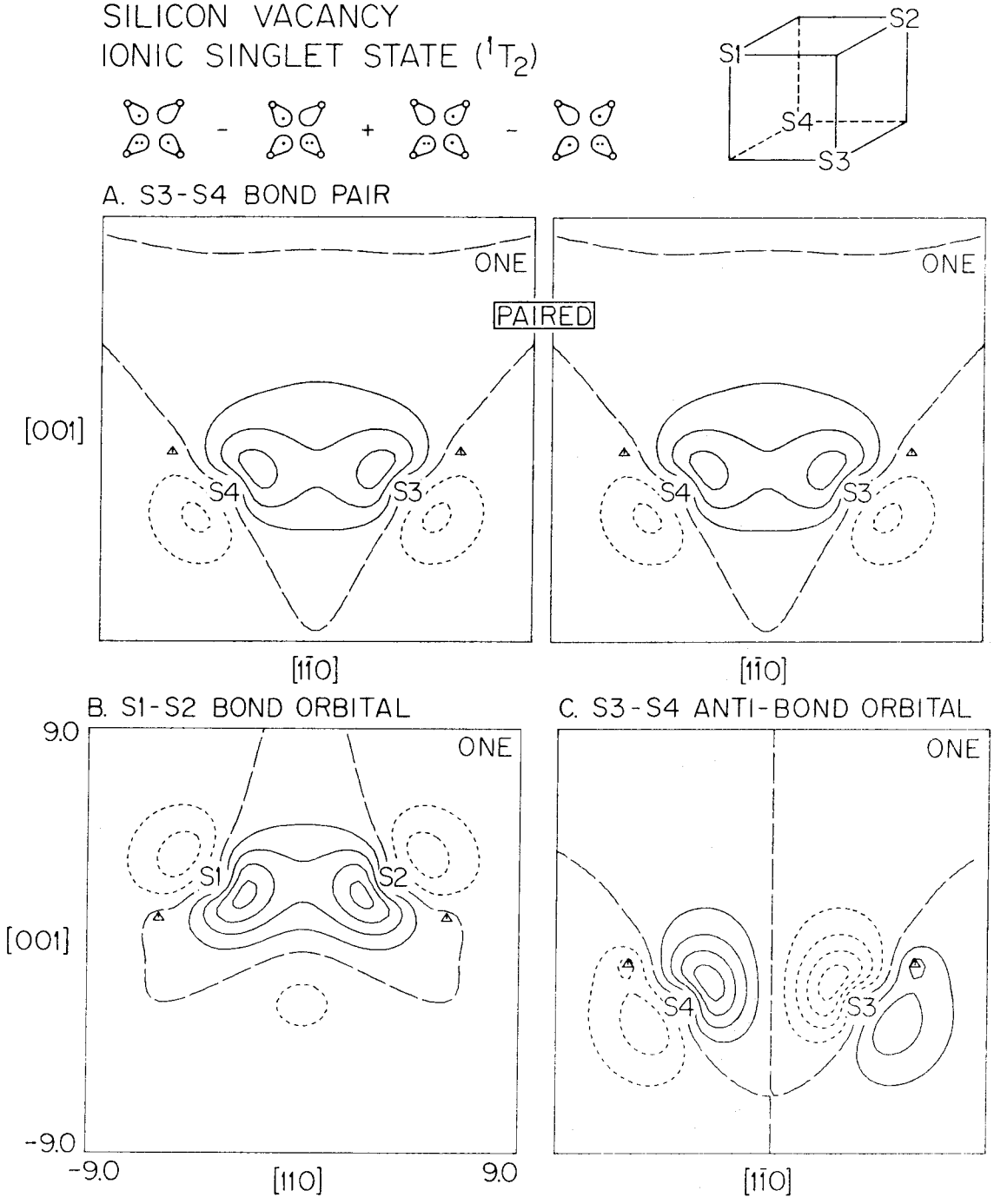
SILICON VACANCY
IONIC SINGLET STATE ($^1T_2$)
S1
S2
S3
S4
A. S3-S4 BOND PAIR
ONE
PAIRED
ONE
[001]
S4
S3
S4
S3
[1$\bar{1}$0]
[1$\bar{1}$0]
B. S1-S2 BOND ORBITAL
C. S3-S4 ANTI-BOND ORBITAL
9.0
ONE
ONE
[001]
S1
S2
S4
S3
-9.0
-9.0
[110]
9.0
[1$\bar{1}$0]

Figure V.3.1.

SILICON VACANCY
IONIC SINGLET STATE ($^1T_2$)

A. GVB BONDING ORBITAL

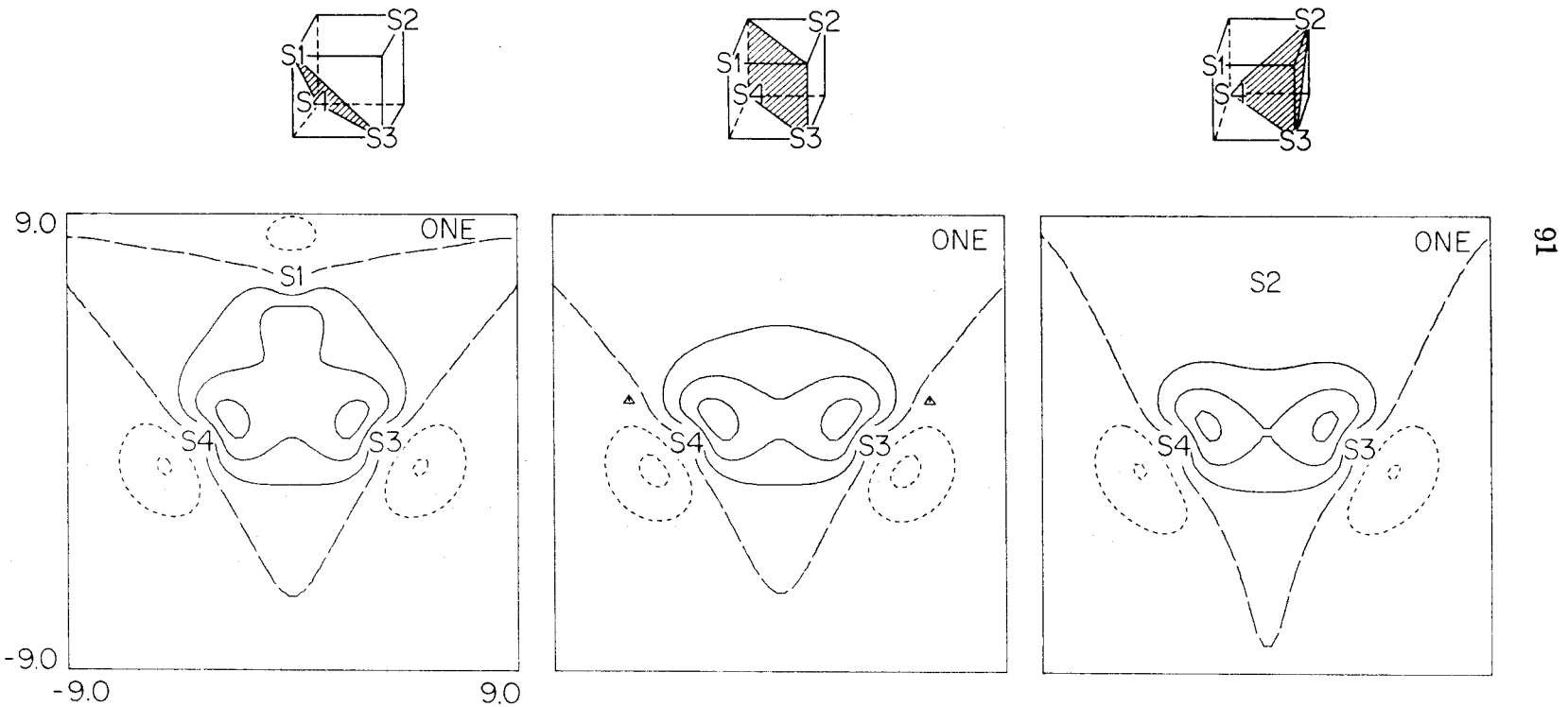

Figure V.3.2.

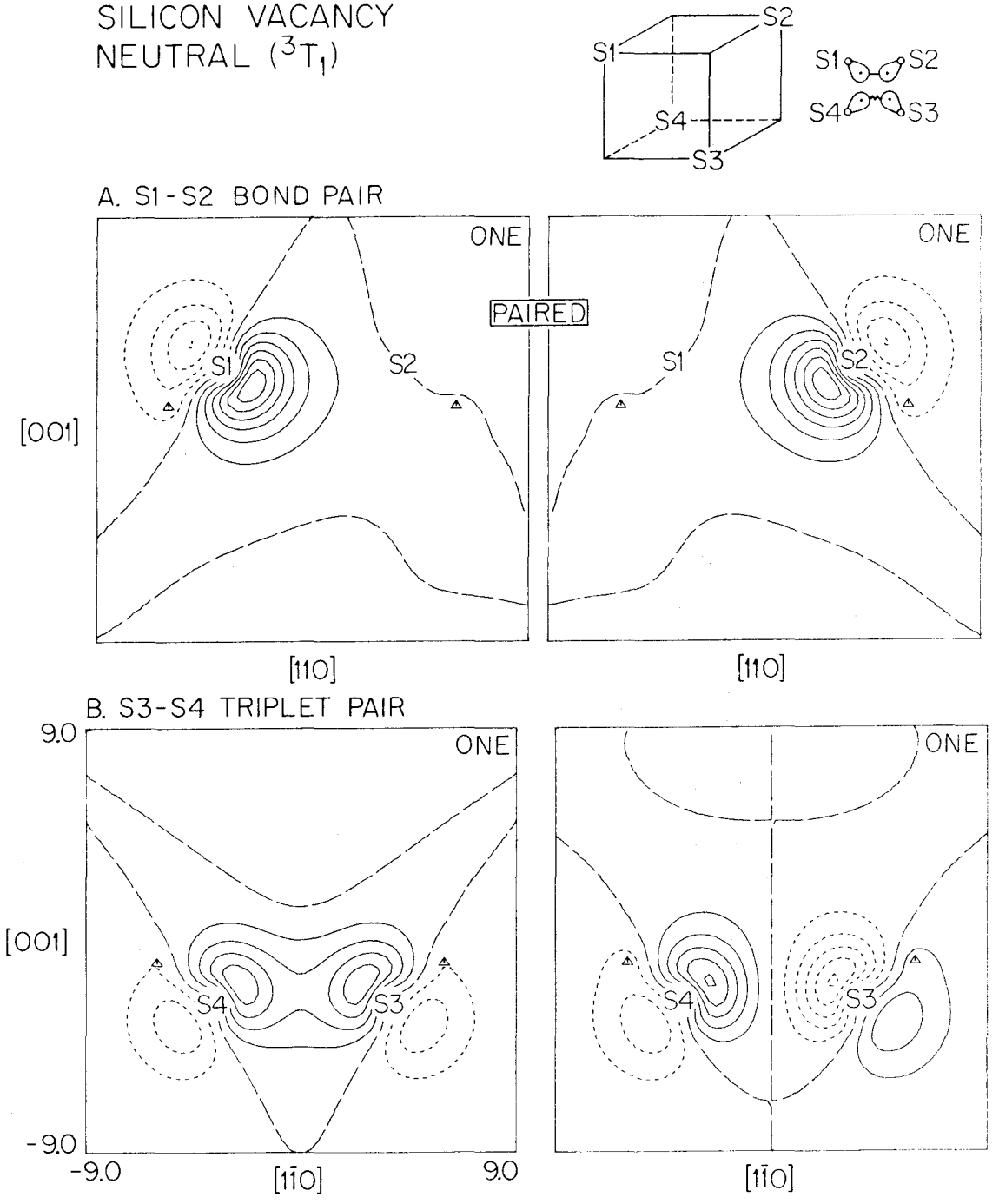
SILICON VACANCY
NEUTRAL ($^3T_1$)
S1
S2
S3
S4
A. S1-S2 BOND PAIR
ONE
PAIRED
ONE
S1
S2
S1
S2
[001]
[110]
[110]
B. S3-S4 TRIPLET PAIR
9.0
ONE
ONE
S4
S3
S4
S3
[001]
-9.0
-9.0
[1$\bar{1}$0]
9.0
[1$\bar{1}$0]

Figure V.4.

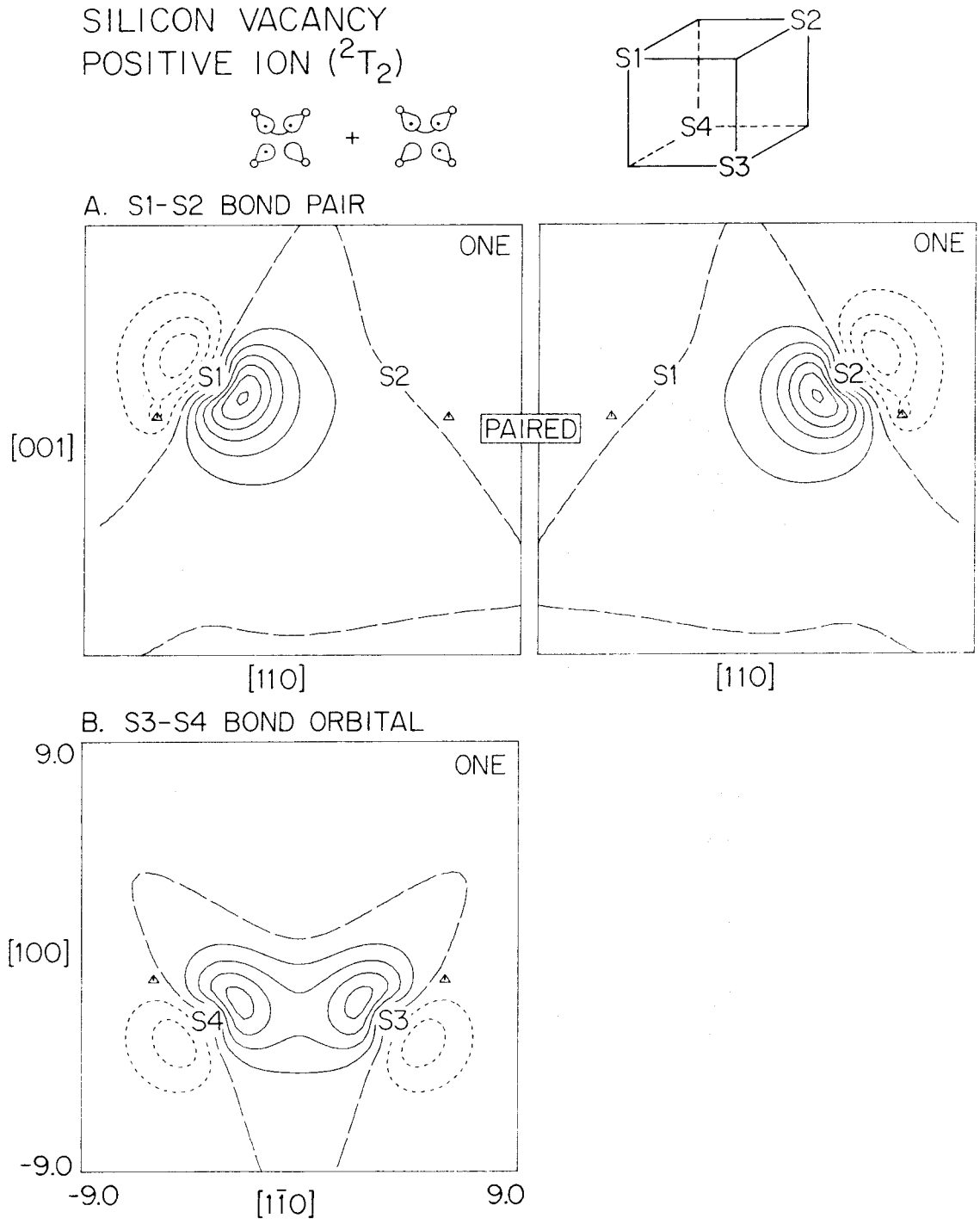
SILICON VACANCY
POSITIVE ION ($^2T_2$)
+
S1
S2
S4
S3
A. S1-S2 BOND PAIR
ONE
S1
S2
PAIRED
ONE
S1
S2
[001]
[110]
[110]
B. S3-S4 BOND ORBITAL
9.0
ONE
[100]
S4
S3
-9.0
-9.0
[1$\bar{1}$0]
9.0

Figure V.5.

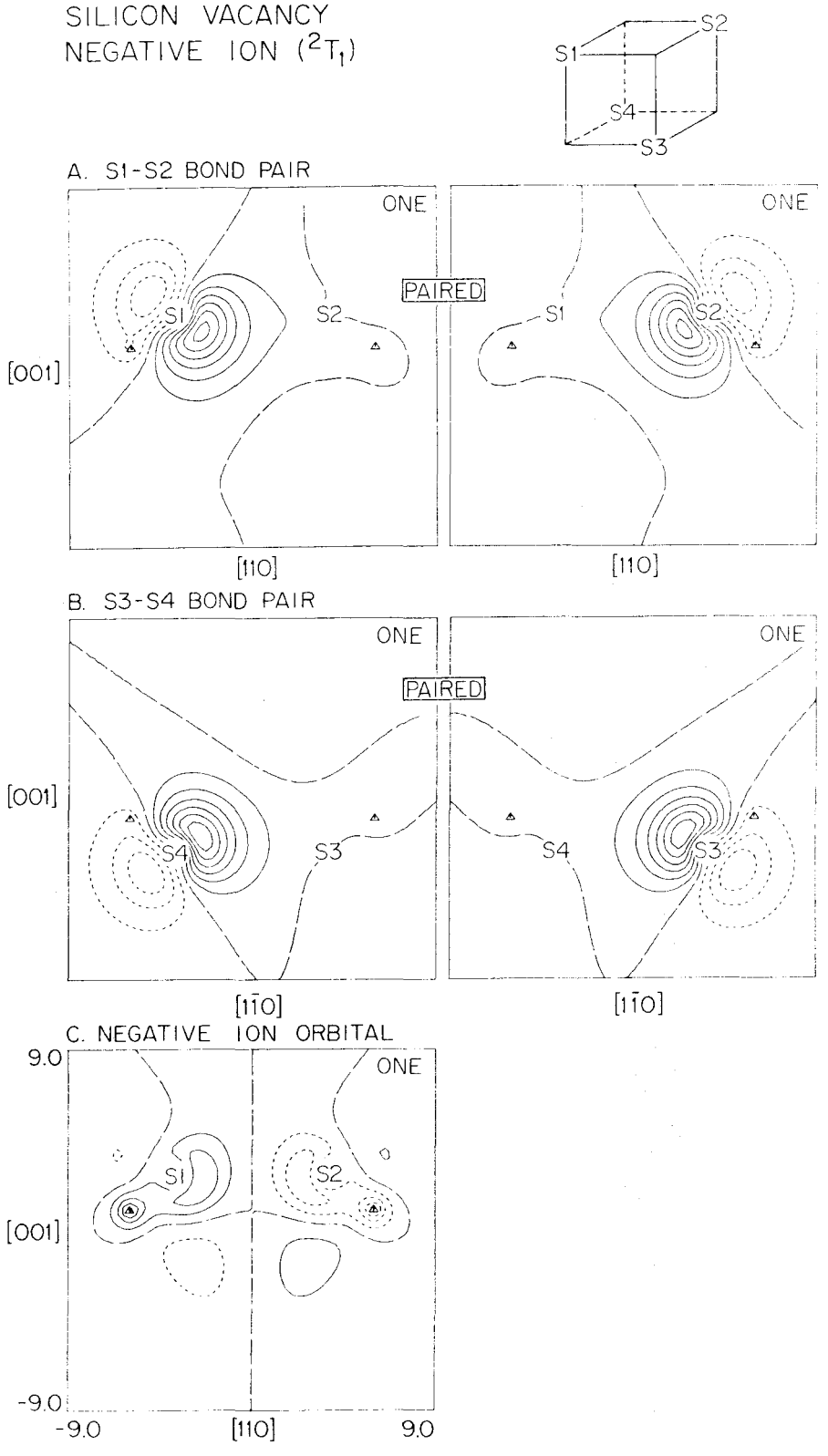
SILICON VACANCY
NEGATIVE ION ($^2T_1$)
S1
S2
S3
S4
A. S1-S2 BOND PAIR
ONE
PAIRED
ONE
S1
S2
S1
S2
[001]
[110]
[110]
B. S3-S4 BOND PAIR
ONE
PAIRED
ONE
S4
S3
S4
S3
[001]
[1$\bar{1}$0]
[1$\bar{1}$0]
C. NEGATIVE ION ORBITAL
9.0
ONE
S1
S2
[001]
-9.0
-9.0
[110]
9.0

Figure V. 6.

VI. SILICON SURFACE STATES

The study of the silicon (111) surface states grew out of using the Si_4H_9 model for finding the equilibrium positions for the vacancy. The work also ties in with other studies of the Si surface being performed by Antonio Redondo of this research group.

The calculations on the positive and negative ion states were carried out using the Si MBS and using a HF description for the states. Both the use of the MBS and of the HF approximation are worst for the negative ion and the resulting bond lengths should be too long in that case. The calculations were performed for several positions of the surface Si along the [111] direction, as was done for C and Si in sections IV and V. The results of these calculations are given in Table VI.1. A cubic spline fit to these results for the positive and negative ions is shown in Figure VI.1. The curve for the neutral case was given in Figure V.1.

We find that the minimum point for the positive ion is 0.582 a.u. = 0.308 Å below the undistorted (tetrahedral) position (that is, shorter bonds) while the negative ion is 0.415 a.u. = 0.219 Å above the undistorted position. This means that the positive ion will move 39% of the interplanar distance into the surface while the negative ion distorts 28% away from the surface. The corresponding Si—Si bond lengths are 2.26 Å, 2.32 Å and 2.43 Å for the positive ion, neutral and negative ion respectively, compared with a 2.35 Å bond length in the crystal.

The calculations were repeated using a full DZ basis by Redondo[28] leading to minima at -.683 a.u., -.152 a.u. and +.400 a.u. for the positive, neutral and negative ions respectively. The error in going from MBS to DZ is worst for the positive ion where it is $\sim .1$ a.u. = .053 Å.

The DZ calculations on the positive ion and the neutral represent a reasonable level of calculation for these species. However, for the negative ion the HF description does not allow for correlations between the two electrons in the dangling bond orbital and hence will lead to an extra error. In order to obtain some quantitative idea of the importance of such correlation effects, we decided to study SiH_3^- as a prototype.

For this study a tetrahedral SiH_3^- was used with a SiH bond length of 1.48 Å. The basis was a DZ basis (including the hydrogens) augmented with diffuse sp functions. The Si core was again replaced by an effective potential. Calculations were performed using both this sp basis and the same basis augmented with d functions. The basis set information is given in Table VI.2. Hartree Fock calculations were performed on the neutral and negative ion as well as GVB calculations for the negative ion.

In performing the GVB calculations on SiH_3^+, a slightly more general form of the NO expansion was used. The deficiency of the HF calculation is that the two lone pair electrons are described by one doubly occupied orbital. A GVB (1-PP) calculation remedies this to a certain extent by allowing the electrons to be radially correlated

(one electron farther from the Si than the other). (See Section II.C.) In our calculations we have also allowed angular correlation. Thus the GVB pair is replaced

$$\phi_a \phi_b + \phi_b \phi_a \rightarrow C_1 \phi_1^2 + C_2 \phi_2^2 + \cdots + C_m \phi_m^2 .$$

In this case we use a four-term expansion and denote the wavefunction GVB (1/4-PP). For SiH_3^- the first NO is much like the HF orbital, the second NO is of the same symmetry but contains an extra radial node, the third and fourth NO's are π functions perpendicular to the direction of the lone pair (first NO). Thus this form of the wavefunction allows simultaneous radial, in-out and angular correlation of the pair.

The results of the HF and GVB calculations for SiH_3 and SiH_3^- are given in Table VI.3. We find that while the sp basis HF calculations yield an electron affinity of SiH_3 of 0.042 eV, the GVB calculation gives an electron affinity of 0.351 eV. In going from the sp basis to the spd basis the energy of the neutral drops 0.60 eV but the electron affinity only changes slightly to 0.381 eV. The conclusion drawn from this calculation is that the correlation effects of the GVB (1/4) wavefunction dominate the electron affinity and that the inclusion of d-functions is of little importance.

On the basis of these results it was decided to recalculate the negative ion DZ potential curve adding diffuse functions to the center atom (SI 1 in Table III.2) and using the GVB (1/4-PP) wavefunction.

The results of these calculations are given in Table VI.4. The minimum point was found to be 0.442 a.u. in the [111] direction (slightly farther from the surface). In Table VI.4 we also present the results of the DZ calculations by Redondo for certain points. We find that the inclusion of diffuse functions lowers the energy of the neutral 5.7 mh = .15 eV and lowers the energy of the positive ion 4.7 mh = .13 eV for the equilibrium neutral geometry. In the case of the negative ion the comparison is between a HF calculation and a GVB calculation. The effects of the diffuse functions is estimated[29] as 10 mh at the -.152 a.u. distance.

The calculated vertical ionization potential and electron affinity (from Table VI.5) are 7.69 eV and 0.71 eV respectively. The adiabatic electron affinity is 1.02 eV. The adiabatic ionization potential must be estimated by assuming that the effect of the additional basis functions is constant. In the case the adiabatic ionization potential is 7.43 eV. The DZ results of Redondo gave vertical and adiabatic ionization potentials of 7.66 and 7.41 respectively, hence the above assumption of a constant correction seems reasonable. The DZ calculations also give vertical and adiabatic electron affinities of 0.35 eV and 0.62 eV respectively. Thus we find that there is a fairly constant correction of 0.4 eV in this case as well.

TABLE VI.1. Total Energy of the MBS-HF calculations for the Si (111) surface complex as a function of the position of the surface atom along the [111] direction. All quantities are in Hartree atomic units. The + direction is away from the surface.

Distance	Negative Ion	Neutral	Positive Ion
0.6	-19.834027	--	--
0.4	-19.835600	--	--
0.2	-19.833479	-19.909681	-19.657557
0.0	-19.828207	-19.915003	-19.669642
-0.2	-19.820352	-19.916103	-19.677884
-0.4	-19.810416	-19.913491	-19.682500
-0.6	--	--	-19.683783
-0.8	--	--	-19.682070
minimum distance	0.415	-0.159	-0.582

TABLE VI.2. Additional basis set information for the SiH_3 and Si_4H_9 calculations. The first two functions for silicon of each symmetry are those of Table III.5. The 2p basis is obtained by adding the 3s and 3p function on silicon while the spd basis is obtained by adding the d function as well.

	Function	Exponent	Coefficient
SILICON	3s[a]	0.03648	1.0
	3p[a]	0.02808	1.0
	1d[b]	1.32201	0.35875
		0.391571	0.76147
HYDROGEN	1s[b]	5.663728	0.0871988
		0.857387	0.5046466
	2s[b]	0.190504	1.0

a) Obtained from the DZ basis (Table III.5) by scaling the outermost function of that basis by the ratio of the last two functions.

b) Obtained from A. Redondo.

TABLE VI.3. HF and GVB Calculations for SiH_3 and SiH_3^-. The basis sets refer to Table VI.2. The total energy is in hartrees, the energy lowering is in millihartrees.

Calculation Species	Basis	Type	Total Energy	ΔE (mh)[a]	Mulliken Populations Si	H
SiH_3	sp	HF	-5.393299	--	3.66	1.11
SiH_3^-	sp	HF	-5.394858	--	4.48	1.17
SiH_3^-	sp	GVB(1/4-PP)	-5.406191	11.51	4.47	1.18
SiH_3	spd	HF	-5.428304	--	3.82	1.06
SiH_3	spd	GVB(1/4-PP)	-5.442423	17.82	4.63	1.12

a) The amount that the energy would increase upon deleting the second third and fourth NO's with the coefficients of the other orbitals held constant.

TABLE VI.4 HF and GVB Calculations for the Si_4H_9 complex. All quantities in Hartree atomic units.

Species	Calculation Basis[a]	Type	Distance in [111] direction (a.u.)	Total Energy (h)	Energy[b] Lowering (mh)	Mulliken Populations[c] Si_1	$Si_{2\ 4}$	$H_{1\ 3}$	$H_{4\ 9}$
Negative Ion	DZR	GVB(1/4)	-0.152	-20.079782	8.75	4.44	3.67	1.19	1.17
Negative Ion	DZR	GVB(1/4)	0.200	-20.089807	9.68	4.36	3.71	1.18	1.16
Negative Ion	DZR	GVB(1/4)	0.600	-20.091231	10.80	4.26	3.76	1.17	1.15
Neutral	DZR	HF	-0.152	-20.053813	--	3.98	3.63	1.13	1.12
Positive Ion	DZR	HF	-0.152	-19.771270	--	3.50	3.63	1.06	1.07
Negative Ion	DZR	--[d]	0.442	-20.091553	--	--	--	--	--
Neutral	DZ	HF	-0.152	-20.048107	--	4.16	3.59	1.12	1.11
Positive Ion	DZ	HF	-0.152	-19.766570	--	3.69	3.60	1.05	1.06
Positive Ion	DZ	--[d]	-0.683	-19.775967	--	--	--	--	--
Negative Ion	DZ	HF	-0.152	-20.061029	--	4.56	3.64	1.18	1.16

a) DZ: Full double zeta basis. These calculations are from A. Redondo, Ref. 28.
DZR: Full double zeta basis plus the 3s and 3p functions of Table VI.2 on Si 1 (Table III.2).

b) The amount that the energy would increase upon deleting the second, third and fourth NO's with the coefficients of the other orbitals held constant.

c) The subscrips refer to the center numbers of Table III.2.

d) The energy is obtained from a cubic spline fit to the calculated points.

TABLE VI.5. Electron Affinity and Ionization Potential for the Si_4H_9 complex. The calculations are given in Table VI.4. All quantities are in electron volts.

	Basis[a]	Vertical[b]	Adiabatic
Electron Affinity	DZ	0.352	.620[c]
	DZR	0.707	1.018
Ionization Potential	DZ	7.661	7.405[c]
	DZR	7.688	7.432[d]

a) DZ: Full double zeta basis. These calculations are from A. Redondo, Reference 28.

DZR: Full double zeta basis plus 3s and 3p functions of Table VI.2 on Si1 (Table III.2).

b) At the equilibrium point for the neutral found using the DZ basis.

c) Obtained by a cubic spline fit to the calculated points.

d) Estimated from the DZ results.

FIGURE CAPTIONS

Figure VI.1. Total Energy of the positive and negative ions of the silicon (111) surface complex as a function of displacement of the apical silicon in the [111] direction. The positive direction is away from the surface.

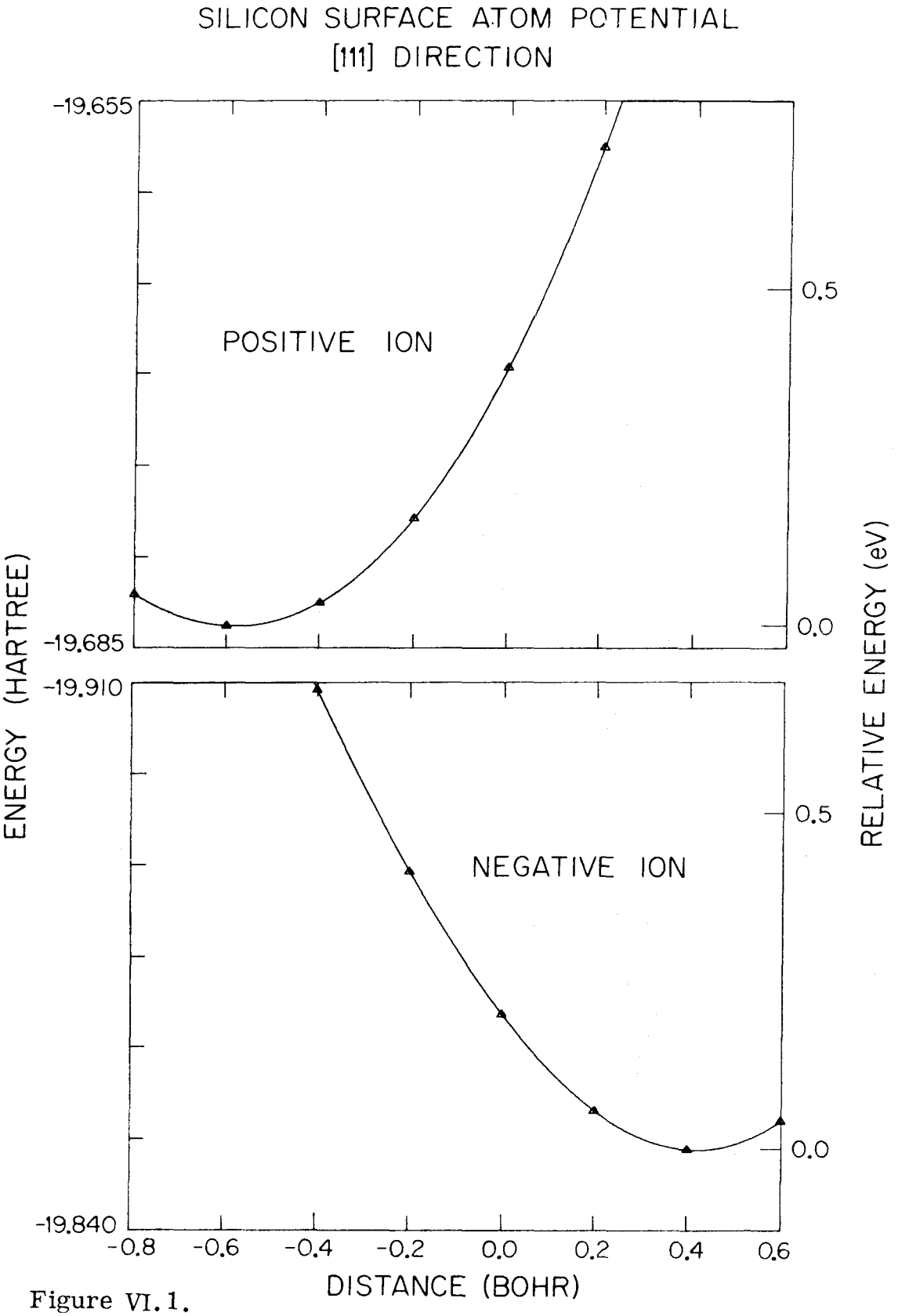
SILICON SURFACE ATOM POTENTIAL
[111] DIRECTION
-19.655
-19.685
POSITIVE ION
0.5
0.0
-19.910
-19.840
NEGATIVE ION
0.5
0.0
ENERGY (HARTREE)
RELATIVE ENERGY (eV)
-0.8
-0.6
-0.4
-0.2
0.0
0.2
0.4
0.6
DISTANCE (BOHR)

Figure VI.1.

VII. LITHIUM AND BORON IMPURITIES IN SILICON

The motivation for studying these two systems is two-fold. The first is that the method used here should make no real distinction between shallow and deep levels and so any differences between shallow and deep levels should "occur naturally" in the calculations. We are implicitly assuming that a localized picture of the shallow impurities can be used, hence the first reason is a test of these ideas. The second motivation is to obtain a way to relate the vacancy levels to the band edges. The shallow levels should "pin down" the valence and conduction band edges so that the position of the various vacancy states within the band gap can be determined.

Before discussing the calculations, we should enlarge slightly on the comments made in section II on these systems. Our interest is in boron as an acceptor and lithium as a donor so we want to look at B, B^-, Li and Li^+ all in the Si_4H_{12} cluster. For B^-, we can form four bonds to the dangling bond orbitals of the cluster. This complex should not have any low-lying excited states since one must break a bond, in effect, to form one. In the case of B, we have already found that there should be $^2A_1$ and $^2T_2$ states. A quick analysis such as in Appendix B leads to the $^2T_2$ being the lower state. The energy separation will be $\sim 4\tau$, $\tau = h_{ab} - \sigma h_{aa}$, as before, and thus will not be small (say 3 eV). In the Li^+ case, we should obtain just the energy level structure of the vacancy with the levels shifted somewhat due to the presence of the positive ion. Perhaps the best way to view the Li impurity is to consider it as a Li^+ ion in the negative ion state of the vacancy. Thus we would expect a $^4A_2$ ground state with a low-lying

$^2T_1$ excited state.

Another point to note is that Li^+ in Silicon is thought to occupy an interstitial rather than a substitutional position.[30] Our argument is that the Li (unionized) is probably substitutional and that after the Li^+ is formed it has a low activation energy for migration, the Li^+ ion being quite small.

For each case discussed above we performed a GVB calculation for the lowest state except for the Li case in which both the $^4A_2$ and $^2T_1$ were calculated. In each case the impurity atom was placed at the origin (Table III.1) and the bulk Si sitances were used. The individual calculations will be discussed as the results are presented.

In Table VII.1 the results of the SCF calculations for the various impurity complexes are given while in Table VII.2 the Mulliken populations from the calculations are presented. The corresponding vacancy calculation is number 2 in Table V.2. For the neutral B, the system was treated as three Si–B bond pairs and one silicon dangling bond orbital. The B^- case was treated as four Si-B bond pairs. Comparing the calculations it is fairly obvious that the Si-B bonds in the two systems are very similar. The overlaps indicate that these are normal bonding orbitals. In Figures VII.1 and VII.2 representative orbitals for the B and B^- cases are shown. For the B complex, one of the three equivalent bonds is presented, as well as the singly occupied orbital. For B^- we show two of the four equivalent bond pairs. The main difference is that the GVB orbital on Si in the Si–B bond delocalized toward the singly occupied orbital in the neutral

case. For the most part the bonding orbitals are quite similar. The electron affinity of $(SiH_3)_4$-B is 3.12 eV from the GVB calculations.

For the Li complex we find that the ground state is the $^4A_2$ state with the $^2T_1$ state ($^2B_1$ component) 0.51 eV higher. The quartet state was solved for using a HF wavefunction. In Figure VII.3 the orbitals of the $^4A_2$ state are shown in two perpendicular Si-Li-Si planes. We see that the doubly occupied orbital is symmetric while the singly occupied orbitals are each antisymmetric although one is the antisymmetric combination of two bond orbitals. In Figure VII.4 the orbitals for the $^2T_1$ state are shown. This state is a bond pair in one bond and a He_2^+-like state (g^2u) in the other bond. This is just the description found previously for $^2T_1$ state of the negative vacancy. Comparing the overlap of the bond pair in this case with the Li^+ calculation (Table VII.1) with the corresponding vacancy calculation (row 2, Table V.2), we see that the Li^+ case overlaps slightly less than the vacancy, while the GVB pair in the $^2T_1$ state overlaps much less than either. In Figure VII.5 the orbitals for the Li^+ calculation are shown. The major difference between this calculation and the vacancy is the nodal surface near the Li^+. The ionization potentials for the two lithium states are 6.214 for the $^2T_1$ and 6.528 for the $^4A_2$.

As before, CI calculations based on the NO's of the GVB calculation were performed to include the major correlation effects which are absent in the GVB-PP wavefunction. First consider the case of $(SiH_3)_4$-B complex. From the neutral GVB-PP calculation there are seven NO's while from the negative ion there are eight (ignoring the

$B(1s)^2$ core and the SiH bonds). To obtain a complete GVB space it is necessary to add a second NO in the region of the singly occupied orbital. This orbital was obtained by orthogonalizing the second NO from the corresponding bond in the B^- calculation to the other orbitals of the B calculation. This yields an eight function GVB space for $(SiH_3)_4$-B. For the negative ion, just the NO's of the GVB calculation were used for the CI calculations. It should be noted that for the $(SiH_3)_4$-B CI basis the SiH bonds were those from the GVB calculation. Since that calculation was for a C_{3V} field, the CI solutions using the orbitals from the neutral calculation will display that symmetry. In the negative ion case, the solutions have full T_d symmetry. In both cases the CI calculations were SD-CI's in the GVB space. The calculation for the states of the neutral were done using both sets of orbitals (neutral and negative ion), primarily as a check on the symmetry of the states, The results of the CI calculations are presented in Table VII.3.

The total CI effect is approximately the same in the two systems, .012 mh for the neutral and .014 mh for the negative ion. The ordering of the states of $(SiH_3)_4$-B is as predicted. The calculated energy difference between the average of the $^2T_1$ levels and the $^2A_2$ level for the neutral basis is 6.04 eV as compared with 5.92 eV for the negative ion basis. For the negative ion, the first excited state is 12.8 eV above the ground state, also as predicted. The electron affinity for $(SiH_3)_4$-B is 2.91 eV from the CI calculations. In Table VII.4 the dominant energy contributions of the CI calculations are presented.

In each case, the relaxation of the perfect pairing restriction is the dominant effect. Thus a full GVB calculation would include some non-singlet spin character in the bond pairs. In addition in the neutral case there is also an orbital rearrangement effect. This derives mostly from the orbitals not having T_d symmetry.

For the CI calculations on the Li complex, a somewhat different choice of the CI basis was made. For the positive ion the four NO's from the GVB calculation were augmented with the valence s and three valence p functions on Li to make an eight basis function space. For the neutral the basis was chosen starting with the $^4A_2$ orbitals. To these we added the valence s and p lithium functions as for the positive ion plus a set of s and directed p functions on Si as was done for the vacancy (see section V). This gives a 16 function space for the neutral case. For the positive ion a full SD-CI was performed, while for the neutral the calculation was a GVB-CI over the HF orbitals plus a SD-CI using the dominant $^4A_2$ configuration as the basic configuration. The results of these calculations are given in Table VII.5. We find that the ordering of the states is as we predicted. The excitation energy for the positive ion is 3.78 eV which is 0.3 eV less than in the silicon vacancy. This should be expected since the Li^+ in the vacancy can help stabilize the charge transfer $^1T_2$ states. A comparison of the vacancy and Li-vacancy states is shown in Figure VII.6. For the case of the neutral we find a spectrum of states very much like the silicon vacancy negative ion, as is also shown in Figure VII.6. In this case as well the spectrum of states is "compressed" relative to the vacancy.

The energy difference between the GVB and CI descriptions is small ($\sim$ 8 mh) for the ground state in both cases. The $^2T_1$ state of the neutral is 0.59 eV above the ground state as compared with 0.51 eV for the GVB calculation. The ionization potential of the $^4A_2$ changes from 6.53 eV for the GVB calculation to 6.66 for the CI, while the ionization potential for the $^2T_1$ state changes from 6.21 eV to 6.07. In Table VII.6 we present the dominant energy contributions for the CI calculations on the lithium complex. For the positive ion we find that there is only a small rearrangement effect after the GVB configurations. In the case of the neutral for the $^4A_2$ state the only CI effects come from changing the shape of the doubly occupied orbital using the p virtuals. For the $^2T_1$ state the CI effect is to change the shape of the second a_1 orbital.

While we have not related the states solved for in these calculations to "true crystal states" per se, we have found that the impurity atoms bond to vacancy orbitals in an easily explained manner. Furthermore we find that the bonds formed in these cases are normal chemical bonds. Our next task is to see how these calculations relate to the observed properties of real materials.

TABLE VII.1 GVB calculations for models of the Li donor and B acceptor states in Si. Quantities are in Hartree atomic units.

Calculation		Total Energy (h)	C_1[a]	C_2[a]	$\Delta E_{(mh)}$[b]	S_{ab}[c]	ϵ[d]
$(SiH_3)_4$-B	GVB(3-PP)	-46.326959	.9931	-.1170	12.09	.7891	-.3933
$(SiH_3)_4$-B^-	GVB(4-PP)	-46.441448	.9933	-.1159	11.63	.7918	-
$(SiH_3)_4$-Li	$^4A_2$ HF	-29.017010	-	-	-	-	-
$(SiH_3)_4$-Li	$^2B_1$ GVB(1-PP)	-28.998105	.7806	-.6250	76.99	.1107	-.3042
$(SiH_3)_4$-Li^+	$^1A_1$ GVB(2-PP)	-28.769749	.8542	-.5200	63.22	.2431	-

a) C_1 and C_2 are the coefficients of the natural orbitals: $\phi_a\phi_b + \phi_b\phi_a = C_1\phi_1\phi_1 + C_2\phi_2\phi_2$.

b) ΔE is the energy lowering due to the presence of the second NO. This is the amount that the energy would increase if the second term in the NO expansion were deleted with the other orbitals held constant.

c) $S_{ab} = \langle \phi_a | \phi_b \rangle$ is the overlap of the GVB orbitals.

d) ϵ is the orbital energy of the singly occupied orbitals.

TABLE VII.2 Mulliken Populations for the calculations in Table VII.1. The subscripts on the Si and H refer to the center numbers in Table III.1.

Calculation	Si_2	$Si_{1,3,4}$	$H_{1,4,9}$	$H_{4,6,11}$	$H_{2,3,5,7,8,12}$		B
$(SiH_3)_4$-B	3.420	3.636	1.127	1.141	1.151		4.917
$(SiH_3)_4$-B^-	3.775	3.775	1.172	1.172	1.172		4.959
	$Si_{1,2}$	$Si_{3,4}$	$H_{1,4}$	$H_{2,3}$	$H_{5,7,9,10}$	$H_{6,8,11,12}$	Li
$(SiH_3)_4$-Li $^4A_2$	3.757	3.757	1.123	1.123	1.123	1.123	2.509
$(SiH_3)_4$-Li $^2B_1$	3.873	3.648	1.132	1.109	1.125	1.116	2.509
$(SiH_3)_4$-Li^+	3.644	3.644	1.084	1.084	1.084	1.084	2.382

TABLE VII.3 CI Calculations for the $(SiH_3)_4$-B complex

	State	B Basis[a] Energy (a.u.)	ΔE (eV)	B^- Basis[b] Energy (a.u.)	ΔE (eV)
$(SiH_3)_4$-B		-46.349046	0.0	-46.313465	0.0
	$^2T_1$	-46.305924	1.173	-46.313464	0.0
		-46.305916	1.174	-46.313462	0.0
	$^2A_2$	-46.098369	6.821	-46.095922	5.919
(GVB)	$^2T_1$	-46.326959			
$(SiH_3)_4$-B^-	$^1A_1$	-		-46.455688	0.0
	$^1T_2$	-		-45.984235	12.829
(GVB)	$^1A_1$	-		-46.441449	

a) CI basis derived from NO's from $(SiH_3)_4$-B GVB(3-PP) calculation.

b) CI basis derived from NO's from $(SiH_3)_4$-B^- GVB(4-PP) calculation.

TABLE VII.4 Dominant contributions to the Configuration Interaction energy for the lowest states of the $(SiH_3)_4$-B complex.

Calculation	Configuration[a]								Number of Equivalent Cases	Energy[b] Lowering (mh)
	σ_1	σ_1^*	σ_2	σ_2^*	σ_3	σ_3^*	σ_4	σ_4^*		
$(SiH_3)_4$-B $^2T_1$	2	0	2	0	2	0	1	0	1	-
B Basis	0	2	2	0	2	0	1	0	3	30.51
	2	0	1	1	1	1	1	0	3	6.60
	2	0	2	0	1	1	0	1	3	4.33
$(SiH_3)_4$-B^- $^1A_1$	2	0	2	0	2	0	2	0	1	-
B^- Basis	0	2	2	0	2	0	2	0	4	42.31
	1	1	1	1	2	0	2	0	6	12.61
	0	2	0	2	2	0	2	0	6	1.79

a) For the B^- basis the functions σ and σ^* are the NO's for the 4 bonds. For the B basis this is also true for σ_1, σ_2, σ_3, σ_1^*, σ_2^*, σ_3^*, while σ_4 is the singly occupied orbital on Si and σ_4^* is a virtual similar to the B^- σ^* orbitals in the direction of the singly occupied orbital.

b) The amount the energy would increase if the configuration were deleted with the coefficients of the other configurations held constant, in millihartrees. The contributions of all equivalent cases are added together.

TABLE VII.5 CI Calculations for the $(SiH_3)_4$-Li complex.

$(SiH_3)_4$-Li^+			$(SiH_3)_4$-Li			
State	Energy (a.u.)	ΔE (eV)	State	Energy (a.u.)	$E-E_{^4A_2}$ [a]	$E-E_{^2T_1}$ [a]
	-28.777019		$^4A_2$	-29.022767	0.0	--
^1E	-28.773091	0.0		-28.942064		
	-28.637193		$^4T_1$	-28.941836	2.218	--
^1T	-28.637192	3.788		-28.941102		
	-28.633166					
				-29.001506		
			$^2T_1$	-29.001381	0.594	0.0
				-28.999973		
				-28.964879		
			^2E		1.593	0.999
				-28.963591		
				-28.945773		
			$^2T_2$	-28.948502	2.061	1.467
				-28.946801		

a) Energy differences are between the average value for the states, in eV.

TABLE VII.6 Dominant contributions to the Configuration Interaction energy for the lowest states of the $(SiH_3)_4$-Li complex.

Calculation	Configuration[a]								Energy[b] Lowering
$(SiH_3)_4$-Li^+	σ_1	σ_2	σ_1^*	σ_2^*					(mh)
^1E	2	2	0	0					126.24
	2	2	0	2					61.27
	0	2	2	0					61.27
	0	0	2	2					28.34
	1	1	2	0					3.75
	1	1	0	2					3.75
$(SiH_3)_4$-Li	a_1	a_1	b_1	b_2	p_1	p_2	p_3	p_4	
$^4A_2$	2	1	1	1	0	0	0	0	717.28
	1	1	1	1	1	0	0	0	1.44
	1	1	1	1	0	1	0	0	0.96
	1	1	1	1	0	0	1	0	0.90
	1	1	1	1	0	0	0	1	0.69
$^2T_1$	2	2	1	0	0	0	0	0	66.98
	2	0	1	2	0	0	0	0	64.11
	1	1	1	2	0	0	0	0	26.39
	2	1	1	0	1	0	0	0	1.28
	2	1	1	0	0	1	0	0	0.84

a) For Li^+, $\sigma_1\,\sigma_1^*\,\sigma_2\,\sigma_2^*$ are the NO's of the GVB calculation, for Li $a_1\,a_1\,b_1\,b_2$ are the HF orbitals of the $^4A_2$ state while $p_1\,p_2\,p_3\,p_4$ are inwardly directed p functions on centers 1, 2, 3, 4, as in the silicon vacancy.

b) The amount the energy would increase if the configuration were deleted with the coefficients of the other configurations held constant in millihartrees.

FIGURE CAPTIONS

Figure VII.1. The GVB orbitals for the $^2T_1$ state of boron in silicon $[(SiH_3)_4\text{-}B]$. The spacing of the contour levels is .03 a.u. with dashed lines representing negative amplitudes. The same spacing is used for all subsequent plots in this section.

Figure VII.2. The GVB orbitals for the $^1A_1$ state of negatively charged boron in silicon $[(SiH_3)_4\text{-}B^-]$.

Figure VII.3. The HF orbitals for the $^4A_2$ state of lithium in silicon $[(SiH_3)_4\text{-}Li]$.

Figure VII.4. The GVB orbitals for the B_1 component of the $^2T_1$ state of lithium in silicon $[(SiH_3)_4\text{-}Li]$.

Figure VII.5. The GVB orbitals for the ^1E state of positively charged lithium in silicon $[(SiH_3)_4\text{-}Li^+]$.

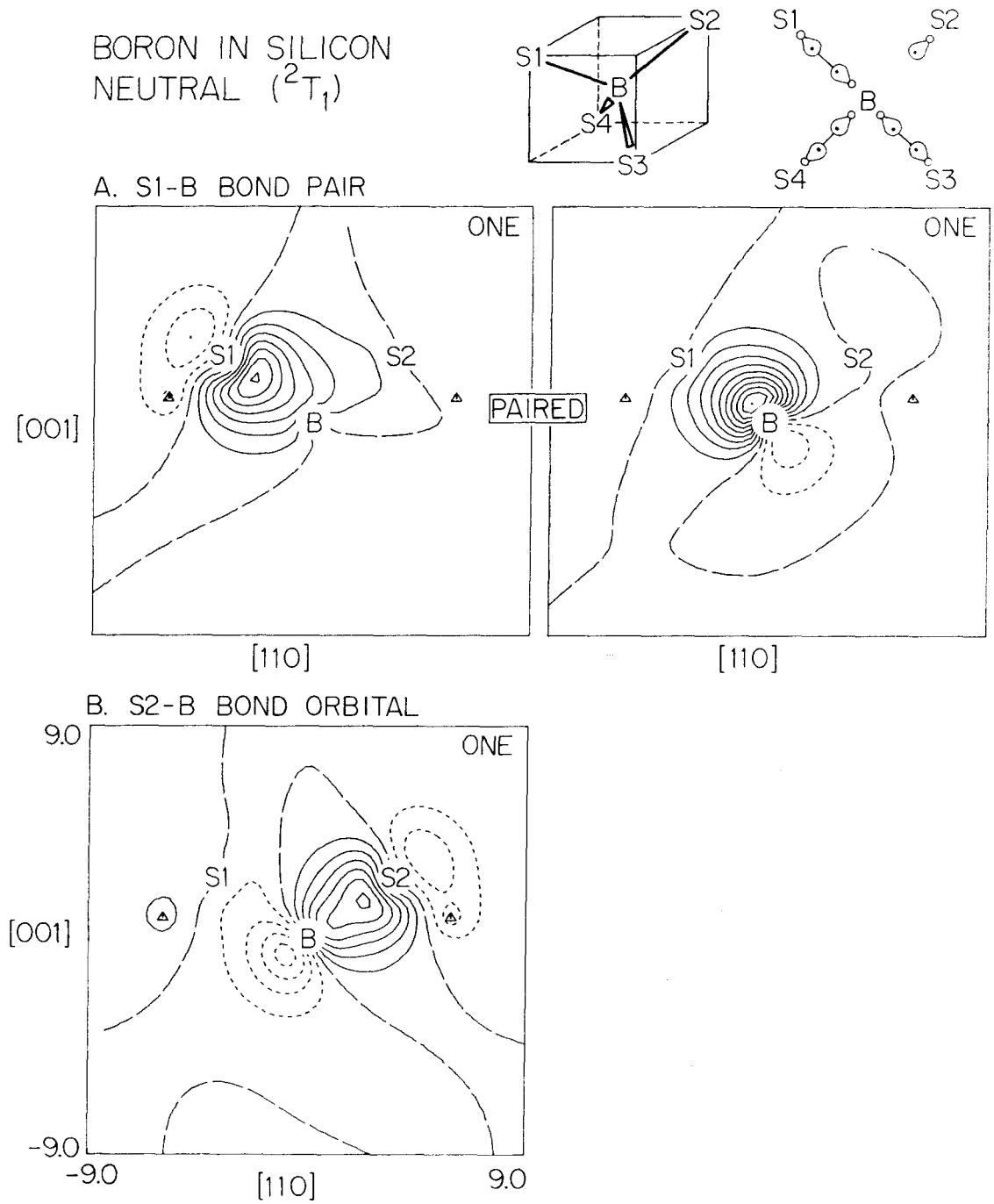
BORON IN SILICON
NEUTRAL ($^2T_1$)
S1
S2
B
S4
S3
A. S1-B BOND PAIR
ONE
PAIRED
[001]
[110]
B. S2-B BOND ORBITAL
9.0
-9.0

Figure VII.1.

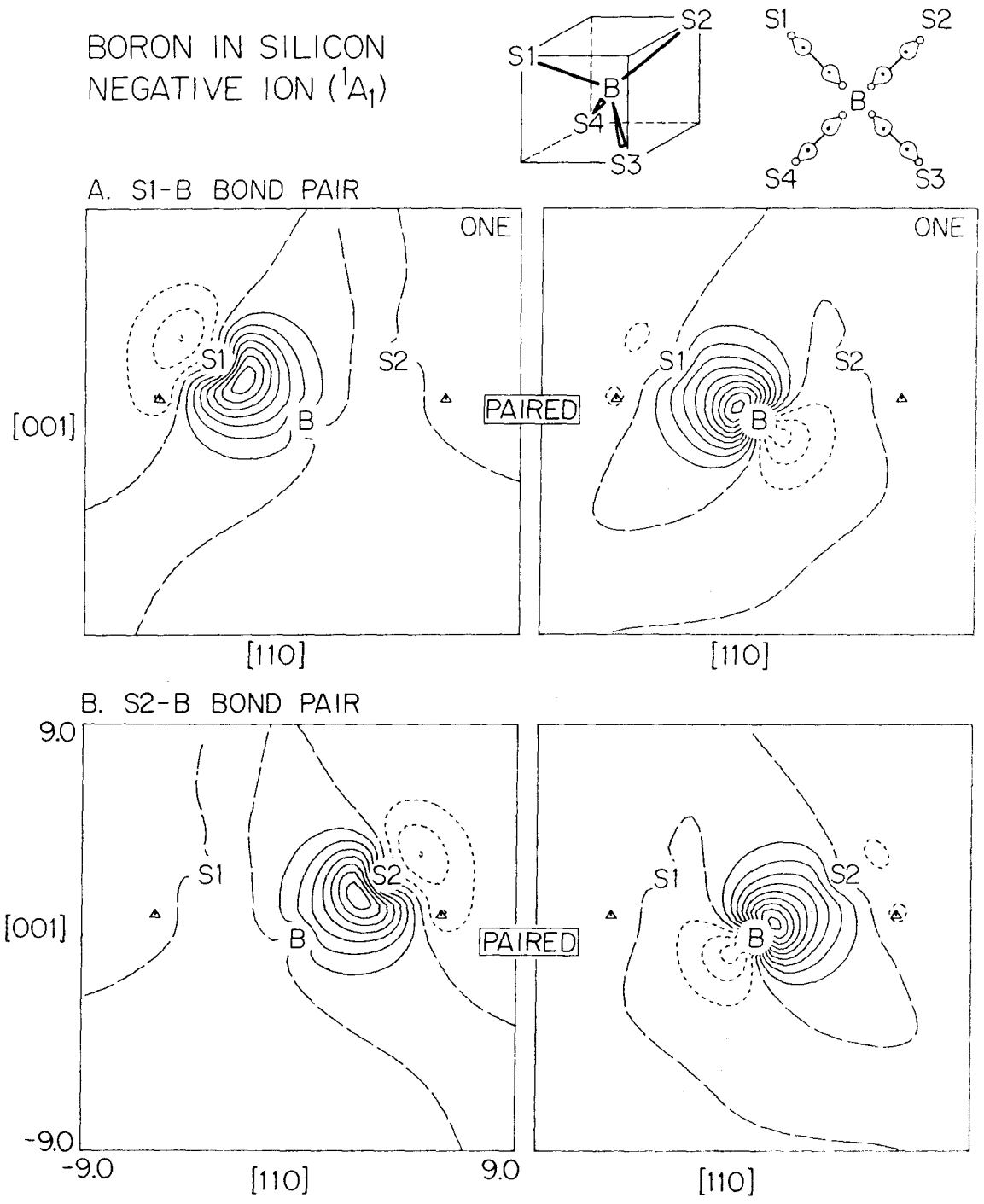
BORON IN SILICON
NEGATIVE ION ($^1A_1$)
S1
S2
S3
S4
B
A. S1-B BOND PAIR
ONE
PAIRED
[001]
[110]
B. S2-B BOND PAIR
9.0
-9.0

Figure VII.2.

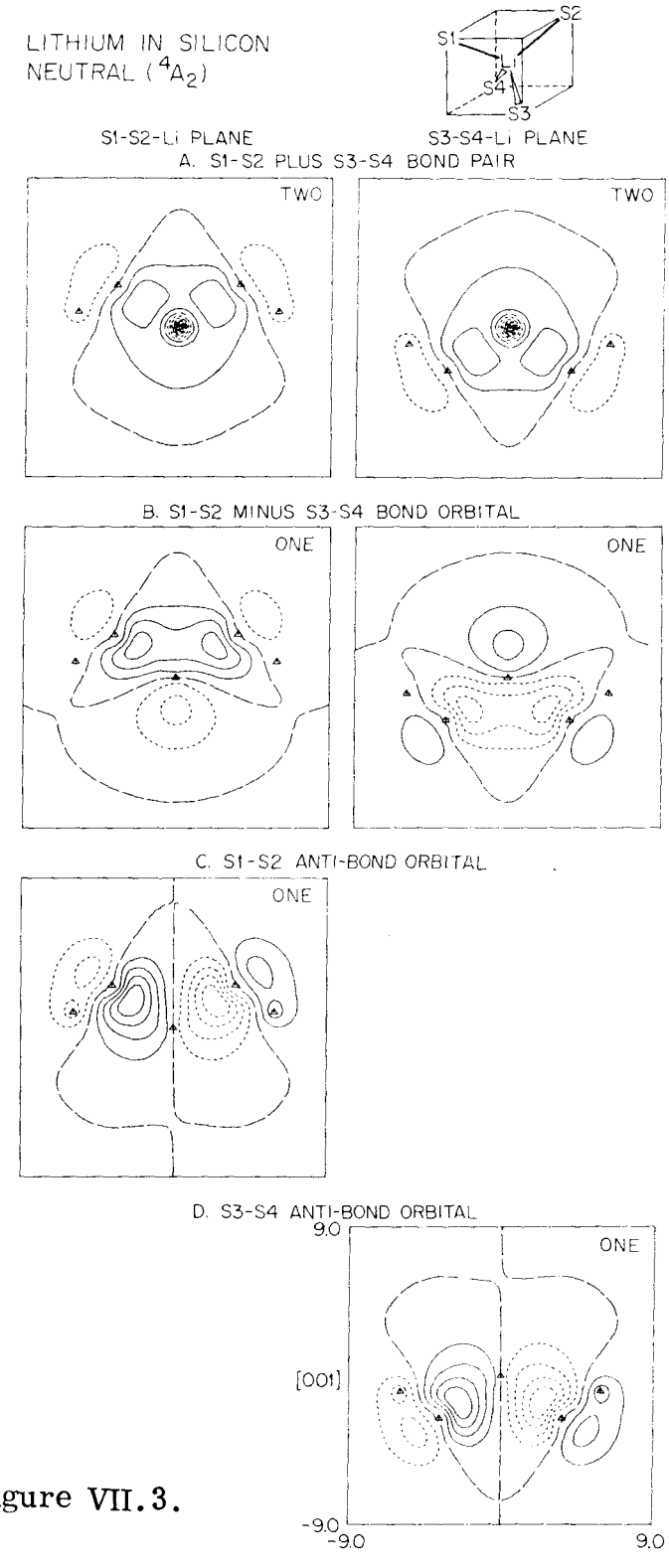
LITHIUM IN SILICON
NEUTRAL ($^4A_2$)
S1
S2
Li
S4
S3
S1-S2-Li PLANE
S3-S4-Li PLANE
A. S1-S2 PLUS S3-S4 BOND PAIR
TWO
TWO
B. S1-S2 MINUS S3-S4 BOND ORBITAL
ONE
ONE
C. S1-S2 ANTI-BOND ORBITAL
ONE
D. S3-S4 ANTI-BOND ORBITAL
9.0
ONE
[001]
-9.0
-9.0
9.0

Figure VII.3.

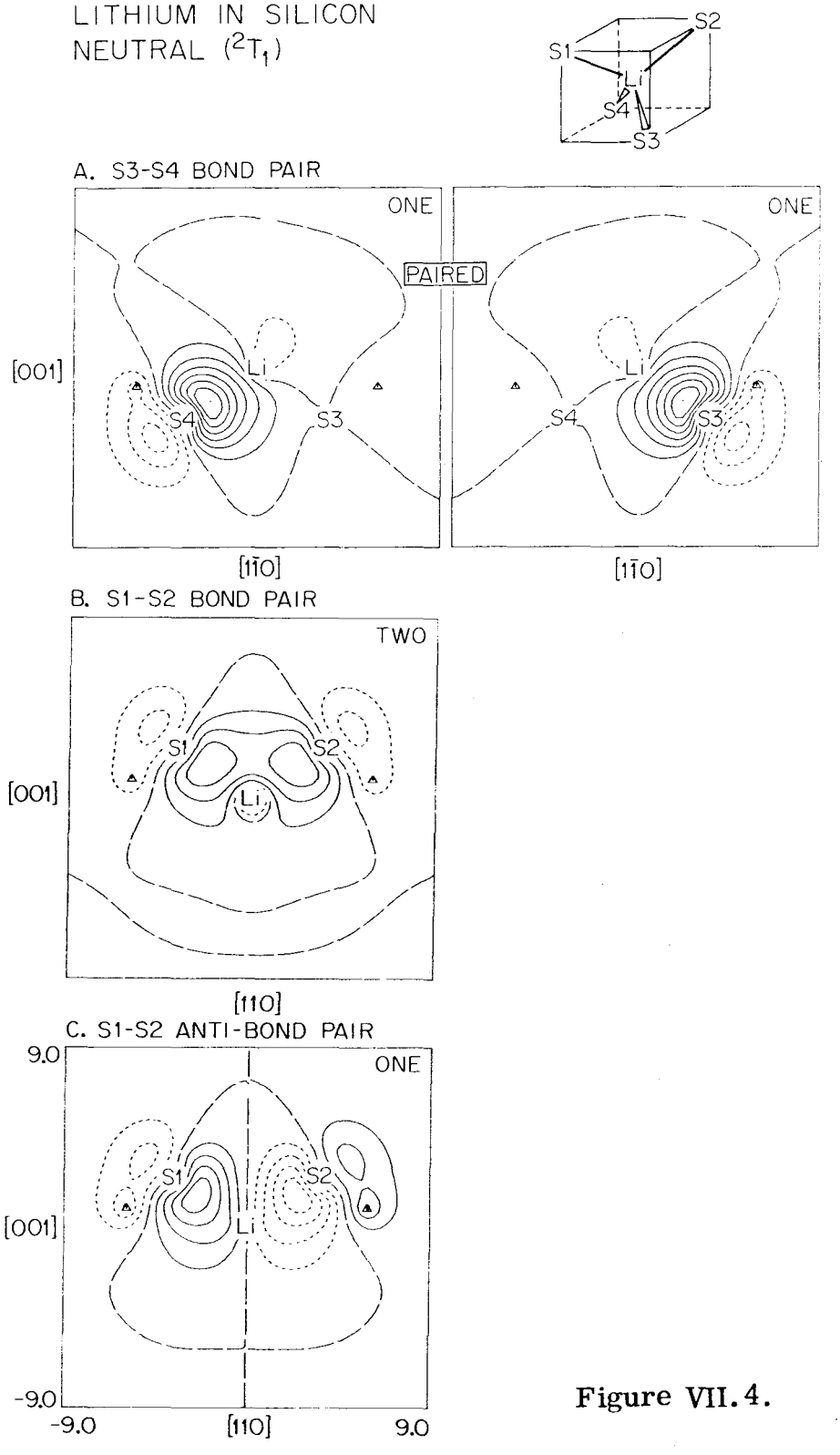
LITHIUM IN SILICON
NEUTRAL ($^2T_1$)
S1
S2
Li
S4
S3
A. S3-S4 BOND PAIR
ONE
PAIRED
ONE
[001]
Li
S4
S3
Li
S4
S3
[1$\bar{1}$0]
[1$\bar{1}$0]
B. S1-S2 BOND PAIR
TWO
[001]
S1
S2
Li
[110]
C. S1-S2 ANTI-BOND PAIR
9.0
ONE
S1
S2
[001]
Li
-9.0
-9.0
[110]
9.0

Figure VII.4.

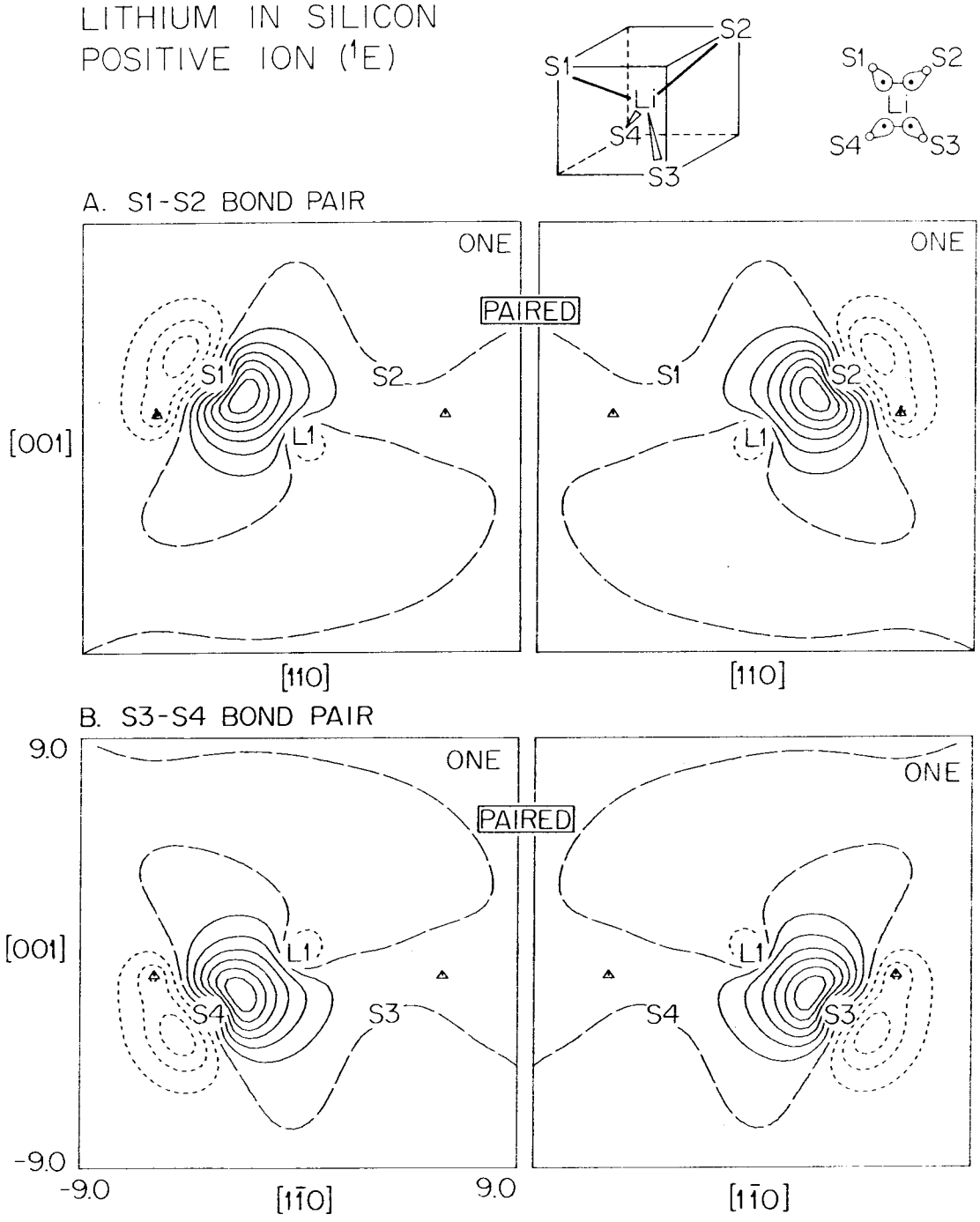
LITHIUM IN SILICON
POSITIVE ION (1E)
S1
S2
Li
S4
S3
A. S1-S2 BOND PAIR
ONE
PAIRED
ONE
S1
S2
S1
S2
L1
L1
[001]
[110]
[110]
B. S3-S4 BOND PAIR
9.0
ONE
PAIRED
ONE
L1
L1
S4
S3
S4
S3
[001]
-9.0
-9.0
9.0
[1$\bar{1}$0]
[1$\bar{1}$0]

Figure VII.5.

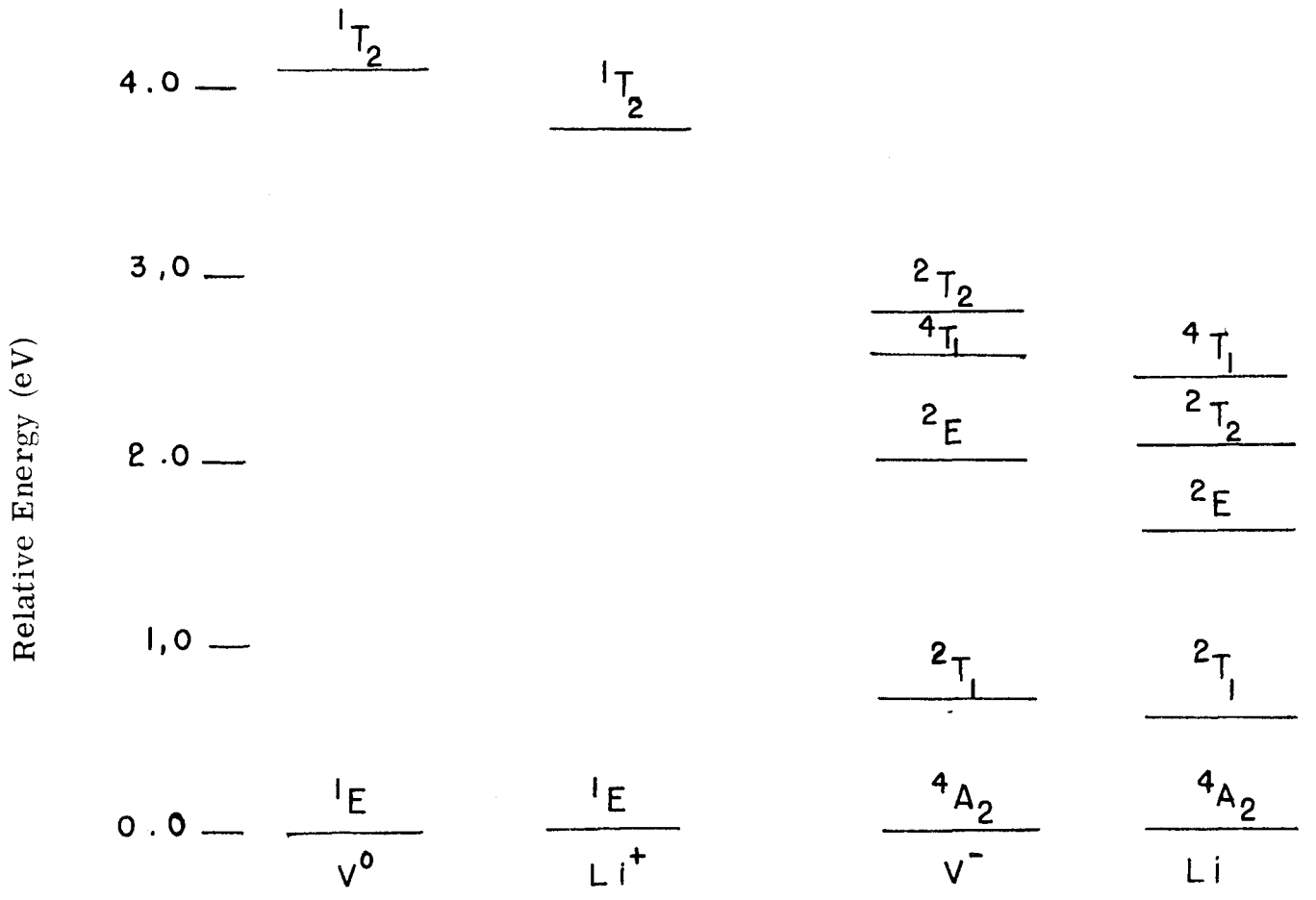

Figure VII.6. Comparison of the states of the neutral (V^0) and negative (V^-) vacancies in silicon with the states of the substitutional lithium (neutral and positive ion).

VIII. DISCUSSION

The calculations performed in this work have included the dominant many body effects present in the clusters and thus should give excitation energies correct to a few tenths of an electron volt. Keeping in mind that distortions have not been allowed, we would expect the methods employed to give a good description of localized states in solids such as the ones studied herein. However, there are cases in which the states are charged or in which the states have dipole or higher moments. In these cases there will be long-range polarization effects that no finite cluster can reproduce. In order to discuss these situations, we have attempted to correct for the polarization effects using a dielectric continuum approximation. The general procedure is as follows: within the cluster the effect of polarization is included since the calculations are self-consistent field calculations. The cluster itself is considered to be a spherical hole in an infinite dielectric. The charge of the cluster or appropriate moments of the charge distribution of the cluster are obtained from the calculation. The energy of interaction of the charge distribution with the medium is then calculated classically and the results are used to correct the calculated energies. The exact formulation of this procedure is given in Appendix C.

One point which has been implied throughout this study is that one must consider the correct many electron states of the system rather than one electron states or molecular orbitals. The usual picture of defects is based on some molecular orbital model whether it is a band

structure[20] or a cluster calculation.[6] While the molecular orbital (MO) approach does provide conceptually simple means of viewing impurity states, it can give misleading or incorrect information, as we shall see.

Consider first the covalent states of the vacancy, that is, ^1E, $^3T_1$, $^5A_2$. In section II we used simple valence bond arguments about the nature of these states which proved to be correct on detailed calculation. For diamond we found the $^3T_1$ state 0.33 eV above the ^1E while the $^5A_2$ state was 1.20 eV above the ^1E. In silicon the $^3T_1$ was found to be 0.18 eV above the ^1E while the $^5A_2$ was 0.60 eV above the ^1E. Experimentally the ground state of the neutral vacancy has been shown to be a ^1E state by thorough piezospectroscopic studies of the GR1 absorption line in irradiated diamonds.[31] In addition there is some evidence for a weakly spin orbit split triplet state with one component 0.008 eV above the ^1E state. The spectral features are consistent with this being a component of a $^3T_1$ state.[31] By comparison virtually every MO calculation based on the Coulson-Kearsley model predicts the $^3T_1$ to be the ground state.[9,32] With the inclusion of "configuration interaction" effects, which amounts to allowing the terms present in the GVB wavefunction, the ^1E usually becomes the ground state. In attempting to explore the effect of many electron effects, Messmer concluded that the average singlet-triplet splitting goes to zero as the cluster size is increased.[33] Unfortunately in using the MO picture he was forced to calculate the average energy of the ^1E, $^1T_2$, $^1A_1$ and $^3T_2$ states to obtain the average singlet energy while the $^3T_2$ energy was

calculated properly. The result of this is illustrated below using our CI results for diamond.

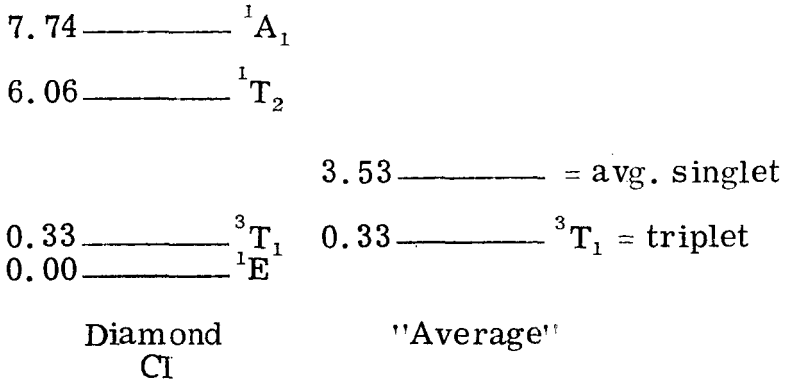

The problem is that in the MO description one has a triply degenerate t_2 orbital which is doubly occupied, $(t_2)^2$, which gives rise to the states ^1E, $^1T_2$, $^1A_1$, $^3T_2$. However, from the valence bond picture we know that i) the $^1T_2$ and $^1A_1$ states are ionic excited states and ii) the $^1T_2$ being a charge transfer state will polarize the cluster and thus its energy will depend on cluster size while the other states will have no such dependence. However, in the MO approach such points are totally lost. In fact our conclusion is that the correct singlet-triplet splitting can be obtained only by the proper inclusion of many-body effects. For instance, the energy lowering in the ^1E state of diamond (GVB calculation) is 3.00 eV per pair, thus a HF description of the ^1E state would be $\sim$ 6 eV above the current calculation. However, the $^5A_2$ state (for which one must use a HF calculation) is only 0.94 eV above the GVB calculation for the ^1E state: Thus we would not predict a ^1E ground state had we used a MO description.

The calculations of the covalent states also allow us to calculate a formation energy for the vacancy. To do this one needs the energies of the "basic units" of the complex. In this case we need the energy of a tetrahedral SiH_3 using the same basis as used in the vacancy calculation. This calculation was performed and the energy is given in Table VIII.1. The binding energy of the vacancy orbitals is quite small, 1.76 kcal/mole, as compared with 53.93 kcal/mole (Table VIII.1) for each Si-Si bond. Thus we find that the vacancy formation energy is endothermic by 213.96 kcal = 9.28 eV. This is only part of the displacement energy which is the energy required to form a vacancy by electron impact, for instance. The displacement energy includes "getting over" whatever barrier is involved in moving the displaced atom from its bonded tetrahedral position. Typical values of the displacement energy are about 13 eV.[34] Thus the "barrier" energy is 3.72 eV.

In performing the polarization corrections of the calculated energies, it is advantageous to start with a few cases for which the experimental results are fairly well established so that the correction can be "calibrated." That is, we would like to understand how well or poorly the method works so that its predictive value can be assessed. For the surface case we consider the cluster to make a hemispherical hole in the surface and that the charge resides at the center of the "hole" for positive and negative ion states:

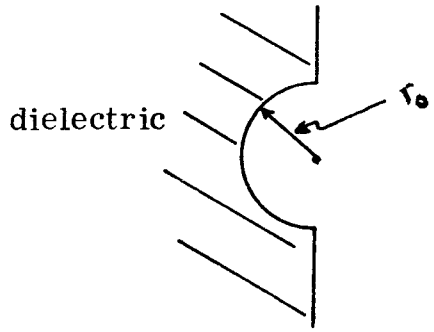

The polarization energy is given by (Appendix C):

$$U = -\tfrac{1}{2}\,\frac{\epsilon - 1}{\epsilon + 1}\,\frac{1}{r_0} \quad \text{(in atomic units)}$$

where ϵ is the dielectric constant of the medium ($\epsilon = 12$ for Si, $\epsilon = 5.7$ for C).

The best material to begin the comparison is silicon in this case. Photoemission studies of the silicon surface indicate that the (111) surface states corresponding to one electron per dangling bond lie 0.5-0.8 eV below the valence band edge.[35,36] This corresponds to a state 5.6-5.9 eV below the vacuum. Thus our calculated ionization potential (IP) should correspond to this number. The electron affinity of the surface per se has not been measured, however, the bulk electron affinity is defined as the bulk IP minus the band gap energy. For silicon this value is 4.0 eV.

The silicon surface calculations presented in section VI gave a vertical IP of 7.69 eV and a vertical electron affinity (EA) of 0.71 eV. Using a sphere radius of 5.99 bohr, which is the distance from the center Si to the hydrogens in the undistorted case, one obtains a

polarization correction of 1.92 eV. The resulting corrected value of the surface IP is 5.77 eV while the corrected surface EA is 2.63 eV. The IP is in very good agreement with experiment while the EA is 1.4 eV low. This could be attributable to: i) an inadequate description of the surface negative ion, ii) using a localized description for an essentially delocalized state, iii) the conduction band actually being 1.4 eV "downhill" from the negative ion surface state.

In the case of diamond, there are no data on surface states such as in the silicon case. The best experimental photoemission data for diamond is that of Cavell[37] et al.. They obtain an ionization potential from the top of the valence band of 6.7±0.3 eV, which also gives an electron affinity of 1.3 eV for diamond.

In section IV, we calculated an ionization potential of 7.32 eV and an electron affinity of -2.56 eV. The electron affinity calculation was done using a HF description of the lone pair of the negative ion with no diffuse functions in the basis. Using a similar sp basis augmented with d functions, Kari and Csizmadia found the electron affinity of methyl (CH_3) to be -1.6 eV. Using a larger basis including diffuse s and p functions as well as d functions, and performing CI calculations, we found the electron affinity of methyl to be -0.49.[44] Thus the value of -2.56 eV from the surface calculation is quite high.

In diamond the radius for the dielectric correction seems to be in the range of distances between the hydrogen position and the second-nearest-neighbor position. (We will discuss the rationale for this later.) For the surface complex these distances are 4.095 and

4.766 bohr. The corresponding corrections are 2.33 eV and 2.00 eV. Hence the ionization potential is in the range 4.99 to 5.32 eV while the electron affinity ranges between -.23 eV and -.56 eV. The correlation effects such as found in CH_3^- could lower these values by ~ 1.1 eV. This would make the EA 0.5-1.0 eV low while the IP would be 1.0 eV low. The implication is i) the positive ion has too low an energy by 1 eV while the negative ion (including correlation) has too high an energy by 1 eV or ii) the measured IP is too large by ~ 1 eV. Given that the sample in the diamond case is insulating and thus could be subject to surface charge problems in the photoelectron experiment ii) is a viable explanation.[38]

Another case in which there is good experimental information is the optical absorption associated with the neutral vacancy in diamond.[31] The experimental study of this spectral feature (the GR1 feature in electron irradiated diamonds) is relatively complete and corresponds to a transition at a tetrahedral site from an E state to a T_2 state. The zero phonon line of the spectrum is at 1.673 eV.

As has been noted previously, the $^1T_2$ state is a charge transfer state and hence can be expected to have sizable polarization corrections. It is instructive to examine the form of the charge distribution before looking at the moments calculated from the wavefunction. We noted in section IV that the $^1T_2$ state is a charge transfer state in which one electron is moved from the 1-2 bond region to the 3-4 bond region. Assuming that one-half an electron is transferred from or to each dangling bond orbital, one obtains the picture

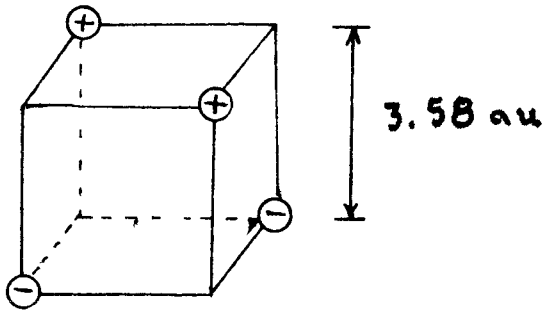

If the $\frac{1}{2}e$ charge is placed at each corner the dipole moment is 3.58 a.u. while the quadrupole moment is Q_{xy} = 9.61 a.u. Comparing this with moments calculated from the GVB wavefunction as given in Table VIII.2, one finds the quadrupole term to be correct but the dipole moment is only 2.45 a.u. Thus there appears to be some deviation from the tetrahedral arrangement given above. One can obtain the necessary information from the Mulliken populations in Table IV.2. The charge transfer between the carbon centers is 0.6 electron which would give a 2.15 a.u. dipole moment. The charge transfer on the hydrogens in the 1,2,3,4 positions is significant, giving rise to the following field source:

H2 H4

-.06 O O +.08

+.08 O O -.06

H1 H3

which is predominantly xy quadrupole in nature. Thus we find that there is significant polarization in the CH bonds leading to large higher moments in the diamond cluster case. By comparison, the silicon hydrogens in the same positions exhibit charge transfers of only .02 electron, mainly due to the lack of flexibility in the minimum basis set

description used for them. Thus we might expect the dipole correction which employs a sphere radius which goes to the hydrogens to be too large. In fact the result is that for that distance (4.17 bohr) the correction is 6.63 eV. Using the choice of the second nearest neighbor sphere (r_0 = 4.76 bohr) gives a correction of 3.28. Obviously if we wished to match experiment we should use a distance intermediate between these two.

We can now return to the point we mentioned in doing the diamond surface calculation. The polarizability of the CH bonds is fairly large and tends to "overcompensate" for the charge transfer. Perhaps some sphere radius "just outside" the cluster radius is more correct, however, the choice is not clear. The values of the $^1E - {}^1T_2$ excitation energy for reasonable values of the sphere radius are given in Table VIII.3. For r_0 in the range 4.5-4.7 bohr we obtain excitation energies in the range 1.07-2.00 eV, which represents about the expected accuracy of such calculations.

As has already been mentioned, the SiH bonds are less polarizable than the CH bonds. Hence the sphere radius can be expected to be somewhat shorter. Here the radius should be between $\frac{1}{4}$ and $\frac{1}{2}$ the distance from the hydrogens to the second-nearest-neighbor position. The resulting radii are 6.35-6.65 bohr which lead to excitation energies in the range 0.97-1.57 eV.

The neutral vacancy excitation in silicon is not observed or at least has not been identified. That result makes it plausible that the excitation energy for the neutral vacancy in silicon is of the same size

as the band gap energy. However, the vacancies in silicon are quite mobile to low temperature, tending to form divacancies rather readily,[39] which might tend to increase the difficulty of observing the transition experimentally.

For the charge states of the vacancy, the experimental situation is somewhat different than in the neutral vacancy case. In this case there is very little evidence for the existence of the charged states in diamond[40] while there have been numerous studies of them in silicon.[41] The primary method used in the study of these species is electron paramagnetic (or spin) resonance. No electronic transitions associated with the positive and negative charge states of the vacancy have been reported, but information is available with regard to the position of these defects in relation to the band edges.

In actuality, the positive (V^+) and negative (V^-) vacancy states in silicon should be considered along with the lithium and boron states as donor and acceptor levels in silicon. To facilitate the discussion we have presented the experiment information on the levels in Figure VIII.1. The boron and lithium levels are very well characterized. Watkins gives two values for the V^+ position, he places the position of the level at .039 eV above the valence band, but finds that the barrier to release the hole of the V^+ state to the valence band is .057 eV. The position of V^- is known only to be more than 0.1 eV from the band edges. The V^- is generated by shining light of energy equal to the band gap on electron irradiated p-type silicon. V^- is also generated by electron irradiation of n-type silicon, otherwise its position is unknown.

To relate our calculations to the experimental quantities, we have to consider just what the level diagram of Figure VIII.1 means. The calculations give state energies while the level structure is based on an MO picture and as such gives one electron energies which, via Koopmans' Theorem relate to ionization potentials. Thus we need to interpret the figure in terms of ionization potentials. For instance, we would say that the experimental IP of Li in silicon is 4.03 eV while that of B^- is 5.05 eV. In Table VIII.4 the calculated and experimental values for the IP's of the various levels are given.

There are a few comments to be made here. The first is that while the IP's of the neutral levels are very similar, that of the negative ions is quite different. The second is that if a simple charge correction is used the energy correction for all cases is 3.8 eV for a radius of 6.06 bohr. This value is correct only for the V^- case. Finally, in terms of the previous calculations, the B^- case is something of an anomaly. (Its energy difference is quite small.) There is also the point that the calculated ground state of the negative ion is a quartet while the epr spectrum is of a doublet state.

Fortunately, the last point is fairly easy to see, the $^4A_2$ state is non-degenerate and thus will exhibit no distortion. The B_1 and B_2 components of the $^2T_1$ state will distort and result in much lower energies. Watkins[41] has estimated an energy lowering on distortion of 2.1 eV based on stress relaxation studies. We have used the $^4A_2$ energy as an upper bound of the V^- energy.

In attempting to "correct" the calculated energies for polarization

effects, we have not really considered the effects of using hydrogens to truncate the cluster. The implicit assumption is that the CH bonds will behave like CC bonds (or like the rest of the crystal). Simply examining the Pauling electronegativities[43] of the atoms we find that the values are H = 2.1, C = 2.5, S_1 = 1.8. Examining the Mulliken populations for the neutral states (^{1}E vacancy), one finds that the populations follow the electronegativities. That is, the carbons have 0.5 extra electrons each while the silicons are each deficient by 0.4 electrons. Hence we might expect there to be a differential effect between positive and negative ion states for a given type of cluster. For instance, the diamond negative ion states have been uniformly too high in energy. The same argument would imply that the silicon positive ion states are too high in energy, while the V^+ and Li^+ calculations might be slightly low if one believes the dielectric correction.

The boron case stands in contrast to all of the other calculations in that in the other cases we found deviations from the dielectric correction of $\sim$1 eV. For all of those states we were dealing with weakly bound or weakly interacting systems. In the case of B the bonds formed are normal chemical bonds as can be seen from Table VIII.1. Note that the boron impurity "costs" only 20 kcal to form as opposed to over 200 kcal for a vacancy. The implication is that the boron system is basically different from the vacancy cases and from the lithium impurity which interacts weakly with the vacancy.

The point of this discussion has not been to make the calculations agree with experiment or explain away the difference. We have sought

to use a fairly simple model to try to understand the kinds of long-range effects which should be included in relating cluster calculations to the infinite solid. We have found that the nature of the states has a definite effect on the charge distribution away from the defect. The inclusion of the hydrogens to "tie off" the bonds to the cluster may build in differential effects so that all states are not really treated equally. Above all, the polarization corrections always work in such a way as to move the calculated value in the direction of better agreement with experiment although going too far in some cases.

The final point concerns the binding of the lithium and boron impurities. From Table VIII.1 we find that the formation of a boron impurity requires 20 kcal/mole while the lithium impurity requires 211 kcal/mole. Clearly the boron is forming strong chemical bonds to the silicons since the bond energy for the boron is nearly that of a silicon. The lithium, however, is a different matter. In section VII the statement was made that lithium probably formed a substitutional impurity but was an interstitial as the positive ion. The basis for this was that the covalent radius of silicon is 1.17 Å[43] while the metallic radius of Li is 1.22 Å.[43] Thus lithium "fits" into the substitutional site and a priori the supposition was that there would be sufficient bond energy to stabilize the substitutional placement. On the basis of this calculation, however, it seems clear that the lithium occupies the tetrahedral interstitial site, which is the same size as the substitutional site. A lithium atom or lithium ion would stabilize a vacancy, and thus might bind at very low temperatures, but would be displaced by mobile silicon atoms (interstitials) at higher temperatures.

TABLE VIII.1 Formation Energies of Various Silicon Clusters.

Basic Energies[a] (hartree)

SiH_3:	-5.372197
B :	-24.526415
Li :	-7.43237
Li^+ :	-7.23620

Σ = Sum of Basic Energies (h)		GVB Energy (h)	Σ - GVB (eV)	Σ - GVB (kcal)
$4(SiH_3)$	= -21.488788	-21.491605	0.0766	1.76
$4(SiH_3) + B$	= -46.015203	-46.326959	8.4834	195.63
$4(SiH_3) + Li$	= -28.921158	-29.017010	0.2241	5.17
$4(SiH_3) + Li^+$	= -28.724988	-28.769749	1.2180	28.09[c]

Si-Si Bond Energy: 53.93 kcal/mole[b]

Formation Energies (kcal)

Si - Vacancy	-213.96
B - Impurity	-20.09
Li - Impurity	-210.55
Li^+ - Impurity	-187.63[c]

a) SiH_3 calculation was performed using the same basis and geometry as one SiH_3 unit of the vacancy. B and Li energies are from references 17 and 20 respectively.

b) Reference 42.

c) Polarization corrections not included.

TABLE VIII.2 Multipole Moments of the GVB wavefunctions for the Ionic excited states ($^1T_2$) of silicon and diamond. All values are in atomic units.

	Dipole Moment	Quadrupole Moments[a,b]	
	P	Qxy	Qz^2
Diamond	2.4515	9.5978	-0.4247
Silicon	3.3119	16.2183	-0.8268
		Octapole Moments[b]	
	z^3	$x^2z = y^2z$	xyz
Diamond	26.6183	17.8322	8.6825
Silicon	58.2829	41.5843	19.7764

a) $Q_{\alpha\beta} = \frac{1}{2}(3r_\alpha r_\beta - r^2\delta_{\alpha\beta})$

b) Only the significant moments are given, all others are less than 0.01.

TABLE VIII.3. Dielectric corrections for the excitation energies of the $^1E - {}^1T_2$ transition in diamond and silicon as a function of sphere radius, The corrections are explained in detail in Appendix C.

Diamond		Silicon		
r_0 (bohr)	ΔE (eV)	r_0 (bohr)	ΔE (eV)	
4.17[a]	6.63	6.06[a]	3.59	
4.50	4.59	6.35	2.85	
4.60	4.09	6.45	2.63	
4.70	3.66	6.55	2.43	
4.76[b]	3.28	7.25[b]	1.48	〈6.65 2.25

a) radius to outer hydrogen position.

b) radius to second-nearest-neighbor position.

TABLE VIII.4. Ionization Potentials of the donor and acceptor complexes in silicon and diamond. All values are in electron volts.

Species	Calculated IP[a]	Experimental IP	Difference
Silicon			
V^0	7.83	5.06	2.77
V^-	0.59	4.1	3.5
B^-	3.12	5.07	1.95
Li	6.73	4.03	2.73
Diamond			
V^0	8.49	-	-
V^-	-1.72	-	-

a) Vacancy IP's are based on SD-CI calculations, the B and Li IP's are from the GVB calculations.

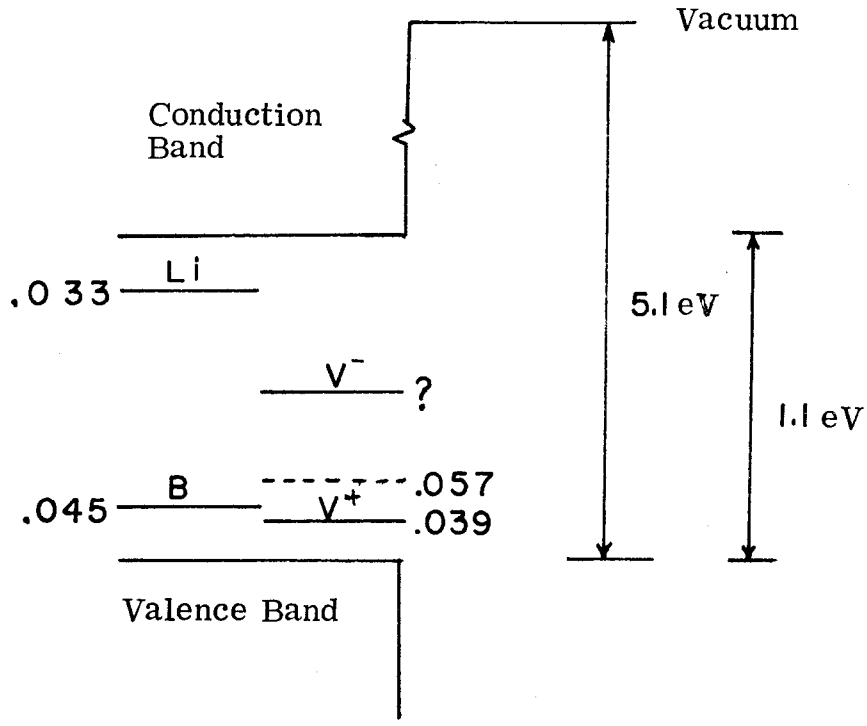

Figure VIII.1. Positions of the donor and acceptor levels in Silicon. The positions of the levels are given in eV from the nearest band edge. The values for boron and lithium are from reference 2c, while those for the positive (V^+) and negative (V^-) vacancy states are from reference 41.

IX. CONCLUSION

Throughout this work, the attempt has been to use methods which are based on fairly simple concepts with regard to how and why molecules bond. The calculations have been done to expand the application of such methods to localized states in solids, i.e., those states which can be treated as molecular in nature. The result is that by the use of valence bond concepts the nature of the states can be understood before the calculations are performed and the results can be interpreted in the same terms afterwards.

In general we find that the lowest states are the covalent states which can be constructed by forming the appropriate number of bonds in the system. The excited states are found from the covalent states by either forming excited states of individual bonds or forming charge transfer (excitation between bonds) states. The ordering of the theoretically determined states agrees with the experiment ordering in the cases studied. In addition we have pointed out that cluster approaches based on MO methods can lead to serious errors in the ordering of states and that these errors stem from not considering the many-electron nature of the states involved.

In comparing the cluster results with experimental quantities, the necessity of including corrections for the "rest of the solid" has been indicated. We find that while simple models for these corrections do not always lead to agreement with experiment, they do include the essential physics of the situation by always correcting in the proper direction.

All of the calculations performed here have included only symmetric relaxations. The actual systems probably do distort and thus methods such as these could be employed to study this question. In addition, with the wealth of epr data on vacancy and impurity systems, one could calculate hyperfine interactions to compare with experiment, even though that is generally a very difficult task unless a different basis is used. Finally, it would be of interest to consider other donor and acceptor systems, specifically aluminum, phosphorous, and perhaps sulfur to obtain a better understanding of the chemical nature of these impurities.

APPENDIX A. Determining the symmetry for the vacancy states.

The starting point for any determination of symmetry is, of course, the structure of the species. If we picture the vacancy as

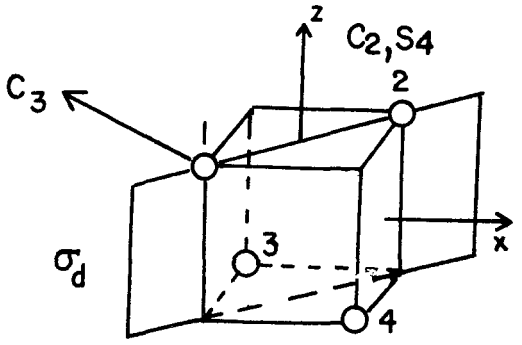

which we will represent as

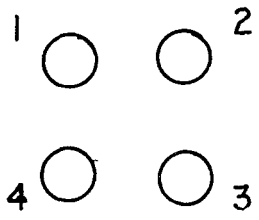

then it is fairly easy to see the effect of the symmetry operations. The symmetry points group is T_d which consists of two-fold rotation axes along x, y and z, four-fold rotary inversions along x, y and z, three-fold rotations along each $(x + y + z) = (1,1,1)$ direction and diagonal mirror planes denoted by the crystallographic planes $[1,1,0]$, $[1,\bar{1},0]$. The character table for T_d is

	E	$8C_3$	$3C_2$	$6S_4$	$6\sigma_d$
A_1	1	1	1	1	1
A_2	1	1	1	-1	-1
E	2	-1	2	0	0
T_1	3	0	-1	1	-1
T_2	3	0	-1	-1	1

We start with four equivalent orbitals, one on each center. For the case of the singlet states, we can construct two covalent structures which correspond to two singlet spin eigenfunctions:

$$\chi_1 = \tfrac{1}{2}(\alpha\beta - \beta\alpha)(\alpha\beta - \beta\alpha)$$

$$\chi_2 = \frac{1}{\sqrt{12}}[2(\alpha\alpha\beta\beta + \beta\beta\alpha\alpha) - (\alpha\beta + \beta\alpha)(\alpha\beta + \beta\alpha)]$$

for which the structures are

where  represents singlet coupling while  represents triplet coupling. Thus we can readily see that the character under C_2 is 2 while under S_4 and σ_d it is zero [for σ_d, the orbital structure χ_1 is character 1 while χ_2 is character -1]. Unfortunately that means that C_3 characterizes the state. We have to rotate χ_1 and χ_2 and solve for the rotated χ's in terms of the original χ's. This is done for a simpler case later, in this case the result in a character of -1 for C_3.

Thus the state is an E state. [Using properties of the symmetric group make this seemingly difficult process quite easy, see for instance M. Hamermesh, Group Theory, Addison-Wesley Publishing Co., Reading, Mass., Chapter 7.]

The case of an ionic state in one bond and a covalent state in the other bond leads to twelve structures of the general form

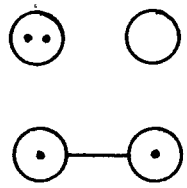

If we consider just the symmetry elements indicated in the figure operating on the twelve structures, we can see that only the σ_d leaves the two structures

unchanged, thus the characters for these twelve structures are

	E	$8C_3$	$3C_2$	$6S_4$	$6\sigma_d$
χ	12	0	0	0	2

This reduces to give the representations A_1, E, T_2, $2T_2$, accounting for $1 + 2 + 3 + 2 \times 3 = 12$ states. Thus the singlet states are $^1A_1$, 2^1E, $^1T_1$, 2^1T_2.

For the triplet case we can start with three triplet spin eigenfunctions:

$$\chi_1 = \frac{1}{\sqrt{2}} (\alpha\beta - \beta\alpha)\alpha\alpha$$

$$\chi_1 = \frac{1}{\sqrt{2}} \alpha\alpha(\alpha\beta - \beta\alpha)$$

$$\chi_3 = \tfrac{1}{2} (\alpha\beta + \beta\alpha)\alpha\alpha - \alpha\alpha(\alpha\beta + \beta\alpha)$$

which correspond to three triplet structures as follows:

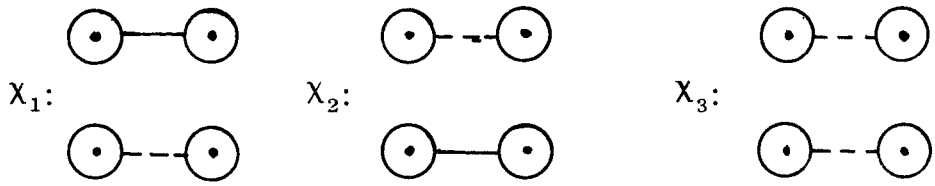

Under interchange of the two centers a ⊙—⊙ is even (character +1) while a ⊙--⊙ is odd (character -1), since they represent singlet and triplet coupling of the two orbitals respectively. Thus we find under C_2 the character is -1 = -1 -1 + 1, and similarly for σ_d the character is -1 = -1 +1 -1. Under S_4, χ_1 and χ_2 interchange while χ_3 goes into itself with two sign changes giving a net character of +1. The C_3 operation transforms the three spin eigenfunctions into each other giving a character of zero. Thus the overall character is

	E	$8C_3$	$3C_2$	$6S_4$	$6\sigma_d$
χ	3	0	-1	1	-1

which corresponds to a T_1 representation.

The excited triplet states of the vacancy arise from a covalent triplet bond and an ionic singlet bond. This again leads to twelve structures of the general form

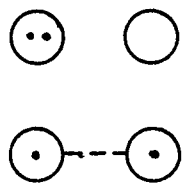

Working out the character for these twelve states, one finds that only σ_d leaves the structures unchanged, but now it gives a minus sign as discussed above. Thus we obtain

	E	$8C_3$	$3C_2$	$6S_4$	$6\sigma_d$
χ	12	0	0	0	-2 .

This can be reduced to the representations A_2, E, $2T_1$, T_2.

For the positive and negative ions the structures we need to consider are basically the same

Negative Ion 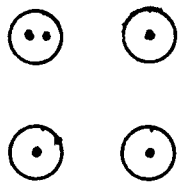 Positive Ion 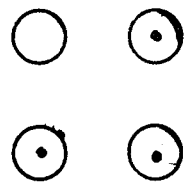

since the doubly occupied orbital and the vacant orbital will have the same transformation properties. Consider first the four quartet structures of the form

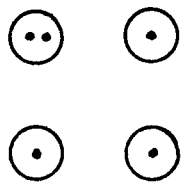

Note that under cyclic permutation of the three singly occupied orbitals the quartet spatial function is even, while under interchange of just two of the orbitals it is odd. Thus the character for the four structures is

	E	$8C_3$	$3C_2$	$6S_4$	$6\sigma_d$
χ	4	1	0	0	-2

which reduces to A_2 and T_1 representations. The doublet states are not quite so straightforward. For each of the above four structures there are two doublet spin eigenfunctions. Two of these could be represented as

where 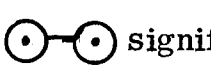 signifies orbitals 3 and 4 singlet coupled and 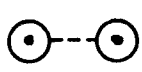 signifies orbitals 3 and 4 triplet coupled. Note that 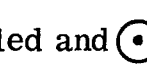 will go into plus itself under interchange of 3 and 4 while 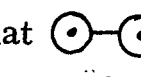 will go into minus itself. Thus under the σ_d we will find a net character of zero (1 + 1 - 1 - 1). The only other problem is working out what happens to the spin functions under a three-fold rotation. The two spin eigenfunctions are

$$\chi_1 = \frac{1}{\sqrt{2}} (\alpha\beta\alpha - \beta\alpha\alpha)$$

$$\chi_2 = \frac{1}{\sqrt{6}} (2\alpha\alpha\beta - \alpha\beta\alpha - \beta\alpha\alpha)$$

Under a three-fold rotation (cyclic permutation) we obtain

$$\chi_1' = C_3 \chi_1 = \frac{1}{\sqrt{2}} (\alpha\alpha\beta - \alpha\beta\alpha)$$

$$\chi_2' = C_3 \chi_2 = \frac{1}{\sqrt{6}} (2\beta\alpha\alpha - \alpha\beta\alpha - \alpha\alpha\beta) .$$

Solving for χ_1' and χ_2' in terms of χ_1 and χ_2 we obtain the matrix

$$\begin{pmatrix} \chi_1' \\ \\ \chi_2' \end{pmatrix} = \begin{pmatrix} -\frac{1}{2} & +\frac{\sqrt{3}}{2} \\ \\ -\frac{\sqrt{3}}{2} & -\frac{1}{2} \end{pmatrix} \begin{pmatrix} \chi_1 \\ \\ \chi_2 \end{pmatrix}$$

and thus the character for C_3 is -1. Thus we obtain the character for the doublets is

	E	$8C_3$	$3C_2$	$6S_4$	$6\sigma_d$
χ	8	-1	0	0	0

which reduces to the representations E, T_1 and T_2.

The states of Li^+ and Li in the vacancy can be considered as adding a Li^+ to the neutral vacancy state or the negative ion state. Thus we would expect to get the same symmetries in the corresponding cases. In the B^- case all of the bonds are doubly occupied and thus the state must be A_1. For the B impurity state we have a structure like

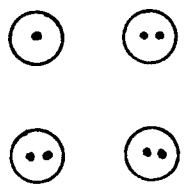

which leads to four equivalent structures. One of these structures transforms into itself under C_3 while two do under σ_d leading to the character

	E	$8C_3$	$3C_2$	$6S_4$	$6\sigma_d$
χ	4	1	0	0	2

This may be reduced to the representations A_1 and T_2.

APPENDIX B. Simple CI Wavefunctions for the Positive and Negative Ion States of the Vacancy.

In order to obtain a qualitative description of the positive and negative ion states we will consider the system to be composed of four equivalent dangling bond orbitals pointing in at the vacancy.[9] Denoting the four centers around the vacancy a, b, c, d, we will label the orbitals as ϕ_a, ϕ_b, ϕ_c, ϕ_d respectively, and will usually use their subscripts, a, b, c, d, to denote the orbitals

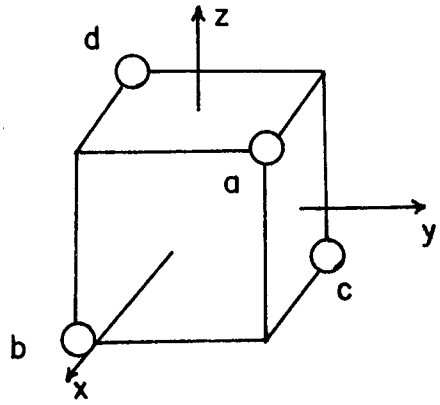

B1. Positive Ion Quartet States

First we consider the quartet states. There are four positive ion wavefunctions differing by which orbital of the four is deleted (i.e., which is the hole). The wavefunctions are

$$\begin{aligned}
\psi_\alpha &= \mathcal{A}(bcd\alpha\alpha\alpha) \\
\psi_\beta &= \mathcal{A}(adc\alpha\alpha\alpha) = C_{2x}\psi_\alpha \\
\psi_\gamma &= \mathcal{A}(dab\alpha\alpha\alpha) = C_{2y}\psi_\alpha \\
\psi_\delta &= \mathcal{A}(cba\alpha\alpha\alpha) = C_{2z}\psi_\alpha
\end{aligned} \qquad \text{(B.1)}$$

where C_{2x} is a two-fold rotation about the x axis, and so forth,

and where $\mathcal{A}$ is the antisymmetrizer $\mathcal{A} = \frac{1}{\sqrt{N!}} \sum \zeta_\tau \hat{\tau}$, each $\hat{\tau}$ being a permutation operator and the ζ_τ its parity.

In T_d symmetry, these four functions lead to A_2 and T_1 symmetries, the A_2 function having the form

$$\Psi_{A_2} = (1 + C_{2x} + C_{2y} + C_{2z})\psi_\alpha = \psi_\alpha + \psi_\beta + \psi_\gamma + \psi_\delta \qquad (B.2)$$

and one component of the T_1 having the form

$$\Psi_{T_1} = (1 + C_{2x} - C_{2y} - C_{2z})\psi_\alpha = \psi_\alpha + \psi_\beta - \psi_\gamma - \psi_\delta \qquad (B.3)$$

Now we want to construct the CI matrix

$$\langle \psi_i | H | \psi_j \rangle$$

for the states of (B.1). Here H is given by (in atomic units)

$$H = \sum_{i=1}^{3} h(i) + \sum_{i>j=1}^{3} \frac{1}{r_{ij}}$$

where

$$h(i) = -\tfrac{1}{2}\nabla_i^2 + V_N(i) + V_{Core}(i)$$

contains, in addition to the usual kinetic energy and nuclear attraction (V_N) terms, the average potential V_{Core}) due to the other bonds and core electrons of the system. Letting

$$A \equiv \langle \psi_\alpha | H | \psi_\alpha \rangle$$

$$B \equiv \langle \psi_\alpha | H | \psi_\beta \rangle \qquad (B.4)$$

we can express the other matrix elements in terms of A and B as follows (remember that H is invariant under the operations of T_d):

$$\langle\psi_\beta|H|\psi_\beta\rangle = \langle C_{2x}\psi_\alpha|H|C_{2x}\psi_\alpha\rangle = \langle\psi_\alpha|H|C_{2x}^{-1}C_{2x}\psi_\alpha\rangle = \langle\psi_\alpha|H|\psi_\alpha\rangle$$

and similarly for the diagonal elements involving ψ_γ and ψ_δ;

$$\langle\psi_\gamma|H|\psi_\alpha\rangle = \langle C_3\psi_\gamma|H|C_3\psi_\alpha\rangle = \langle\, \mathcal{A}(dbc\alpha\alpha\alpha)|H|\,\mathcal{A}(cad\alpha\alpha\alpha)\rangle$$

where C_3 takes a into b, b into c, c into a and d into itself. Since

$$\mathcal{A}(dbc\alpha\alpha\alpha) = +\psi_\alpha$$

(that is, C_3 represents an even permutation) we find that

$$\langle\psi_\gamma|H|\gamma_\alpha\rangle = \langle\psi_\alpha|H|\psi_\beta\rangle = B.$$

Applying the same C_3 one more time leads to

$$\langle\psi_\beta|H|\psi_\gamma\rangle = B.$$

Using a different C_3 axis, one finds that the same relationships hold for transforming ψ_γ into ψ_δ. We can consider the matrix element

$$\langle\psi_\delta|H|\psi_\gamma\rangle = \langle S_4\psi_\delta|H|S_4\psi_\gamma\rangle$$

using the S_4 which is a → d, d → b, b → c, c → a, to give

$$\langle S_4\psi_\delta|H|S_4\psi_\gamma\rangle = \langle\,\mathcal{A}(acd\alpha\alpha\alpha)|H|\,\mathcal{A}(bdc\alpha\alpha\alpha)\rangle = \langle -\psi_\beta|H|-\psi_\alpha\rangle = B.$$

The resulting CI Hamiltonian matrix is

$$\underline{H} \simeq \begin{pmatrix} A & B & B & B \\ B & A & B & B \\ B & B & A & B \\ B & B & B & A \end{pmatrix} \tag{B.5}$$

A similar analysis can be performed for the overlap matrix to give

$$\underline{S} \simeq \begin{pmatrix} I & S & S & S \\ S & I & S & S \\ S & S & I & S \\ S & S & S & I \end{pmatrix} \tag{B.6}$$

where

$$I = \langle \psi_\alpha | \psi_\alpha \rangle$$
$$S = \langle \psi_\alpha | \psi_\beta \rangle \tag{B.7}$$

From (B.2) the energies of the A_2 and T_1 states are obtained by applying the vectors $\begin{pmatrix} 1 \\ 1 \\ 1 \\ 1 \end{pmatrix}$ and $\begin{pmatrix} 1 \\ 1 \\ -1 \\ -1 \end{pmatrix}$ respectively to (B.5) and (B.6). The resulting energies are

$$E_{A_2} = \frac{A+3B}{I+3S} = A + \frac{3(B-SA)}{I+3S}$$

$$E_{T_1} = \frac{A-B}{I-S} = A - \frac{(B-SA)}{I-S} \tag{B.8}$$

Now we want to consider the form of the various terms in order to get some idea of the ordering of the states. Looking first at the overlap terms we have

$$I = \langle \psi_\alpha | \psi_\alpha \rangle = \langle \mathcal{A}(bcd\alpha\alpha\alpha) | \mathcal{A}(bcd\alpha\alpha\alpha) \rangle$$
$$= \sqrt{N!}\, \langle bcd\alpha\alpha\alpha | \mathcal{A}(bcd\alpha\alpha\alpha) \rangle$$
$$= 1 - 3\sigma^2 + 2\sigma^3 \qquad \text{(B. 9)}$$

where $\sigma = \langle \phi_a | \phi_b \rangle$ is the overlap between the one electron orbitals. Similarly

$$S = \langle \psi_\alpha | \psi_\beta \rangle = \langle \mathcal{A}(adc\alpha\alpha\alpha) | \mathcal{A}(bcd\alpha\alpha\alpha) \rangle$$
$$= -\sqrt{N!}\, \langle acd\alpha\alpha\alpha | \mathcal{A}(bcd\alpha\alpha\alpha) \rangle$$
$$= -(\sigma - 2\sigma^2 + \sigma^3) \qquad \text{(B.10)}$$

Neglecting the diagonal terms in the $\underline{H}$ matrix explicitly containing σ we obtain

$$A = \sqrt{N!}\, \langle bcd\alpha\alpha\alpha | H | \mathcal{A}(bcd\alpha\alpha\alpha) \rangle$$
$$= 3\langle b|h|b\rangle + 3\langle a(1)b(2)|\frac{1}{r_{12}}|a(1)b(2)\rangle - 3\langle a(1)b(2)|\frac{1}{r_{12}}|b(1)a(2)\rangle$$
$$\equiv 3h_{aa} + 3J_{ab} - 3K_{ab}$$
$$= 3(h_{aa} + J_{ab} - K_{ab}) \qquad \text{(B.11)}$$

In the case of the B term we want to keep terms containing σ,

$$B = -\sqrt{N!}\, \langle acd\alpha\alpha\alpha | H | \mathcal{A}(bcd\alpha\alpha\alpha) \rangle$$
$$= -\{\langle b|h|a\rangle + 2\sigma\langle c|h|c\rangle + \langle bc|\frac{1}{r_{12}}|ac\rangle - \langle bc|\frac{1}{r_{12}}|ca\rangle$$
$$+\langle bd|\frac{1}{r_{12}}|ad\rangle - \langle bd|\frac{1}{r_{12}}|da\rangle + \sigma\langle cd|\frac{1}{r_{12}}|cd\rangle - \langle cd|\frac{1}{r_{12}}|dc\rangle\}$$
$$\equiv -(h_{ab} + 2J_{abc} - 2K_{abc}) - \sigma(2h_{aa} + J_{ab} - K_{ab}) \qquad \text{(B.12)}$$

Rather than simply substitute the appropriate terms into (B. 8) it is perhaps more instructive to examine the difference in energy between the two states. From (B. 8) we have

$$E_{A_2} = A + \frac{3(B - SA)}{I + 3S} \equiv A + \frac{3\tau}{I + 3S}$$

$$E_{T_1} = A - \frac{(B - SA)}{I - S} = A - \frac{\tau}{I - S}$$

$$E_{A_2} - E_{T_1} = \frac{3\tau}{I + 3S} + \frac{\tau}{I - S} = \frac{4\tau I}{(I + 3S)(I - S)}$$

$$= 4\tau/(I + 2S - 3S^2/I) \qquad \text{(B.13)}$$

Thus the ordering of the states is simply determined by the sign of τ. The form of τ is

$$\tau = (B - SA) = -(h_{ab} - \sigma h_{aa}) - (2J_{abc} - 2K_{abc} - 2\sigma J_{ab} + 2\sigma K_{ab}) \qquad \text{(B.14)}$$

We can get some idea of the sign of the first term by considering H_2^+. Starting with 1s orbitals on each center, ϕ_a and ϕ_b, we obtain two states

$$\Psi_g = a + b, \quad \Psi_u = a - b .$$

Going through the same arguments as above, we obtain the following energy expressions

$$E_g = \frac{h_{aa} + h_{ab}}{1 + \sigma} = h + \frac{h_{ab} - \sigma h_{aa}}{1 + \sigma}$$

$$E_u = \frac{h_{aa} - h_{ab}}{1 - \sigma} = h - \frac{h_{ab} - \sigma h_{aa}}{1 - \sigma}$$

$$E_g - E_u = \frac{\tau_0}{1 - \sigma^2} \quad \text{where } \tau_0 = h_{ab} - \sigma h_{aa}$$

In H_2^+ τ_0 is large and negative. Thus the g state of H_2^+ is the ground state.

In the case of the positive vacancy we need to worry about the J and K terms. Using the Mulliken approximation for J_{abc} we find

$$\langle ab|\frac{1}{r_{12}}|ac\rangle \cong \tfrac{1}{2}\sigma\{\langle ab|\frac{1}{r_{12}}|ab\rangle + \langle ac|\frac{1}{r_{12}}|ac\rangle\} \cong J_{ab}\sigma \quad \text{(B.15)}$$

so that the terms $2J_{abc} - 2\sigma J_{ab}$ approximately cancel. The remaining K terms are small, K_{ab} goes as σ^2/R where R is the separation between centers, while using the Mulliken approximation for K_{abc} gives

$$K_{abc} \cong \tfrac{1}{4}\sigma^2 (J_{aa} + 3J_{ab}) \quad \text{(B.16)}$$

so that the exchange terms in τ could be expected to nearly cancel. The result is that the ordering of the states will be determined by the one-electron quantities, which in turn are just as in H_2^+. The result is that τ should be positive ($\sim -h_{ab}$, $h_{ab} < 0$) and thus the $^4T_1$ state should be below the $^4A_2$. Indeed we find this to be the case, the separation in diamond being 4.75 eV.

B2. Negative Ion Quartet States

For the negative ion, we can take the wavefunctions (B.1) and simply "add" the missing doubly occupied orbital. The wavefunctions are, then,

$$\begin{aligned}
\psi_\alpha &= \mathcal{A}(a^2bcd\alpha\beta\alpha\alpha\alpha) = \mathcal{A}(aabcd\alpha\beta\alpha\alpha\alpha) \\
\psi_\beta &= \mathcal{A}(b^2adc\alpha\beta\alpha\alpha\alpha) = C_{2x}\psi_\alpha \\
\psi_\gamma &= \mathcal{A}(c^2dab\alpha\beta\alpha\alpha\alpha) = C_{2y}\psi_\alpha \\
\psi_\delta &= \mathcal{A}(d^2cba\alpha\beta\alpha\alpha\alpha) = C_{2z}\psi_\alpha
\end{aligned} \tag{B.17}$$

We can rearrange the wavefunctions ψ_β, ψ_γ, ψ_δ into

$$\begin{aligned}
\psi_\beta &= \mathcal{A}(abbcd\alpha\beta\alpha\alpha\alpha) \\
\psi_\gamma &= \mathcal{A}(acbcd\alpha\beta\alpha\alpha\alpha) \\
\psi_\delta &= \mathcal{A}(adbcd\alpha\beta\alpha\alpha\alpha)
\end{aligned}$$

so that the "odd" orbital is always second and no sign changes occur. Evaluating the matrix elements as was done for the positive ion one obtains

$$A' \equiv \langle\psi_\alpha|H|\psi_\alpha\rangle = 5h_{aa} + J_{aa} + 9J_{ab} - 6K_{ab} \tag{B.18}$$

$$B' \equiv \langle\psi_\alpha|H|\psi_\beta\rangle = h_{ab} + 2J_{ab} + 2J_{abc} + \sigma(4h_{aa} + 6J_{ab} - 6K_{ab})$$

where $J_{aab} = \langle a|J_a|b\rangle$. We can form the same functions as in (B.2) and (B.3). The Hamiltonian matrix has the same form as (B.5) simply replacing A by A′ and B by B′. The overlap matrix is also the same with I′ and S′ being given by

$$S' = \langle \psi_\alpha | \psi_\beta \rangle = \sigma - 5\sigma^3 + O(\sigma^4)$$

$$I' = \langle \psi_\alpha | \psi_\alpha \rangle = 1 - 5\sigma^2 + O(\sigma^3) \qquad \text{(B.19)}$$

We can now substitute the appropriate terms into equations (B.13). The term we want to examine again is $\tau = (B' - S'A')$. Substituting B.18 and B.19 into the expression for τ we obtain

$$\begin{aligned} \tau &= h_{ab} + 2J_{aab} + 2J_{abc} + \sigma(4h_{aa} + 6J_{ab} - 6K_{ab}) \\ &\quad - \sigma(5h_{aa} + J_{aa} + 9J_{ab} - 6K_{ab}) \\ &= h_{ab} - \sigma h_{ab} + 2J_{aab} + 2J_{abc} - \sigma J_{aa} - 3\sigma J_{ab} \end{aligned} \qquad \text{(B.20)}$$

Again using the Mulliken approximation for Jaab we find that

$$\begin{aligned} 2J_{aab} &\cong \tfrac{1}{2} \cdot 2 \cdot \sigma \cdot (\langle aa | aa \rangle + \langle ab | ab \rangle) \\ &= \sigma(J_{aa} + J_{ab}) \end{aligned}$$

thus, using (B.15) we find that all of the J terms cancel to give $\tau = h_{ab} - \sigma h_{aa}$. We now have back the case of H_2^+ once more. τ is dominated by h_{ab} which is negative so that we find the $^4A_2$ state <u>below</u> the $^4T_1$ state for the negative ion. This ordering is opposite from the ordering in the positive ion and results from $B' > 0$ while $B < 0$.

The difference in the ordering of the states in the two cases is similar to the difference between H_2^+ and He_2^+. The positive ion wavefunctions could be written in the form

$$\psi_\alpha + \psi_\beta = \mathcal{A}[(a + b)\, cd\, \alpha\beta\alpha] \qquad \text{(B.21)}$$

while the negative ion is

$$\psi_\alpha + \psi_\beta = \mathcal{A}[(a^2b + b^2a)\,cd\,\alpha\beta\alpha\alpha\alpha]. \tag{B.22}$$

In this form the similarity between (B.21) and H_2^+ and between (B.22) and He_2^+ is apparent.

If we consider He_2^+, as in the case of H_2^+, we start with a 1s orbital on each center, ϕ_a and ϕ_b from which we can construct two functions

$$\begin{aligned}\psi_\alpha &= \mathcal{A}[\phi_a\,\phi_a\,\phi_b\,\alpha\beta\alpha] \\ \psi_\beta &= \mathcal{A}[\phi_b\,\phi_b\,\phi_a\,\alpha\beta\alpha]\end{aligned} \tag{B.23}$$

which we can use to construct symmetry functions

$$\begin{aligned}\Psi_g &= \psi_\alpha + \psi_\beta \\ \Psi_u &= \psi_\alpha - \psi_\beta .\end{aligned} \tag{B.24}$$

We can evaluate the Hamiltonian and overlap matrices as we have done before to obtain the energy expressions. The key term is

$$\begin{aligned}B = \langle \psi_\alpha | H | \psi_\beta \rangle &= \langle \mathcal{A}(aab\alpha\beta\alpha) | H | \mathcal{A}(bba\alpha\beta\alpha)\rangle \\ &= \langle \mathcal{A}(aab\alpha\beta\alpha) | H | -\mathcal{A}(abb\alpha\beta\alpha)\rangle \\ &= -(h_{ab} + 2J_{abb} + \sigma 2h_{aa} + \sigma J_{ab} - \sigma K_{ab}) \\ S = \langle \psi_\alpha | \psi_\beta \rangle &= -\sigma + \sigma^3\end{aligned} \tag{B.25}$$

If we evaluate the energy expressions we find that

$$E_g = A + \frac{B - SA}{1 + S} = A - \frac{\tau}{1 - \sigma}$$

$$E_u = A - \frac{B - SA}{1 - S} = A + \frac{\tau}{1 + \sigma} \qquad \text{(B.26)}$$

$$\tau = h_{ab} - \sigma h_{aa} - \sigma J_{ab} .$$

Here we expect the τ term to be dominated by h_{ab} and to be negative. Thus we find that the u states is favored in He_2^+ and that relative to H_2^+ the ordering is inverted.

B3. Positive Ion Doublet States

The wavefunctions for the doublet states are constructed from the same set of orbital products as used in (B.1), except that in the doublet case there are two possible spin eigenfunctions:

$$\chi_1 = \frac{1}{\sqrt{2}} (\alpha\beta\alpha - \beta\alpha\alpha)$$

$$\chi_2 = \frac{1}{\sqrt{6}} (\alpha\alpha\beta - \alpha\beta\alpha - \beta\alpha\alpha) . \qquad \text{(B.27)}$$

Thus rather than the four configurations obtained in (B.1) there will be eight in this case. Constructing symmetry functions for one component each of T_1, T_2 and E, we find that

$$\psi_{T_1} = \mathcal{A}(cdb\,\chi_2) + \mathcal{A}(dca\,\chi_2) - \mathcal{A}(abd\,\chi_2) - \mathcal{A}(bac\,\chi_2)$$

$$\psi_{T_2} = \mathcal{A}(cdb\,\chi_1) + \mathcal{A}(dca\,\chi_1) - \mathcal{A}(abd\,\chi_2) - \mathcal{A}(bac\,\chi_1)$$

$$\psi_E = \mathcal{A}(cdb\,\chi_1) + \mathcal{A}(dca\,\chi_1) + \mathcal{A}(abd\,\chi_1) + \mathcal{A}(bac\,\chi_1).$$

(B.29)

Rather than construct the entire 8×8 matrix, it is only necessary to calculate certain matrix elements. We will retain only those terms in the off-diagonal matrix elements which are first order in overlap of the form σh_{aa}, σJ_{aa}, σJ_{ab} and σK_{ab}. Any other terms involving σ would have an overall dependence of σ^2 or higher. The matrix elements that we need in the energy expressions are given below.

$$
\begin{aligned}
\langle \mathcal{A}(cdb\,\chi_1)|H|\,\mathcal{A}(cdb\,\chi_1)\rangle &= 3(h_{aa} + J_{ab}) = A + 3K_{ab} \\
\langle \mathcal{A}(cdb\,\chi_1)|H|\,\mathcal{A}(dca\,\chi_1)\rangle &= h_{ab} + 2J_{abc} - K_{abc} + \sigma(2h_{aa} + J_{ab} + K_{ab}) \\
&= B + K_{abc} + \sigma(2h_{aa} + J_{ab} + K_{ab}) \\
\langle \mathcal{A}(cdb\,\chi_2)|H|\,\mathcal{A}(dca\,\chi_2)\rangle &= -(B + 3K_{abc}) - \sigma(2h_{aa} + J_{ab} - K_{ab}) \\
\langle \mathcal{A}(cdb\,\chi_1)|H|\,\mathcal{A}(abd\,\chi_1)\rangle &= -\tfrac{1}{2}(B + 4K_{abc}) - \tfrac{1}{2}\sigma(2h_{aa} + J_{ab} - 2K_{ab}) \\
&= \langle \mathcal{A}(cdb\,\chi_1)|H|\,\mathcal{A}(bac\,\chi_1)\rangle \\
\langle \mathcal{A}(cdb\,\chi_2)|H|\,\mathcal{A}(abd\,\chi_2)\rangle &= \tfrac{1}{2}B + \tfrac{1}{2}\sigma(2h_{aa} + J_{ab} + 2K_{ab}) \\
&= \langle \mathcal{A}(cdb\,\chi_2)|H|\,\mathcal{A}(bac\,\chi_1)\rangle
\end{aligned}
\qquad \text{(B.30)}
$$

where A and B are given by (B.11) and (B.12) respectively and

$$
\begin{aligned}
\langle \mathcal{A}(cdb\,\chi_1)|\,\mathcal{A}(cdb\,\chi_1)\rangle &= 1 + O(\sigma^2) \\
\langle \mathcal{A}(cdb\,\chi_1)|\,\mathcal{A}(dca\,\chi_1)\rangle &= \sigma + O(\sigma^3) \\
\langle \mathcal{A}(cdb\,\chi_2)|\,\mathcal{A}(dca\,\chi_2)\rangle &= -\sigma + O(\sigma^3) \\
\langle \mathcal{A}(cdb\,\chi_1)|\,\mathcal{A}(abd\,\chi_1)\rangle &= -\tfrac{1}{2}\sigma = \langle \mathcal{A}(cdb\,\chi_1)|\,\mathcal{A}(abd\,\chi_1)\rangle \\
\langle \mathcal{A}(cdb\,\chi_2)|\,\mathcal{A}(abd\,\chi_2)\rangle &= -\tfrac{1}{2}\sigma = \langle \mathcal{A}(cdb\,\chi_2)|\,\mathcal{A}(abd\,\chi_2)\rangle
\end{aligned}
\qquad \text{(B.31)}
$$

The appropriate energy expressions are constructed as before and are given by

$$E_{T_2} = A + 3K_{ab} + \frac{2B + 5K_{abc} + \sigma(4h_{aa} + 2J_{ab} - K_{ab}) - 2\sigma(A + 3K_{ab})}{1 + 2\sigma}$$

$$E_{T_1} = A + 3K_{ab} - \frac{2B + 3K_{abc} + \sigma(4h_{aa} + 2J_{ab} - K_{ab}) - 2\sigma(A + 3K_{ab})}{1 - 2\sigma}$$

$$E_E = A + 3K_{ab} - 3K_{abc} + 3\sigma K_{ab} \qquad \text{(B.32)}$$

The first two expressions can be reduced considerably using (B.16) after expanding the A and B terms to give

$$E_{T_2} = A + 3K + \frac{2(h_{ab} - \sigma h_{aa}) + 3K_{abc} - \sigma K_{ab}}{1 + 2\sigma}$$

$$E_{T_1} = A + 3K - \frac{2(h_{ab} - \sigma h_{aa}) + K_{abc} + \sigma K_{ab}}{1 - 2\sigma} \qquad \text{(B.33)}$$

Again we have the situation in which the splitting of the energy levels is determined by a "τ-like" term. In (B.16) it was shown that $K_{abc} \sim \sigma^2$, furthermore, K_{ab} goes as σ^2/R_{ab}, so that the K terms should all be smaller than the one electron quantities. As before (hab - σhaa) can be expected to be large and negative. The ordering of the states is, then

$$E_{^2T_2} < E_{^2E} < E_{^2T_1}.$$

If we go back to (B.13) and (B.14) and make the substitution (B.15), we obtain

$$E_{^4A_2} = A - \frac{3(h_{ab} - \sigma h_{aa}) + 2\sigma K_{ab} - 2K_{abc}}{1 - 3\sigma}$$

$$E_{^4T_1} = A + \frac{(h_{ab} - \sigma h_{aa}) + 2\sigma K_{ab} - 2K_{abc}}{1 + \sigma} \qquad (B.34)$$

At this point we would argue that the overall ordering of the states of the positive vacancy are determined by the term $(h_{ab} - \sigma h_{aa})$. If we redefine τ,

$$\tau = h_{ab} - \sigma h_{aa} \qquad (B.35)$$

and ignore the K terms, we obtain

$$E_{^2T_2} \cong A + \frac{2\tau}{1+2\sigma}$$

$$E_{^4T_1} \cong A + \frac{\tau}{1+\sigma}$$

$$E_{^2E} \cong A$$

$$E_{^2T_1} \cong A - \frac{2\tau}{1-2\sigma}$$

$$E_{^2A_1} \cong A - \frac{3\tau}{1-3\sigma} \qquad (B.36)$$

where we have listed the terms in order of increasing energy going down the page. This is the calculated ordering found for both diamond and silicon.

B4. Negative Ion Doublet States

At this point it should be possible to infer from section B2 what to expect in the case of the negative ion doublet states. In the discussion of He_2^+ we saw that the off-diagonal Hamiltonian matrix elements changed sign from H_2^+ to He_2^+. That is, the addition of the doubly-occupied pair in the He_2^+ wavefunctions caused an extra sign change in evaluating these matrix elements. For the negative ion doublets, then, we have wavefunctions of the form $\mathcal{A}[a^2cdb(\alpha\beta\alpha\beta\alpha - \alpha\beta\beta\alpha\alpha)]$ and expect the same behavior. We have already calculated

$$\begin{aligned} E_{^2A_2} &\cong A' + \frac{3\tau}{1+3\sigma} \\ E_{^4T_1} &\cong A' - \frac{\tau}{1-\sigma} \end{aligned} \tag{B.37}$$

If we simply start with (B.36) and reverse the signs of all the τ and σ terms we should obtain the appropriate result. Doing so and reordering the ascending order we obtain

$$\begin{aligned} E_{^4A_2} &\cong A' + \frac{3\tau}{1+3\sigma} \\ E_{^2T_1} &\cong A' + \frac{2\tau}{1+2\sigma} \\ E_{^2E} &\cong A' \\ E_{^4T_1} &\cong A' - \frac{\tau}{1-\sigma} \\ E_{^2T_2} &\cong A' - \frac{2\tau}{1-2\sigma} . \end{aligned} \tag{B.38}$$

Thus for the negative ion, the sign change in the τ and σ terms cause an ordering of states which is the reverse of the positive ion. This is the case in silicon and is correct except for the $^4T_1$ and $^2T_2$ states of diamond.

APPENDIX C. DIELECTRIC CORRECTIONS

The inclusion of polarization effects in the description of localized states is not a new idea. For instance, a classical electrostatic calculation of the polarization of an alkali halide lattice due to an extra charge was used by Mott and Littleton[45] in describing electrolytic conduction in solid salts. The energy correction formulae were later used by Fowler[46] to study the effect of polarization on the spectra of alkali halide crystals.

In this case we will first describe the general problem and its solution and then will give a few more specific examples. The starting point is a cavity in an infinite dielectric. The calculated molecular cluster resides inside the cavity and gives rise to a multipole field. The approach is to find the energy of interaction of the field with the medium. The solution is by the method of images. Consider the geometry

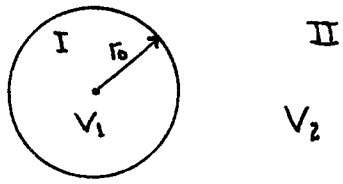

where V_1 is the source potential and V_2 is the image potential. In region I the potential ϕ_I is

$$\phi_I(\vec{r}) = V_1(\vec{r}) + V_2(\vec{r})$$

while in region II

$$\phi_{II}(\vec{r}) = \frac{1}{\epsilon}\,\tilde{V}_1(\vec{r})$$

where we have defined

$$\tilde{V}_1(\vec{r}) = \tilde{C}\,V_1(\vec{r})$$
$$V_2(\vec{r}) = C\,V_1(\vec{r})\ .$$

Using the boundary conditions at the sphere we find that

$$\hat{n}\cdot(\vec{D}_2 - \vec{D}_1) = 0 \Rightarrow\quad 1 - C = \epsilon\,\tilde{C}$$

$$\phi_I = \phi_{II} \Rightarrow\quad 1 + C = \frac{1}{\epsilon}\,\tilde{C}\ .$$

Thus one obtains

$$\tau = \frac{2\epsilon}{\epsilon + 1}$$

$$\phi_{II}(\vec{r}) = \frac{1}{\epsilon}\cdot\frac{2\epsilon}{\epsilon+1}\cdot V_1(\vec{r})$$

$$= \frac{2}{\epsilon+1}\,V_1(\vec{r})$$

We wish to find the energy density in region II, U where

$$U = -\tfrac{1}{2}\int_{II}\vec{P}_2\cdot\vec{E}_1\,dv$$

$$\vec{P} = \frac{1}{4\pi}(\vec{D} - \vec{E}),\quad \vec{D} = \epsilon\,\vec{E}$$

$$\Rightarrow\ \vec{P} = \frac{\epsilon - 1}{4\pi}\,\vec{E}\ .$$

We now use the relations

$$\vec{E}_1 = -\vec{\nabla} V_1 \qquad \vec{E}_2 = -\vec{\nabla} \phi_{II}$$

thus obtaining

$$\vec{P}_2 = -\frac{\epsilon - 1}{4\pi} \cdot \frac{2}{\epsilon + 1} \vec{\nabla} V_1(\vec{r})$$

$$\Rightarrow U = -\frac{1}{4\pi} \frac{\epsilon - 1}{\epsilon + 1} \int_{II} \vec{\nabla} V_1 \cdot \vec{\nabla} V_1 \, dv \ .$$

We now use Green's Theorem to obtain

$$\int_{II} \vec{\nabla} V_1 \cdot \vec{\nabla} V_1 \, dr = \int_S V_1 \vec{\nabla} V_1 \cdot d\vec{A} - \int_{II} V_1 \nabla^2 V_1 \, dr \ .$$

However, in region II $\nabla^2 V_1 = 0$, thus the second term is zero. Note now that $d\vec{A}$ points <u>inward</u> in the $\hat{r}$ direction, thus we have

$$d\vec{A} = -\hat{r} \, r_0^2 \sin\theta \, d\theta \, d\phi$$

for a sphere of radius r_0. Consequently only the $\hat{r}$ term in $\vec{\nabla}$ will contribute to the integral. We now take V_1 to be a general multipole potential,

$$V_1 = 4\pi \sum_{\ell m} \frac{1}{2\ell + 1} \, q_{\ell m} \, \frac{Y_{\ell m}(\theta, \phi)}{r^{\ell+1}}$$

where $$q_{\ell m} = \int Y^*_{\ell m}(\theta', \phi') \, r'^{\ell} \, \rho(r') \, d\vec{r} \ .$$

Thus

$$V_1 \vec{\nabla} V_1 = V_1 \frac{\partial V_1}{\partial r} \hat{r} = V_1 \sum_{\ell m} -(\ell+1) \frac{4\pi}{2\ell+1} q_{\ell m} \frac{Y_{\ell m}(\theta,\phi)}{r^{\ell+1}} \hat{r}$$

$$U = -\frac{1}{4\pi} \frac{\epsilon-1}{\epsilon+1} \sum_{\ell m} \sum_{\ell' m'} (\ell+1) \int r_0^{-(2\ell+1)} q_{\ell m} q_{\ell' m'} Y_{\ell m} Y_{\ell' m'} \, d\Omega$$

$$= -\frac{1}{4\pi} \frac{\epsilon-1}{\epsilon+1} \sum_{\ell m} \sum_{\ell' m'} (\ell+1) \int r_0^{-(2\ell+1)} q_{\ell m} q^*_{\ell' m'} (-1)^{2m'} Y_{\ell m} Y_{\ell' m'} \, d\Omega$$

$$= -\frac{1}{4\pi} \frac{\epsilon-1}{\epsilon+1} \sum \frac{\ell+1}{r_0^{2\ell+1}} \cdot \left(\frac{4\pi}{2\ell+1}\right)^2 (q_{\ell m} q^*_{\ell m}) \, .$$

If we take $\rho(\vec{r})$ to be a point charge, e, we obtain

$$U = -\frac{1}{4\pi} \frac{\epsilon-1}{\epsilon+1} (4\pi)^2 \cdot 1 \cdot \left(\frac{1}{\sqrt{4\pi}}\right)^2 \frac{e^2}{r_0} = -\frac{\epsilon-1}{\epsilon+1} \frac{e^2}{r_0} \, .$$

Similarly for a dipole 2ea in the z direction, we obtain

$$q_{10} = \sqrt{\frac{3}{4\pi}} P$$

$$U = -\tfrac{2}{3} \frac{\epsilon-1}{\epsilon+1} \frac{P^2}{r_0^3}$$

If we define the quadrupole moment as

$$Q_{\alpha\beta} = \tfrac{1}{2} (3 r_\alpha r_\beta - r^2 \delta_{\alpha\beta})$$

then the energy correction is

$$U = -\frac{3}{5}\frac{\epsilon - 1}{\epsilon + 1}\{(Q_{xx} - Q_{yy})^2 + Q_{zz}^2 + 4(Q_{xy}^2 + Q_{xz}^2 + Q_{yz}^2)\}\frac{1}{r_0^5} .$$

Higher order corrections are easily obtained in terms of the $q_{\ell m}$ or using real spherical harmonics (x, y, z etc.).

For a charge q on the surface we use the geometry

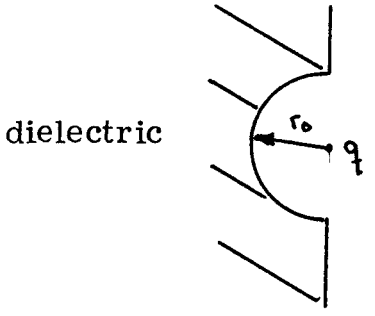

The energy expression becomes

$$U = -\frac{1}{4\pi}\frac{\epsilon - 1}{\epsilon + 1}\int \frac{q^2}{r^4}\, d\vec{r}$$

where the integral is over the dielectric, thus one obtains

$$U = -\frac{q^2}{4\pi}\frac{\epsilon - 1}{\epsilon + 1}\int_0^{2\pi}\int_{\pi/2}^{\pi}\int_{r_0}^{\infty}\frac{r^2}{r^4}\sin\theta\, d\theta\, d\phi\, dr$$

$$= -\frac{q^2}{2}\frac{\epsilon - 1}{\epsilon + 1}\left[-\cos\theta\right]_{\pi/2}^{\pi}\left[-\frac{1}{r}\right]_{r_0}^{\infty} = -\frac{q^2}{2}\left(\frac{\epsilon - 1}{\epsilon + 1}\right)\frac{1}{r_0} .$$

This is one half the result for a charge in a cavity as one might have expected.

REFERENCES

1. (a) J. C. Phillips, Bonds and Bands in Semiconductors (Academic Press, New York, N.Y., 1973);
(b) W. A. Harrison, Solid State Theory (McGraw-Hill Company, New York, N.Y., 1970).

2. (a) W. Kohn, Solid State Physics, F. Seitz and D. Turnbull, eds., (Academic Press, New York, N.Y., 1957) Vol. 5, p. 258;
(b) W. Kohn and J. M. Luttinger, Phys. Rev. 97, 1721 (1955); ibid., 48, 915 (1955);
(c) F. Bassani, G. Iadonisi and B. Preziosi, Rep. Prog. Phys. 37, 1099 (1974). Reference (c) contains the most complete review of the theory of impurity state excluding cluster calculations.

3. S. T. Pantelides and C. T. Sah, Phys. Rev., B10, 621, 638 (1974).

4. A. M. Stoneham, Radiation Effects in Semiconductors, J. W. Corbett and G. D. Watkins, eds., (Gordon and Breach, London, 1971), p. 8.

5. (a) A. B. Lidiard, Radiation Damage and Defects in Semiconductors, J. E. Whitehouse, ed., (Institute of Physics, London, 1972), p. 238;
(b) C. A. Coulson, ibid., p. 249.

6. R. P. Messmer and G. D. Watkins, Phys. Rev. B7, 2568 (1973). References 4-6 contain a reasonable survey of methods for vacancy states.

7. W. A. Goddard III and R. C. Ladner, J. Am. Chem. Soc., 93, 6750 (1971).

8. W. A. Goddard, T. H. Dunning, W. J. Hunt, P. J. Hay, Accts. Chem. Res. 6, 368 (1973).

9. C. A. Coulson and M. J. Kearsley, Proc. Roy. Soc. (London) A231, 433 (1957).

10. (a) T. Yamaguchi, J. Phys. Soc. Japan 17, 1359 (1962).

(b) C. A. Coulson and F. P. Larkins, J. Phys. Chem. Solids, 32, 2245 (1971).

(c) F. P. Larkins, J. Phys. Chem. Solids, 32, 965 (1971).

11. In H_2, if we consider the singlet (S) and triplet (T) states constructed from localized orbitals on each center, ℓ and r, the VB wavefunctions are given by

$$\Psi_S = \mathcal{A}[(\ell r + r\ell)\,\alpha\beta]$$

$$\Psi_T = \mathcal{A}[(\ell r - r\ell)\,\alpha\beta]$$

Evaluating the energy using the same orbitals in each case on obtains

$$E_S = \frac{E_0 + E_X}{1 + S^2} = E_0 + \frac{E_X - E_0 S^2}{1 + S^2}$$

$$E_T = \frac{E_0 - E_X}{1 - S^2} = E_0 - \frac{E_X - E_0 S^2}{1 - S^2}$$

where

$$E_0 = \langle \ell r | H | \ell r \rangle$$

$$E_X = \langle \ell r | H | r \ell \rangle = 2\langle \ell | r \rangle \langle \ell | h | r \rangle + \langle \ell r \left| \frac{1}{r_{12}} \right| r \ell \rangle$$

$$= 2Sh_{\ell r} + K_{\ell r}$$

For H_2 $S \geq 0$

$K_{\ell r} \geq 0$

$h_{\ell r} \leq 0$

$S|h_{\ell r}| > K_{\ell r}$

thus the singlet state will be lower. The ratio of the splitting from E_0 for the two states is

$$\frac{1 + S^2}{1 - S^2}$$

which becomes close to 1 (no splitting) as $S \rightarrow 0$.

12. W. A. Goddard and R. J. Blint, Chem. Phys. Letters, 14, 616 (1972).

13. (a) W. A. Goddard, A. Redondo and T. C. McGill, Solid State Comm. (to be published).

(b) A. Redondo, private communication.

14. J. C. Slater, Quantum Theory of Molecules and Solids (McGraw-Hill, New York, N.Y., 1965), Volume 2.

15. T. H. Dunning, private communication.

16. S. Huzinaga, J. Chem. Phys., 42, 1293 (1965).

17. T. H. Dunning, J. Chem. Phys., 53, 2823 (1970).

18. (a) C. F. Melius, Ph.D. Thesis, California Institute of Technology, 1972.

(b) C. F. Melius and W. A. Goddard, Phys. Rev., A10, 1528 (1974).

(c) C. F. Melius, B. D. Olafson and W. A. Goddard, Chem. Phys. Letters, 28, 457 (1974).

19. A. Redondo, W. A. Goddard and T. C. McGill, to be published.

20. L. R. Kahn, P. J. Hay and I. Shavitt, J. Chem. Phys., 61, 3530 (1974).

21. C. D. Clark and J. Walker, Proc. Roy. Soc (London) A334, 241 (1973).

22. W. A. Lathan, W. J. Hehre and J. A. Pople, J. Am. Chem. Soc., 93, 808 (1974).

23. In general we will consider two bond regions, one between centers 1 and 2 and one between 3 and 4. Thus for bond 1-2 we define

$$g_1 = \phi_1 + \phi_2 = \ell_1 + r_1$$
$$u_1 = \phi_1 - \phi_2 = \ell_1 - r_1$$

where ϕ_1 and ϕ_2 are localized functions on centers 1 and 2. Similarly we have

$$g_2 = \phi_3 + \phi_4 = \ell_2 + r_2$$
$$u_2 = \phi_3 - \phi_4 = \ell_2 - r_2 \ .$$

24. In He_2^+ the ground state is

$$\mathcal{A}[(\ell\ell r - rr\ell)\alpha\beta\alpha] = \mathcal{A}[g^2 u\alpha\beta\alpha]$$

while for H_2^+ the ground state is $g = \ell + r$.

25. F. W. Bobrowicz, Ph.D. Thesis, California Institute of Technology, 1974.

26. G. D. Watkins, Radiation Damage in Semiconductors (Dunod, Paris, 1965), p. 95.

27. F. P. Larkins and A. M. Stoneham, J. Phys., C4, 143, 154 (1971).

28. A. Redondo, private communication.

29. No Hartree Fock Calculations were performed for the larger basis. This estimate was obtained by replacing the GVB pair with the first NO of the pair (ϕ_1^2). This amounts to adding the energy lowering to the GVB energy to obtain the estimated HF energy.

30. R. L. Aggarwal, P. Fisher, V. Mourzine and A. K. Ramdas, Phys. Rev., 137, A882 (1965).

31. (a) Reference 21.

(b) For a review of other radiation produced centers as well as earlier work on the GR1 center see C. D. Clark and E. W. J. Mitchell, Radiation Effects in Semiconductors, J. W. Corbett and G. D. Watkins, eds., (Gordon and Breach, London, 1972), p. 257.

32. Of the calculations in references 9 and 10, only that of reference 10(a) obtains the correct ordering.

33. G. D. Watkins and R. P. Messmer, Phys. Rev. Letters, 32, 1244 (1974).

34. J. W. Corbett, J. C. Bourgoin and C. Weigel, Radiation Damage and Defects in Semiconductors, J. E. Whitehouse, ed., (Institute of Physics, London, 1972), p. 1.

35. L. F. Wagner and W. E. Spicer, Phys. Rev. Letters, 28, 1381 (1972).

36. D. E. Eastman and W. D. Grobman, Phys. Rev. Letters, 28, 1378 (1972).

37. R. G. Cavell, S. P. Kowalczyk, L. Ley, R. A. Pollack, B. Mills, D. A. Shirley and W. Perry, Phys. Rev., B7, 5313 (1973).

38. The explanation of the problems related to photoemission experiments was provided by Dr. Steve Cunningham.

39. G. D. Watkins, Radiation Damage and Defects in Semiconductors, J. E. Whitehouse, ed., (Institute of Physics, London, 1972), p. 228.

40. J. A. Baldwin, Phys. Rev. Letters, 10, 220 (1963).

41. G. D. Watkins, General Electric Technical Information Series, Report No. 74 CRD202, Sept. 1974. The text of an invited paper given at the International Conference on Lattice Defects in Semiconductors, Freiburg, Germany, July 22-25, 1974.

42. D. D. Wagman, W. H. Evans, V. B. Parker, I. Halow, S. M. Bailey and R. H. Schumm, Selected Values of Chemical Thermodynamics Properties, National Bureau of Standards (U.S.), Technical Note 270-3 (1968).

43. L. Pauling, The Nature of the Chemical Bond, (Cornell University Press, Ithaca, N.Y., 1960), Chap. 7, p. 221.

44. G. T. Surratt and W. A. Goddard III, to be published.

45. N. F. Mott and M. J. Littleton, Trans. Faraday Soc., 34, 485 (1938).

46. W. B. Fowler, Phys. Rev., 151, 657 (1966).